



Aalto University
School of Engineering

Jaak Kadak

Effect of steel strength on the welded joint between a plate and two tubular cross-sections

Master's thesis submitted in partial fulfillment of the requirements for the degree of Master of Science in Technology.

In Espoo 26.5.2014

Supervisor: Professor Jari Puttonen

Instructors: Wei Lu D.Sc. (Tech.), Arto Sivill M.Sc. (Tech.)

AALTO UNIVERSITY SCHOOLS OF TECHNOLOGY PO Box 12100, FI-00076 AALTO http://www.aalto.fi		ABSTRACT OF THE MASTER'S THESIS	
Author: Jaak Kadak			
Title: Effect of steel strength on the welded joint between a plate and two tubular cross-sections			
School: School of Engineering			
Department: Civil and Structural Engineering			
Professorship: Structural Engineering and Building Physics		Code: Rak-43	
Supervisor: Professor Jari Puttonen Instructors: Wei Lu D.Sc. (Tech.), Arto Sivill M.Sc. (Tech.)			
<p>The aim of this thesis is to study the behaviour of a K-type bottom edge joint that is used in a WQ truss. The behaviour of the joint is studied under static loads using Finite Element (FE) analysis. The joint consists of Rectangular Hollow Sections (RHS) as bracing members, a division plate and a steel plate as a lower chord. The current thesis studies the behaviour of the joints with steel grades S460 and S550.</p> <p>In the literature review, the properties of high strength steel and material models used in FE analysis are discussed. Numerical analyses for joints with steel grades S460 and S550 were conducted with an FE package ABAQUS/Standard. Both the joint and the truss are modelled to account for global effects of the truss on the behaviour of the joint. For the sake of computational efficiency, only the joint of the truss is modelled with solid elements, and the surrounding truss members are modelled with beam elements. Both geometrical and material non-linearity are taken into account in the analyses. Possible criteria for the limit load were defined and the model was validated against the results from the previous research. Parametric studies were then conducted on the joint to investigate the effects of such parameters as the steel grade, the thickness of both division plate and lower chord, inclination angle of bracing members, and the width of bracing members on the deformation and limiting load of the joints.</p> <p>The criterion for the limiting load was considered to be met when the equivalent plastic strains exceeded 5 % at any element centroid in the joint model. The criterion observed for all studied models was the local yielding of the tension bracing member. According to the numerical analysis, the criterion was met in the interface between the weld and the vertical flange of the bracing member. Smoothing the geometrical discontinuity regions would reduce the stress concentrations, possibly leading to higher limit loads. A tendency for smaller relative displacements at the limit load was seen with higher steel grade. A full scale loading tests need to be performed to validate the results from numerical analysis against the true behaviour of the joint. For future research the effect of using undermatched filler materials in welds and the effect of heat affected zones (HAZ) on the joint capacity need to be considered.</p>			
Date: 26.5.2014		Language: English	Number of pages: 88 + 12
Keywords: FE analysis, high strength steel, rectangular hollow section, k-type truss joint			

AALTO-YLIOPISTO TEKNIIKAN KORKEAKOULUT PL 12100, 00076 Aalto http://www.aalto.fi		DIPLOMITYÖN TIIVISTELMÄ	
Tekijä: Jaak Kadak			
Työn nimi: Teräslujuuden merkitys levyn ja kahden putken hitsatulle liitokselle			
Korkeakoulu: Insinööritieteiden korkeakoulu			
Laitos: Rakennustekniikan laitos			
Professori: Talonrakennustekniikka		Koodi: Rak-43	
Työn valvoja: Professori Jari Puttonen			
Työn ohjaajat: TkT Wei Lu, DI Arto Sivill			
<p>Diplomityössä tutkitaan WQ-ristikossa usein käytettävän reunimmaisesta K-liitoksen käyttäytymistä. Liitokseen vaikuttaa ristikolta tuleva staattinen kuormitus. Tarkastelussa käytetään elementtimenetelmää (FEM). Liitos koostuu poikkileikkaukseltaan suorakulmion muotoisista rakenneputkista, jakolevystä sekä alapaarteen muodostavasta teräslevystä. Liitoksen toimintaa selvitetään teräslaaduilla S460 ja S550.</p> <p>Kirjallisuuskatsauksessa tutkitaan korkealujuuksisen teräksen ominaisuuksia ja numeerisessa analyysissä käytettäviä materiaalimalleja. Numeerinen analyysi suoritettiin elementtimenetelmään perustuvalla ABAQUS/Standard –laskentaohjelmalla. Ristikon globaalien vaikutusten huomioon ottamiseksi sekä ristikko että liitos mallinnettiin. Laskenta-ajan vähentämiseksi vain liitosalue mallinnettiin solidielementeillä, muu osa ristikkoa mallinnettiin palkkielementeillä. Sekä geometrinen että materiaallinen epälineaarisuus otettiin laskennassa huomioon. Mahdollisten murtumistapojen määrittämisen jälkeen mallia validoitiin vertailulla aiempiin tutkimuksiin. Tämän jälkeen selvitetiin parametrisella analyysillä, miten teräksen lujuusluokka, alapaarteen ja jakolevyn paksuudet, uumasauvojen kaltevuuskulma sekä uumasauvojen leveys vaikuttavat liitoksen venymiin ja rajakuormaan.</p> <p>Rajakuorman katsottiin olevan saavutettu, kun plastiset venymät ylittivät 5 % jossakin liitoksen osaa kuvaavan elementin keskipisteessä. Kaikkien tutkittujen mallien tapauksessa murtotavaksi osoittautui uumasauvan paikallinen myötääminen, joka tapahtui lähellä uumasauvan uuman ja hitsin yhtymäkohtaa. Geometrinen epäjatkuvuuskohtien pyöristäminen vähentäisi jännityskeskittymiä näillä alueilla ja johtaisi mahdollisesti suurempiin laskennallisiin rajakuormiin. Suurempaa teräslujuutta käytettäessä huomattiin taipumus pienempiin suhteellisiin siirtymiin murtokuormalla. Murtokokeiden suorittaminen oikealla rakenteella on suotavaa numeerisen mallin tulosten oikeelliseksi varmentamiseksi. Jatkotutkimuksessa on kiinnitettävä erityisesti huomiota alilujien hitsausaineiden ja muutosvyöhykkeen (HAZ) vaikutukseen liitoksen kestävyteen.</p>			
Päivämäärä: 26.5.2014		Kieli: englanti	Sivumäärä: 88 + 12
Avainsanat: elementtimenetelmä, korkealujuusteräs, putkiprofiili, K-liitos			

Foreword

This thesis is a part of the development project driven by Ruukki Oyj and Finnmap Consulting Oy. I am grateful for these two companies for funding this thesis. Additionally, I thank CSC - IT Center for Science Ltd for providing the licence for Abaqus software.

I would also like to thank my instructors Dr. Wei Lu and Mr. Arto Sivill whose advice and enthusiasm for explaining the theory is highly appreciated. In addition, I would like to express my gratitude to my supervisor Professor Jari Puttonen for his valuable comments and ideas.

I am also grateful to my fellow master's thesis writers and doctoral students in the Rebuilding of Aalto University as well as my colleagues in Finnmap Consulting Oy as they have kept up the good spirit on a daily basis. Finally, special thanks to my friends and family who have been understanding and supportive through the whole writing process.

In Espoo 26.5.2014

Jaak Kadak

Table of Contents

Abstract

Tiivistelmä

Foreword

Table of Contents

Symbols

List of abbreviations

1	Introduction.....	1
1.1	Background of the project.....	1
1.2	Truss.....	1
1.3	Joint.....	3
1.4	Methods.....	4
1.5	Outline of the thesis.....	4
2	Literature review.....	6
2.1	High-strength steel.....	6
2.2	Truss joint.....	12
2.2.1	K-joints.....	12
2.2.2	Design of welds.....	17
2.2.3	Limit state criteria.....	23
2.3	Previous studies.....	27
3	Finite element modelling.....	28
3.1	Geometrical model.....	28
3.2	FE Meshes.....	29
3.3	Material properties.....	32
3.3.1	Elastic-plastic model with linear strain hardening.....	33
3.3.2	Simplified stress-strain curve.....	34
3.4	Boundary conditions.....	36
3.5	Analysis step.....	36
4	Validation and analysis of results.....	38
4.1	Geometries of joint.....	38
4.2	Convergence tests.....	38
4.3	Criteria to determine the limit load.....	40
4.4	Effect of the material model on limit loads.....	45
4.5	Comparison with previous studies.....	49
5	Parametric studies.....	51
5.1	Models with $\theta = 30^\circ$ and $150 \times 150 \times 10$ bracing members.....	53
5.1.1	Model 1-1: $t_0 = 40$ mm, $t_p = 25$ mm.....	53
5.1.2	Model 1-2: $t_0 = 20$ mm, $t_p = 25$ mm.....	53
5.1.3	Model 1-3: $t_0 = 40$ mm, $t_p = 35$ mm.....	54
5.1.4	Conclusion of models with $\theta = 30^\circ$ and $150 \times 150 \times 10$ bracing members..	55
5.2	Models with $\theta = 45^\circ$ and $150 \times 150 \times 10$ bracing members.....	57
5.2.1	Model 2-1: $t_0 = 40$ mm, $t_p = 25$ mm.....	57
5.2.2	Model 2-2: $t_0 = 20$ mm, $t_p = 25$ mm.....	57
5.2.3	Model 2-3: $t_0 = 40$ mm, $t_p = 35$ mm.....	58
5.2.4	Conclusion of models with $\theta = 45^\circ$ and $150 \times 150 \times 10$ bracing members..	59
5.3	Models with $\theta = 60^\circ$ and $150 \times 150 \times 10$ bracing members.....	61

5.3.1	Model 3-1: $t_0 = 40$ mm, $t_p = 25$ mm.....	61
5.3.2	Model 3-2: $t_0 = 20$ mm, $t_p = 25$ mm.....	61
5.3.3	Conclusion of models with $\theta = 60^\circ$ and $150 \times 150 \times 10$ bracing members..	62
5.4	Models with $\theta = 30^\circ$ and $250 \times 150 \times 10$ bracing members.....	64
5.4.1	Model 4-1: $t_0 = 40$ mm, $t_p = 25$ mm.....	64
5.4.2	Model 4-2: $t_0 = 20$ mm, $t_p = 25$ mm.....	64
5.4.3	Model 4-3: $t_0 = 40$ mm, $t_p = 35$ mm.....	65
5.4.4	Conclusion of models with $\theta = 30^\circ$ and $250 \times 150 \times 10$ bracing members..	66
5.5	Models with $\theta = 45^\circ$ and $250 \times 150 \times 10$ bracing members.....	68
5.5.1	Model 5-1: $t_0 = 40$ mm, $t_p = 25$ mm.....	68
5.5.2	Model 5-2: $t_0 = 20$ mm, $t_p = 25$ mm.....	68
5.5.3	Conclusion of models with $\theta = 45^\circ$ and $250 \times 150 \times 10$ bracing members..	69
5.6	Models with $\theta = 60^\circ$ and $250 \times 150 \times 10$ bracing members.....	71
5.6.1	Model 6-1: $t_0 = 40$ mm, $t_p = 25$ mm.....	71
5.6.2	Model 6-1: $t_0 = 20$ mm, $t_p = 25$ mm.....	71
5.6.3	Conclusion of models with $\theta = 60^\circ$ and $250 \times 150 \times 10$ bracing members..	72
5.7	Comparison of brace inclination angles.....	74
5.8	Comparison with EN 1993-1-8.....	77
6	Conclusions.....	80
6.1	Recommendations for future studies.....	83
	References.....	84
	Appendix.....	88

Symbols

a	[mm]	is the throat thickness of the fillet weld
b_0	[mm]	is the width of the chord cross-section
b_1	[mm]	is the width of the tension bracing member cross-section
b_2	[mm]	is the width of the compression bracing member cross-section
f_{eu}	[MPa]	is the strength of the electrode material
f_u	[MPa]	is the ultimate strength of the steel
$f_{vw,d}$	[MPa]	is the design shear strength of the weld
f_y	[MPa]	is the yield strength of the steel
h_0	[mm]	is the height of the chord cross-section
h_1	[mm]	is the height of the tension bracing member cross-section
h_2	[mm]	is the height of the compression bracing member cross-section
l	[-]	is the length of the weld
t	[mm]	is the thickness of the rectangular hollow section
t_0	[mm]	is the thickness of the chord cross-section
t_1	[mm]	is the thickness of the tension bracing member cross-section
t_2	[mm]	is the thickness of the compression bracing member cross-section
E	[MPa]	is the modulus of elasticity
$F_{w,Ed}$	[kN/m]	is the design value of the weld force per unit length
$F_{w,Rd}$	[kN/m]	is the design weld resistance per unit length
$F_{w,Rd,j}$	[kN]	is the design weld resistance in the joint
N_0	[kN]	is the normal force applied to the chord
N_1	[kN]	is the normal force applied to the tension bracing member
N_2	[kN]	is the normal force applied to the compression bracing member
P_0	[-]	is the “dead load” in RIKS analysis
P_{ref}	[-]	is the reference load vector in RIKS analysis
β_w	[-]	is the correlation factor for fillet welds
γ_{M0}	[-]	is the partial safety factor for resistance of cross-sections
γ_{M2}	[-]	is the partial safety factor for resistance of cross-sections in tension to fracture
γ_{M5}	[-]	is the partial safety factor for resistance of joints in hollow section lattice girder
ε	[-]	is the nominal strain

ε_{true}	[-]	is the true strain
θ_1	[°]	is the inclination angle of the tension bracing member
θ_2	[°]	is the inclination angle of the compression bracing member
λ	[-]	is the load proportionality factor in RIKS analysis
λ_{ov}	[-]	is the overlap ratio of the joint
ν	[-]	is the Poisson's ratio of the material
σ	[MPa]	is the nominal stress
σ_{true}	[MPa]	is the true stress

List of abbreviations

FE	finite element
RHS	rectangular hollow section
CLD	compression load-displacement (curve)
TLD	tension load –displacement (curve)

1 Introduction

1.1 Background of the project

The aim of this thesis was to investigate a novel K-joint, which is used in a single span WQ truss. The letter W in the abbreviation “WQ” stands for *welded* and the letter Q refers to the shape of the cross-section of the WQ edge beam. Failure mechanisms and critical aspects are studied by Finite Element (FE) modelling with steel grades S460 and S550.

This thesis is a part of the WQ truss research, which aims at developing basis for designing the whole truss so that it is both economical and efficient. Earlier researches include, among others, the study of overlapping joints with lower steel grades of S355 and S420 (Jurmu 2011), but the use of high strength steels S460 and S550 is expected to lead to lighter and more economical solutions.

1.2 Truss

The studied joint is often used as a part of the WQ truss. As seen in Figure 1, WQ truss consists of a WQ beam as an upper chord, rectangular hollow section (RHS) members as bracing members, and steel plate as the bottom chord. The cross-section of the WQ truss is shown in Figure 2. WQ trusses are used for instance as floor carriers in shopping malls. Loading for this type of truss comes usually from hollow core panels, surface concrete and imposed load of $5 - 10 \text{ kN/m}^2$. In this study, permanent and imposed loads are summed and simultaneously applied on the top chord of the truss, as seen in Figure 3. Only vertical loads were considered in this study. WQ trusses give good flexibility for HVAC installations compared to normal steel beams.

WQ beam is a beam with a box-type cross-section shown in Figure 4. The beam is used to support intermediate floors and ceilings made either of hollow-core slabs or thin-shell slabs. The height of the beam is usually defined by the height of the hollow-core slab. The width of the upper chord is chosen according to structural requirements. WQ centre beams are symmetric profiles that support slabs on both sides of the beam. WQ edge beams are asymmetric profiles supporting slabs only on one side of the beam. (Rautaruukki Oyj 2009)

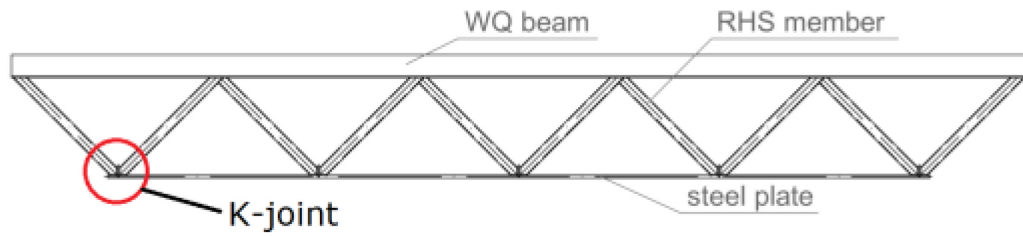


Figure 1: WQ truss.

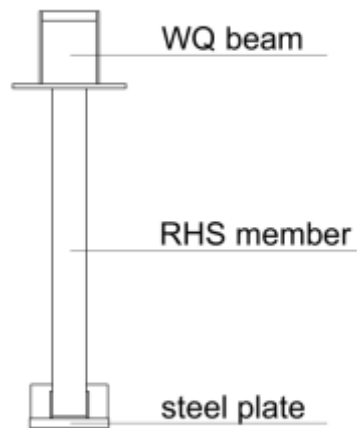


Figure 2: Cross-section of the truss.

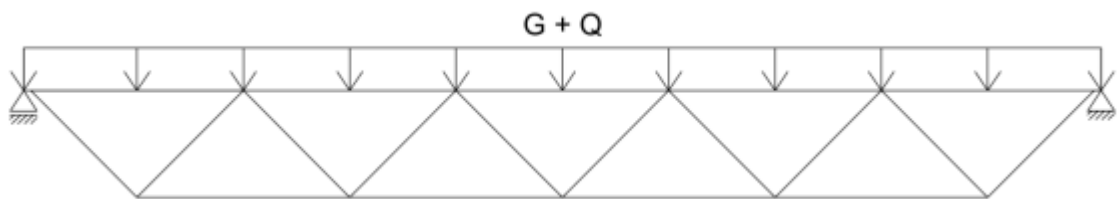


Figure 3: Loads on the truss.

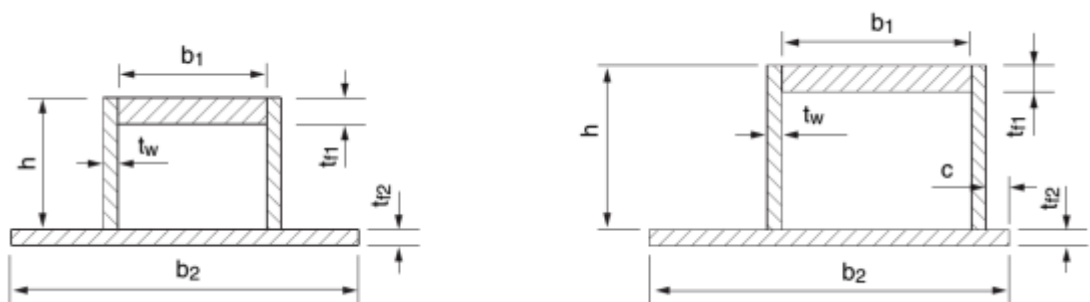


Figure 4: WQ centre beam (on the left) and WQ edge beam. (Alternated from Ongelin & Valkonen 2010)

1.3 Joint

A novel K-joint consisting of a steel plate as the bottom chord, and RHS tubes for bracing members (Figure 5) is studied. To strengthen the joint, a division plate is used between bracing members. No clear rules for designing this type of joint have been established. The joint is located close to the edge of the bottom chord (Figure 6), as that is the place where the largest axial forces for bracing members are located in the truss.

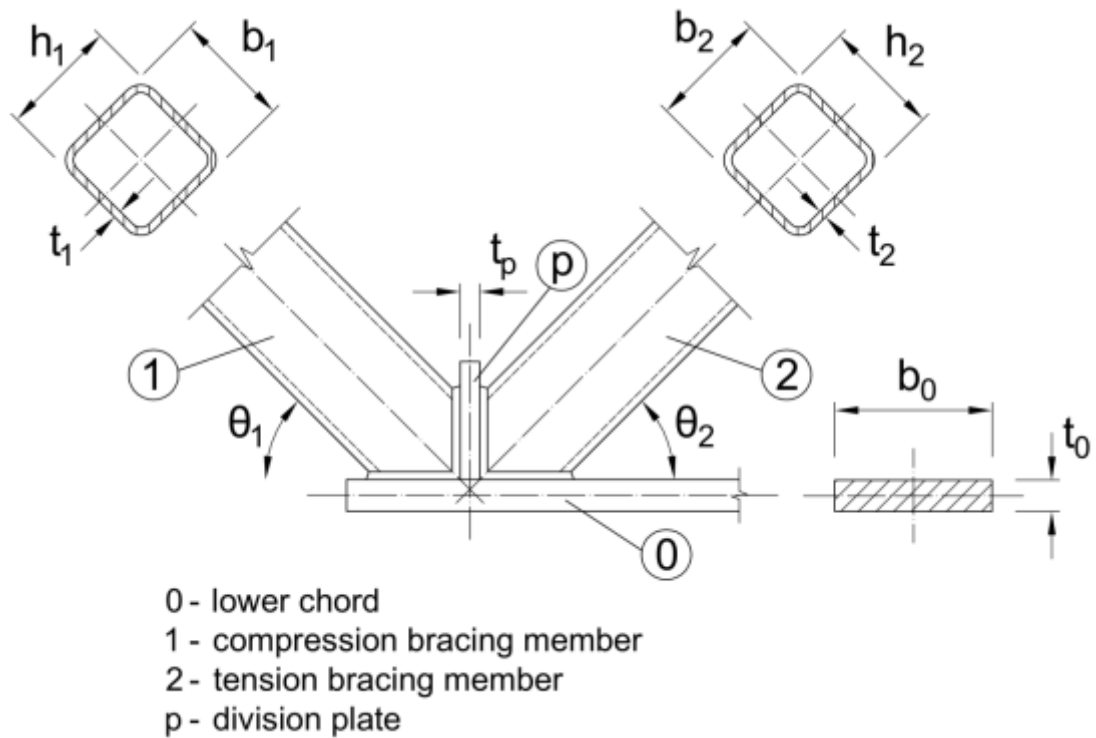


Figure 5: Studied K-joint.

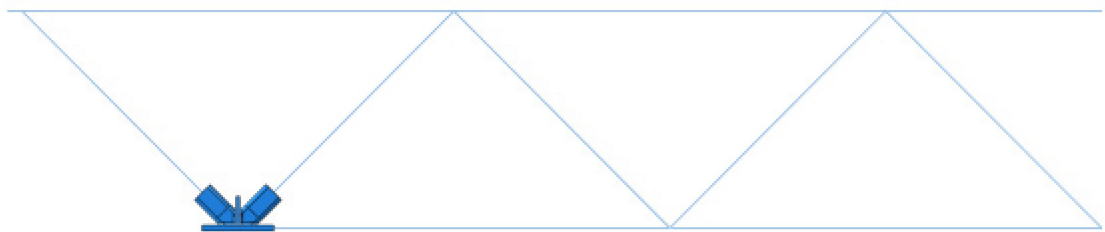


Figure 6: Joint location in the truss.

1.4 Methods

The truss was pre-dimensioned using an Excel-sheet provided by Finnmap Consulting Oy. The equations used in pre-dimensioning sheet are based on the joint where the steel plate is used as a bottom chord (Jurmu 2011). An objective of the pre-dimensioning was to confirm that the geometry from Jurmu's thesis (2011) can also be used with higher steel grades in this study, making then two studies easily comparable with each other. Pre-dimensioning was done to ensure that the WQ beam does not act as a single beam, carrying the rest of the truss as a load.

Finite element (FE) analysis was performed to study the effects of different steel grades and geometrical properties on this type of joint. FE models were created with a FE software Abaqus/CAE version 6.12 and the FE analysis was performed with Abaqus/Standard version 6.12.

The numerical analysis was executed according to the requirements for documentation of the numerical analysis according to the Recommended Practice DNV-RP-C208 (2013).

1.5 Outline of the thesis

Chapter 2 introduces the literature review. First, the WQ beam and WQ truss are introduced. Second, the properties of high strength steel are explained. Third, the welded truss joint is explained. This part concentrates on different K-type joints and possible failure types that may occur in these joints.

Chapter 3 concentrates on FE modelling aspects of the joint. The geometrical model used in FE analysis will be shown. Also, element types, mesh densities, material properties, and boundary conditions are discussed in this chapter.

Chapter 4 discusses about the validation of the model and analysis of the results. The FE model is validated by comparing the results of the present model to the results received by Jurmu (2011). Additionally, a convergence test is made to define a sufficient mesh density. Different material models are also compared and failure types defined. So far, no full-scale test results of the joint are available.

In Chapter 5, the parametric analysis is carried out to study the effect of model variations on results. Different phenomena occurring in analysis are discussed here.

Finally, Chapter 6 introduces conclusions and recommendations for the design of the joint studied giving recommendations for further research topics of the joint.

2 Literature review

2.1 High-strength steel

In this thesis, high strength steel grades are considered to be grades S460 and higher. There are many motives for using high strength steels in construction. For instance, it is possible to reduce the material thickness of the structure therefore reducing the self-weight of the structure, giving higher imposed load capacity. Lower production weights also result in lower handling costs. Additionally, the environmental issues are addressed by lower weight resulting in lower fuel consumption and exhaust emissions when transporting constructions. (Sperle 1997.)

The effects of high strength steels on reduction of wall thickness and weight are also pointed out by Sedlacek and Müller in their studies (2001). Figure 7 shows that reduction of thickness and weight of structures can be achieved when using higher grade steels. According to the figure, thickness and weight can be reduced by nearly half to achieve the same structural capacity when increasing steel grade from S355 to S550.

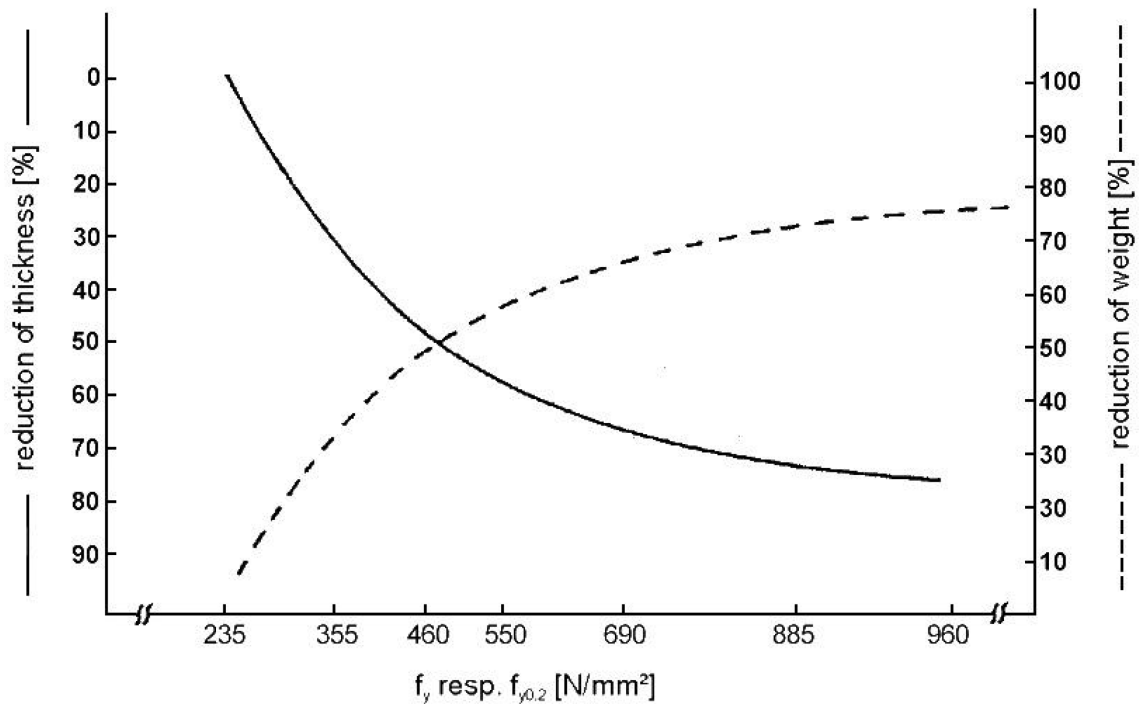


Figure 7: Reduction of wall thickness and weight with increasing strength of steel when the structural capacity is unchanged. (Sedlacek & Müller 2001)

According to Sedlacek and Müller (2001), for steel grades up to S460, a certain minimum ductility of material is assumed to be available in the design rules, therefore

- local restraints due to deformations are neglected, and hinged connections are assumed instead,
 - residual stresses due to fabrication and welding are neglected,
 - stress concentration factors are neglected, linear mean stress distributions are used,
 - simplified plastic distributions of stresses are used, forces in connections are assumed to be equally distributed
 - unlimited plastic rotation capacity is assumed in “plastic hinges”
- (Sedlacek & Müller 2001.)

Due to yielding resulting from a relatively large yielding plateau and strain hardening of steel grades S235 to S460, the phenomena listed are considered not to have effects on the ultimate limit state behaviour of structural components. Sedlacek and Müller (2001) concluded in their studies that due to sensitivities to flaws for steel grades higher than S460, it would be appropriate to use strain oriented design.

As shown in Figure 8, the strain ϵ associated with the tensile strength f is smaller the higher the strength f is. Therefore, high strength steels are considered to be more sensitive than ordinary steels, when high local ductility of the material is required in structural details.

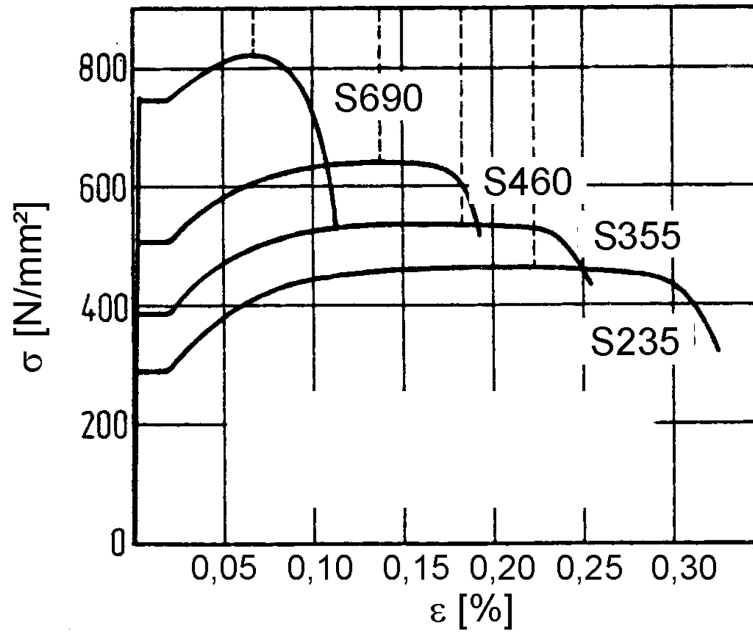


Figure 8: Load-deflection lines for different steel grades. (Sedlacek and Müller 2001)

Before the year 2007, the European unified technical design rules for steel structures in Eurocode 3 were applicable to steel grades S235 to S460. Then, the “Eurocode 3. Design of steel structures. Part 1-12: Additional rules for the extension of EN 1993 up to steel grades S700” was published, giving additional rules to EN 1993-1-1 to EN 1993-1-11, and additional rules to application parts of EN 1993-2 to EN 1993-6. These rules are valid for steel grades greater than S460 up to S700. In these rules for higher strength steel, lower ductility requirements are required compared to steel grades from S235 up to S460. Ductility requirements are expressed in terms of limits for:

- the ratio f_u / f_y of the specified minimum ultimate tensile strength f_u to the specified minimum yield strength f_y ;
- the elongation at failure
- the ultimate strain ϵ_u where ϵ_u corresponds to the ultimate strength f_u .

Table 1 shows the recommended minimum values for steel grades S460 and S550. It can be seen that lower ductility values are accepted for steel grade S550.

Table 1: Recommended ductility requirements for steel grades S460 and S550.

	<i>S460</i>	<i>S550</i>
f_u / f_y	1.10	1.05
<i>elongation at failure</i>	15 %	10 %
ϵ_u	$15f_y/E$	$15f_y/E$
<i>E</i> is the modulus of elasticity of steel		

According to standard SFS-EN 1993-1-5 Annex C, the following material models can be used in FE modelling (Figure 9):

- a) elastic-plastic without strain hardening;
- b) elastic-plastic with a nominal plateau slope;
- c) elastic-plastic with linear strain hardening;
- d) true stress-strain curve modified from the test results.

The true strain ϵ_{true} and true stress σ_{true} can be obtained as follows (SFS-EN 1993-1-5 2007):

$$\epsilon_{true} = \ln(1 + \epsilon) \quad (2)$$

where ϵ_{true} is the true strain [-]
 ϵ is the nominal strain [-]

$$\sigma_{true} = \sigma(1 + \epsilon) \quad (3)$$

where σ_{true} is the true stress [Pa]
 σ is the nominal stress [Pa]

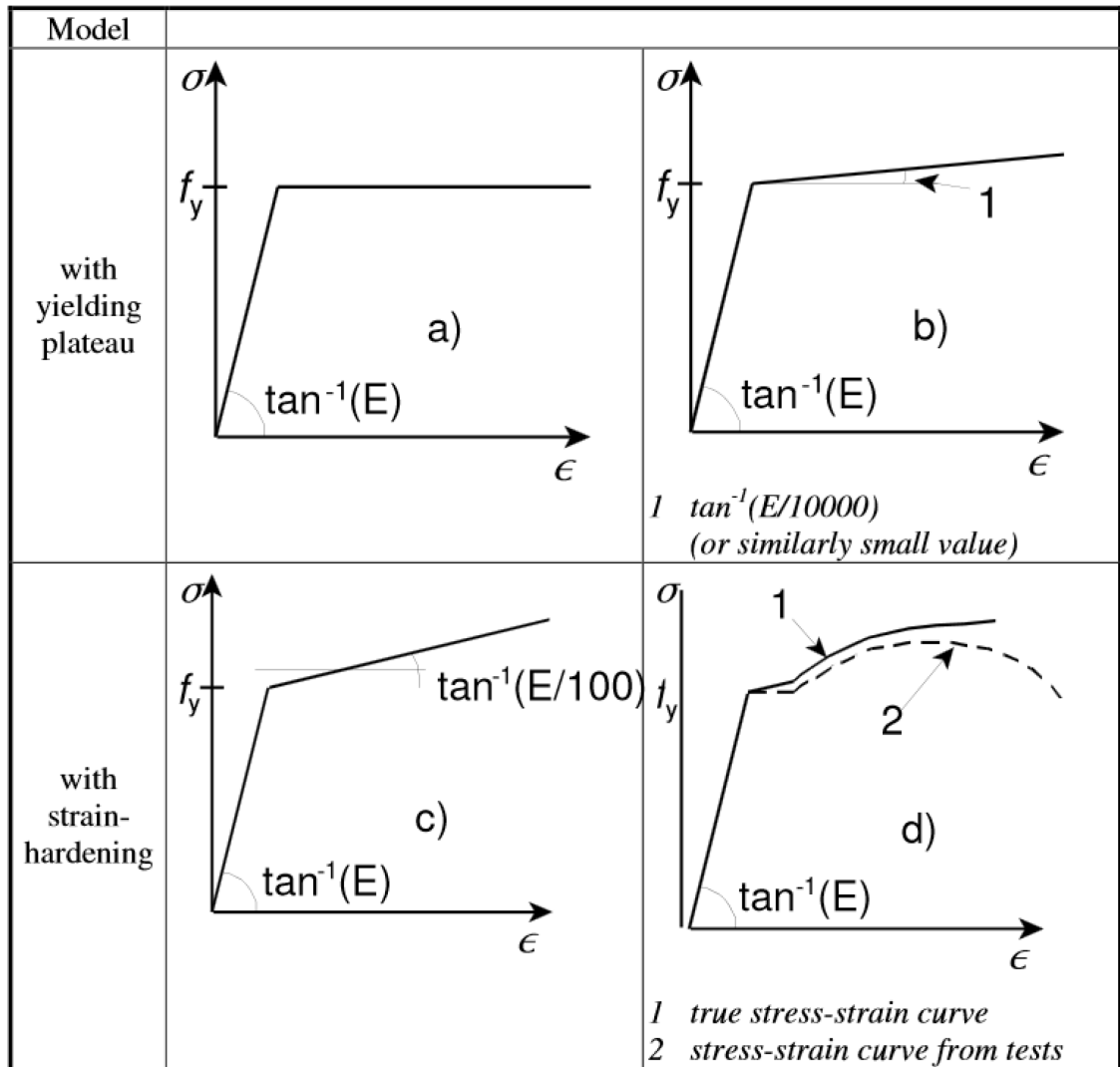


Figure 9: Modelling of material behaviour (SFS-EN 1993-1-5 2007)

In this research, the strain hardening of the material was taken into account. Material models c and d were also compared.

Two general types of stress-strain curves can be distinguished: a sharp-yielding type (Figure 10a) and gradual-yielding type (Figure 10b) (Yu & LaBoube 2010). According to Yu & LaBoube (2010), for gradual-yielding steel, the yield stress is determined by either the offset method (Figure 11a) or the strain-underload method (Figure 11b). The offset method is often used for research work of stainless and alloy steels. When using the offset method, the stress required to produce an offset amount of a certain amount is taken as the yield stress. Generally, this offset amount is specified as 0.2%. The strain-underload method is used for mill tests of sheet or strip carbon and low-alloy steels.

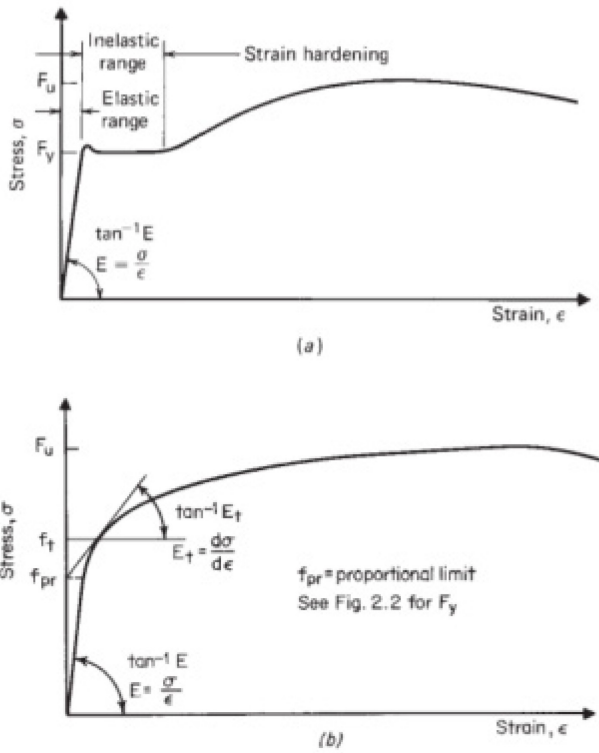


Figure 10: Stress-strain curves of steel: (a) sharp yielding, (b) gradual yielding. (Yu & LaBoube 2010)

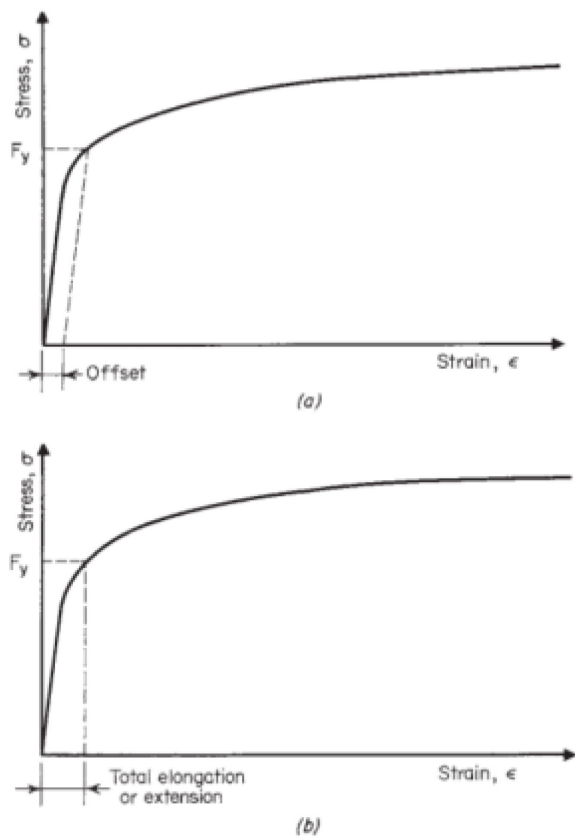


Figure 11: Determination of yield stress for gradual-yielding steel: (a) offset method; (b) strain-underload method. (Yu & LaBoube 2010)

2.2 Truss joint

2.2.1 K-joints

A design guide has been made (Packer et al. 2009) for K-joints where Rectangular Hollow Section (RHS) tubes have been used both as a chord and bracing members. A book of the background to design with structural hollow sections (Wardenier et al. 2010) includes design rules for welded joints between hollow and open sections. Both works present possible failure types for K-joints. The design of welded RHS joints is based on potential limit states shown in Figure 12.

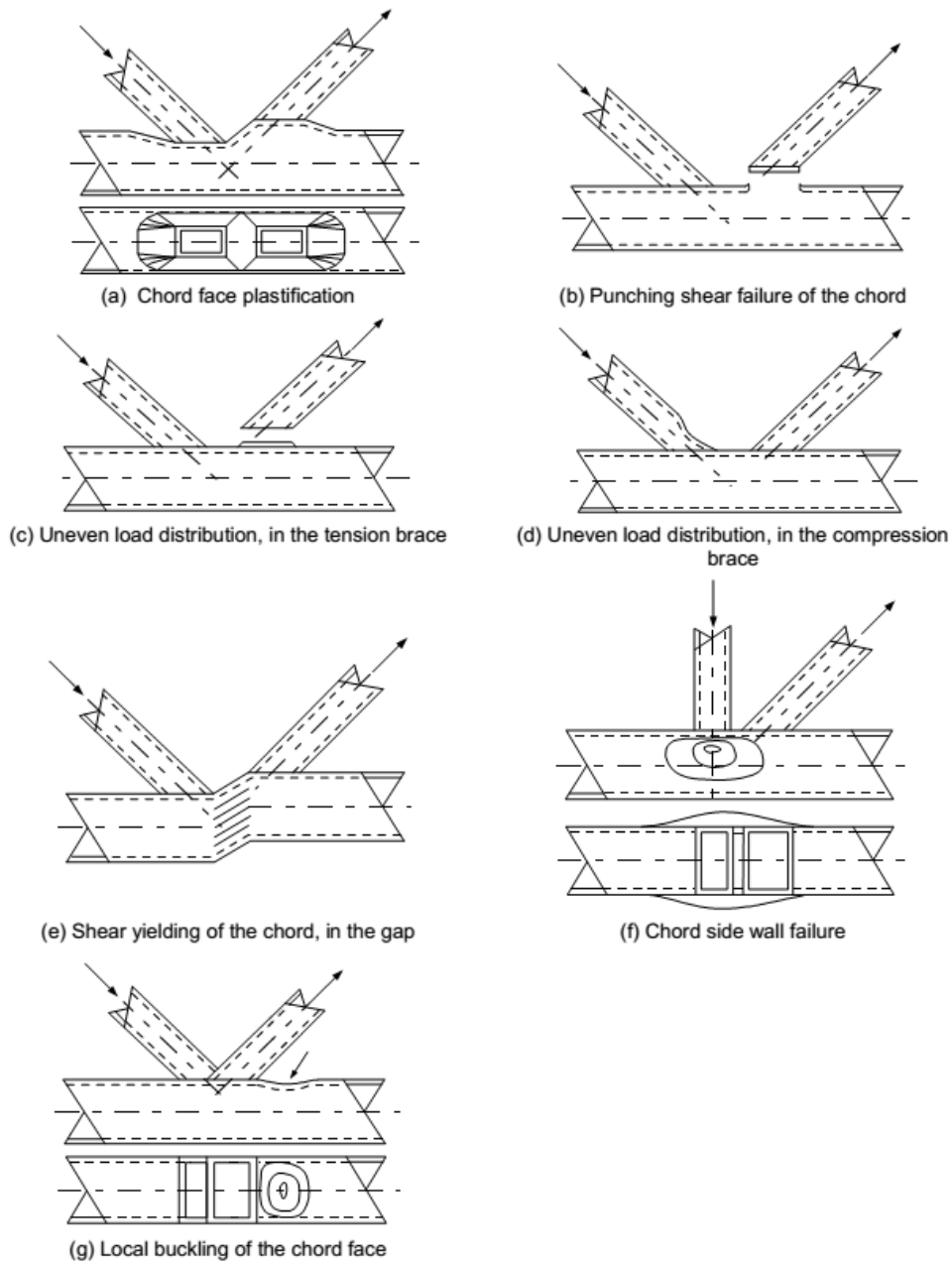


Figure 12: Failure types for K-type RHS truss joints. (Packer et al. 2009)

The following criteria should be checked to define the resistance of overlap joints between hollow sections with $25 \% \leq \lambda_{ov} \leq 100 \%$ (Figure 13):

- (1) Local yielding of the overlapping brace.
- (2) Local chord member yielding at the location of joints, based on interaction between axial load and bending moment.
- (3) Shear of the connection between the brace(s) and the chord. (Packer et al. 2009.)

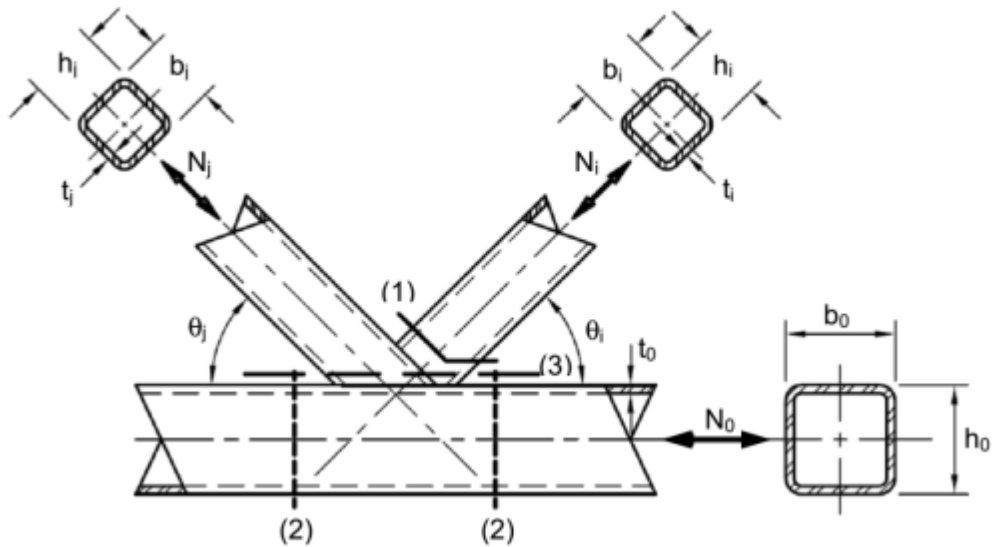


Figure 13: Overlap joint configuration. (Packer et al. 2009)

Overlap ratio λ_{ov} is defined as follows:

$$\lambda_{ov} = \frac{q}{p} \times 100 \% \quad (1)$$

where p and q are defined in Figure 14.

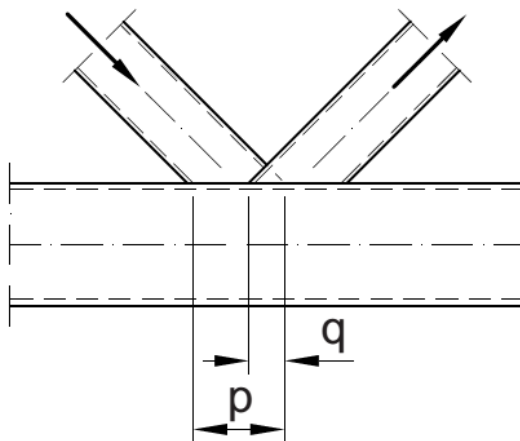


Figure 14: Definition of overlap. (Ongelin & Valkonen 2012)

When Jurmu investigated a K-joint made of steel grades S355 and S420 shown in Figure 23 (a) in his thesis (2011), he found two possible failure types for the joint:

- (1) Local yielding of the overlapping brace.
- (2) Shear of the connection between the brace and the chord.

The latter type was seen when the angle between bracing member and chord was 30° and the thickness of the chord member was 40 mm. In other model variations, the local yielding of the bracing member was observed as the failure type.

Equations for resistance of welded K-joints with RHS or circular members are given in EN 1993-1-8 (2005). Brace resistance for overlap K-joints with different overlap ratios can be defined as shown in Table 2. If the division plate is used to reinforce the joint because of the insufficient overlap, the rules in Table 3 should be used.

According to these equations, the design resistance of overlap joints reinforced with a division plate depends on the member widths, heights, and thicknesses.

Table 2: "Table 7.10: Design axial resistances of welded joints between square or circular hollow section." (EN 1993-1-8)

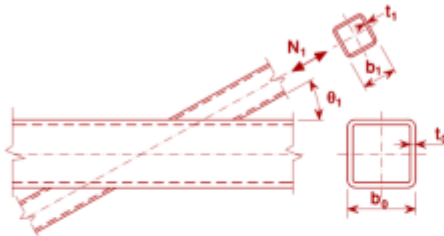
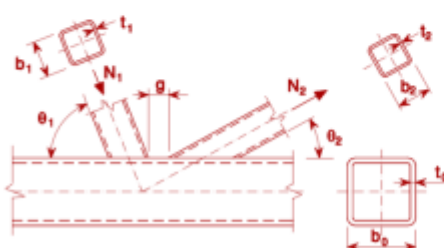
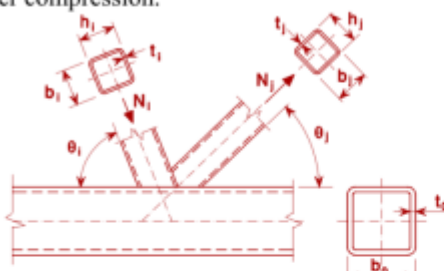
Type of joint	Design resistance [$i = 1$ or 2 , $j =$ overlapped brace]
T, Y and X joints	Chord face failure $\beta \leq 0,85$
	$N_{i,Rd} = \frac{k_n f_{y0} t_0^2}{(1 - \beta) \sin \theta_1} \left(\frac{2\beta}{\sin \theta_1} + 4\sqrt{1 - \beta} \right) / \gamma_{M5}$
K and N gap joints	Chord face failure $\beta \leq 1,0$
	$N_{i,Rd} = \frac{8,9 \gamma^{0,5} k_n f_{y0} t_0^2}{\sin \theta_i} \left(\frac{b_1 + b_2}{2b_0} \right) / \gamma_{M5}$
K and N overlap joints *)	Brace failure $25\% \leq \lambda_{ov} < 50\%$
Member i or member j may be either tension or compression but one should be tension and the other compression.	$N_{i,Rd} = f_{yi} t_i \left(b_{eff} + b_{e,ov} + \frac{\lambda_{ov}}{50} (2h_i - 4t_i) \right) / \gamma_{M5}$
	Brace failure $50\% \leq \lambda_{ov} < 80\%$
	$N_{i,Rd} = f_{yi} t_i [b_{eff} + b_{e,ov} + 2h_i - 4t_i] / \gamma_{M5}$
	Brace failure $\lambda_{ov} \geq 80\%$
	$N_{i,Rd} = f_{yi} t_i [b_i + b_{e,ov} + 2h_i - 4t_i] / \gamma_{M5}$
Parameters b_{eff} , $b_{e,ov}$ and k_n	
$b_{eff} = \frac{10}{b_0/t_0} \frac{f_{y0} t_0}{f_{yi} t_i} b_j \quad \text{but } b_{eff} \leq b_i$	For $n > 0$ (compression):
$b_{e,ov} = \frac{10}{b_j/t_j} \frac{f_{yj} t_j}{f_{yi} t_i} b_i \quad \text{but } b_{e,ov} \leq b_i$	$k_n = 1,3 - \frac{0,4n}{\beta}$
	but $k_n \leq 1,0$
	For $n \leq 0$ (tension):
	$k_n = 1,0$
For circular braces, multiply the above resistances by $\pi/4$, replace b_1 and h_1 by d_1 and replace b_2 and h_2 by d_2 .	
*) Only the overlapping brace member i need be checked. The brace member efficiency (i.e. the design resistance of the joint divided by the design plastic resistance of the brace member) of the overlapped brace member j should be taken as equal to that of the overlapping brace member.	

Table 3: "Table 7.18: Design resistances of reinforced welded K and N joints between RHS or CHS brace members and RHS chords." (EN 1993-1-8)

Type of joint	Design resistance [$i = 1$ or 2]
Reinforced with flange plates to avoid chord face failure, brace failure or punching shear.	
	$l_p \geq 1,5 \left(\frac{h_1}{\sin \theta_1} + g + \frac{h_2}{\sin \theta_2} \right)$ $b_p \geq b_0 - 2t_0$ $t_p \geq 2t_1 \text{ and } 2t_2$ <p>Take $N_{i,Rd}$ as the value of $N_{i,Rd}$ for a K or N joint from Table 7.12, but with t_0 replaced by t_p for chord face failure, brace failure and punching shear only.</p>
Reinforced with a pair of side plates to avoid chord shear failure.	
	$l_p \geq 1,5 \left(\frac{h_1}{\sin \theta_1} + g + \frac{h_2}{\sin \theta_2} \right)$ <p>Take $N_{i,Rd}$ as the value of $N_{i,Rd}$ for a K or N joint from Table 7.12, but with t_0 replaced by $(t_0 + t_p)$ for chord shear failure only.</p>
Reinforced by a division plate between the brace members because of insufficient overlap.	
	$t_p \geq 2t_1 \text{ and } 2t_2$ <p>Take $N_{i,Rd}$ as the value of $N_{i,Rd}$ for a K or N overlap joint from Table 7.12 with $\lambda_{ov} < 80\%$, but with b_j, t_j and f_{yj} replaced by b_p, t_p and f_{yp} in the expression for $b_{e,ov}$ given in Table 7.10.</p>

2.2.2 Design of welds

According to SFS-EN 1993-1-8, the design resistance of a fillet weld can be determined using either the directional method or the simplified method. In the directional method for designing the resistance of the welds, the forces in the weld are divided into components parallel and transverse to the longitudinal axis of the weld and normal and transverse to the plane of its throat (Figure 15.)

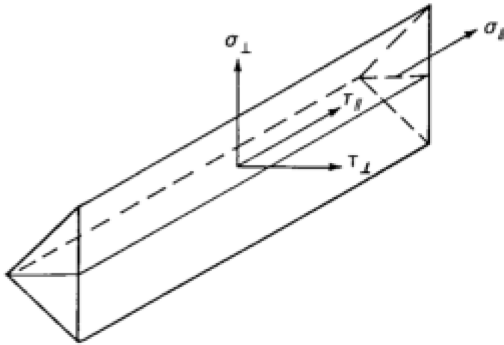


Figure 15: Stresses on the throat section of a fillet weld. (SFS-EN 1993-1-8 2005)

When verifying the design resistance of the weld, the normal stress σ_{\parallel} parallel to the axis is not considered. The reasons for this are discussed by Ballio and Mazzolani (1983). They support the assumption of neglecting σ_{\parallel} with the example of an I-beam. They reason by mentioning that the stress σ_{\parallel} is not really present in the weld, but it is present in the cross-section consisting of the weld and connected parts, when the external load is applied on the beam. The weld just connects parts together, and the seams are loaded with shear stresses τ_{\parallel} , which act against the sliding between flanges and web, therefore representing the stresses due to the connection.

In the directional method, the design resistance of the fillet weld is sufficient if the following are both satisfied:

$$\sqrt{\sigma_{\perp}^2 + 3(\tau_{\perp}^2 + \tau_{\parallel}^2)} \leq \frac{f_u}{\beta_w \cdot \gamma_{M2}} \quad (2)$$

and

$$\sigma_{\perp} \leq 0.9 \frac{f_u}{\gamma_{M2}} \quad (3)$$

where f_u is the nominal ultimate tensile strength of the weaker part joined [MPa]
 β_w is the correlation factor taken from Table 4
 γ_{M2} is the safety factor

Table 4: Correlation factor β_w for fillet welds. (SFS-EN 1993-1-8 2005)

Standard and steel grade			Correlation factor β_w
EN 10025	EN 10210	EN 10219	
S 235 S 235 W	S 235 H	S 235 H	0,8
S 275 S 275 N/NL S 275 M/ML	S 275 H S 275 NH/NLH	S 275 H S 275 NH/NLH S 275 MH/MLH	0,85
S 355 S 355 N/NL S 355 M/ML S 355 W	S 355 H S 355 NH/NLH	S 355 H S 355 NH/NLH S 355 MH/MLH	0,9
S 420 N/NL S 420 M/ML		S 420 MH/MLH	1,0
S 460 N/NL S 460 M/ML S 460 Q/QL/QL1	S 460 NH/NLH	S 460 NH/NLH S 460 MH/MLH	1,0

In the simplified method, the design resistance of a fillet weld can be determined from equations (4 - 6). The design resistance can be assumed adequate, if the resultant of all forces per unit length transmitted by the weld satisfy the following criterion at every point along its unit length:

$$F_{w,Ed} \leq F_{w,Rd} \quad (4)$$

where $F_{w,Ed}$ is the design value of the weld force per unit length [kN/m]
 $F_{w,Rd}$ is the design weld resistance per unit length [kN/m].

Independent of the orientation of the weld throat plane to the applied force, the design resistance per unit length $F_{w,Rd}$ in equation (4) should be determined from:

$$F_{w,Rd} = f_{vw,d} a \quad (5)$$

where $f_{vw,d}$ is the design design shear strength of the weld [MPa]
 a is the throat thickness of the fillet weld [mm].

Figure 16 shows how the effective throat thickness of the fillet weld is defined.

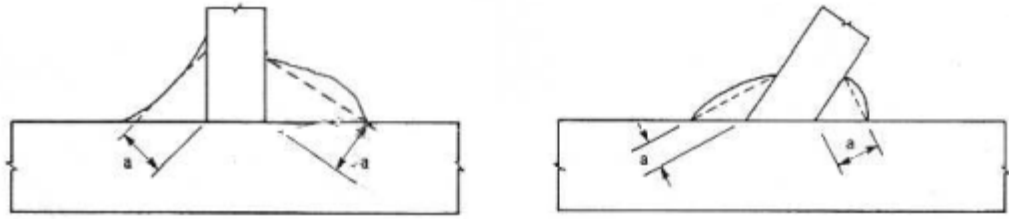


Figure 16: Throat thickness of a fillet weld. (SFS-EN 1993-1-8 2005)

The design shear strength $f_{vw,d}$ of the weld should be determined from:

$$f_{vw,d} = \frac{f_u / \sqrt{3}}{\beta_w \gamma_{M2}} \quad (6)$$

where f_u is the steel strength [MPa].

According to EN 1993-1-8, the correlation factor for steel grade S460 should be taken as $\beta_w = 1.0$. EN 1993-1-12 expands this rule also for steel grades greater than S460 up to S700.

Günther, Hildebrand, et al. (2009) carried out experimental and numerical investigations for the load bearing capacity and safety against brittle fracture at lap joints with longitudinal fillet welds, cruciform joints with transverse fillet welds, and butt joints with partial penetration double-V-groove welds of high strength steels. Steel grades investigated were S460 and S690. Test specimens studied are shown in Figure 17. The design resistance of the steel grade S460 was pointed out to currently be lower compared to steel grade S355 because of the higher β_w value, as shown in Table 5.

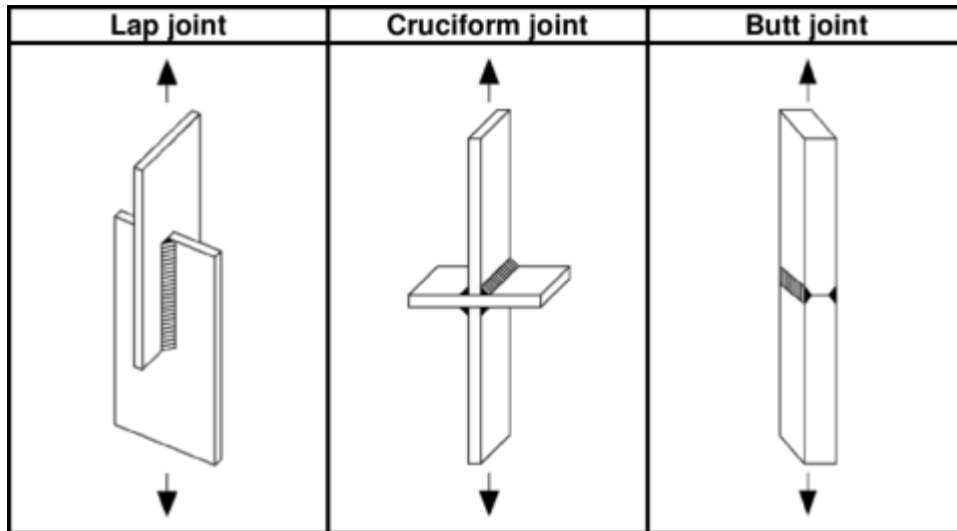


Figure 17: Types of joints of the test specimens. (Günther et al. 2009)

Table 5: Values for the design weld resistance according to EN 1993 in case of fillet welds, $t \leq 40$ mm. (Günther, Hildebrand et al. 2009)

Steel grade		S235 ¹⁾	S355 ¹⁾	S460 ²⁾	S690 ³⁾
f_y	[MPa]	235	355	460	690
f_u	[MPa]	360	510	540	770
β_w	[MPa]	0.8	0.9	1.0	1.0
$f_y/(\beta_w \cdot \gamma_{M2})$	[MPa]	360	453	432	616
EN 10025 [4] ¹⁾ Part 2, ²⁾ Part 3 and 4, ³⁾ Part 6					

β_w values were evaluated for matching conditions, taking into account the minimum partial safety factor for the resistance of the welds $\gamma_{M2} = 1.25$. Matching conditions imply that the nominal strength of the filler metal is the same than as of base material.

The experimentally determined ultimate loads for longitudinal fillet welded lap joints were compared to the theoretical predicted loads for steel grade S460. Compared to existing design specifications in EN 1993-1-8 (2005) the test results showed an increase of 15 % for the load bearing capacity of longitudinal fillet welded lap joints. In the German National Annex DIN EN 1993-1-8/NA the correlation factor has been fixed to $\beta_w = 0.85$ instead of 1.0 for steel grade S460 based on given results. Figure 18 shows the comparison of test results with theoretical predicted loads for longitudinal fillet welded lap joints. The theoretical predicted loads were obtained by using the equations (1) and (2). The evaluation led to $\beta_w = 0.79$ for steel grade S460. For cruciform joints, a similar approach lead to the correlation factor $\beta_w = 0.68$ for steel grade S460, using matching

conditions. Figure 19 shows the comparison for cruciform joints with transverse fillet welds. The proposal of recommendations for correlation factors β_w is shown in Table 6.

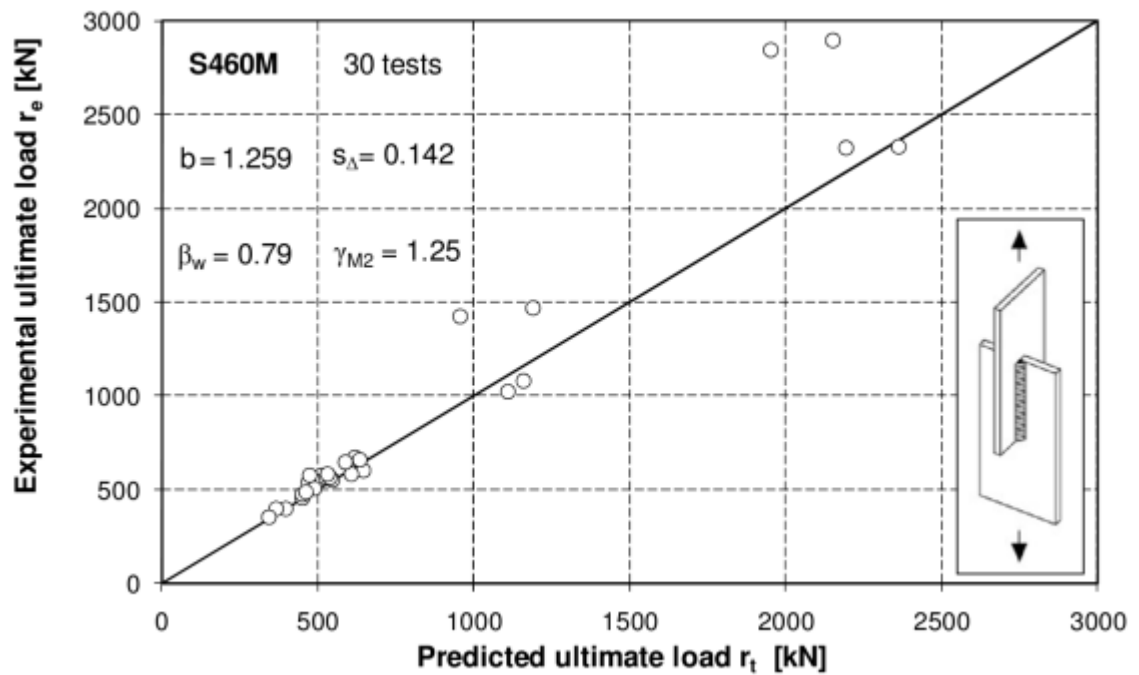


Figure 18: Plot of test results r_e over theoretical predicted results r_t according to equations (1) and (2) for longitudinal fillet welded lap joints and steel grade S460M. (Günther et al. 2009)

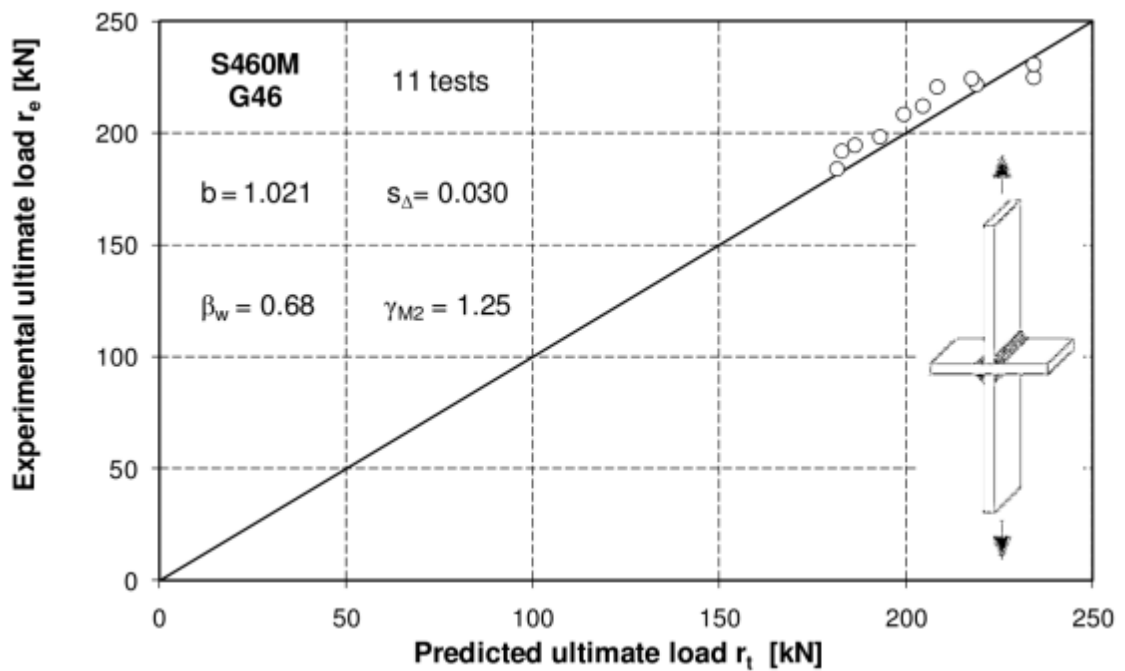


Figure 19: Plot of test results r_e over theoretical predicted results r_t according to equations (1) and (2) for cruciform joints with transverse fillet welds and steel grade S460M. (Günther et al. 2009)

Table 6: Proposal of correlation factors according to Eurocode 3 for high strength steels S460M and S690Q. (Günther, Hildebrand et al. 2009)

Steel grade	S460M	S690Q/QL
	β_w	β_w
Longitudinal fillet welds	0,85	1,2
Transverse fillet welds	0,7	1,0
Partial penetration double V-groove welds (butt joints)	0,85	1,0

Studies show (Björk et al. 2010, Khursid & Mumtaz 2011) have shown that the ductility of joints is increased when under matched filler metal is being used. EN 1993-1-12 allows using under matched electrodes for steels with grades greater than S460 up to S700, meaning that the filler metal is permitted have strength lower than that of the base material. According to EN 1993-1-12, the resistance of such connections should be based on the strength of the filler metal.

Collin and Johansson (2005) studied experimentally welds in high strength steel. Two series of welds were studied: butt welds and fillet welds. The purpose of the study was to develop a design formula covering under matching as well as over matching electrodes. An observation was made that the weld strength was closer to the strength of the stronger material, whether it was the electrode material or the base material. However, a more conservative expression as hypothesis of the weld strength was taken:

$$f_w = \frac{f_u + f_{eu}}{2} \quad (7)$$

where f_w is the weld strength [MPa]
 f_u is the steel strength [MPa]
 f_{eu} is the strength of the electrode material [MPa]

The expression had already been proposed earlier for overmatching electrodes as a conclusion of the IIW international test series (Ligtenberg 1968). Collin and Johansson (2005) state that the formula is valid for both under and overmatching electrodes.

Günther, Hildebrand et al. (2009) conducted tests on lap joints and cruciform joints with different strengths of base metal and filler metal. When matching conditions were chosen, connections made of steel grade S460M showed clearly higher strength than

those made of steel grade S355J2. Joints made of steel grade S690Q had only slightly higher strength compared to joints with steel grade S460M. When the influence of the filler metal strength was investigated, a higher load bearing capacity with higher strength of the filler metal was noticed. Also, the joints with base metal S690 had a lower deformation capacity than joints made of steel grade S460. Cruciform joints with matching conditions showed higher strengths when using steel grade S690Q instead of S460M as base metal.

The minimal throat thickness of the fillet weld assuming that the resistance of the weld is equal to the base material strength can be calculated using the following equation (Ongelin & Valkonen 2012):

$$a \geq 2 \cdot \frac{\beta_w}{\sqrt{2}} \cdot \frac{\gamma_{M2}}{\gamma_{M0}} \cdot \frac{f_y}{f_u} \cdot t \quad (8)$$

where

a	is the minimal throat thickness of the fillet weld [mm]
β_w	is the correlation factor for fillet welds [-]
γ_{M0}	is the partial factor for resistance of cross-sections [-]
γ_{M2}	is the partial factor for resistance of cross-sections in tension to fracture [-]
f_y	is the yield strength of the steel [MPa]
f_u	is the ultimate strength of the steel [MPa]
t	is the thickness of the rectangular hollow section [mm]

2.2.3 Limit state criteria

Khursid and Mumtaz studied the behaviour of load carrying welded joints with different consumables and weld penetration ratios in their thesis (2011). They made 2D non-linear numerical analyses for evaluating the ultimate capacity. The numerical analyses were verified with experimentations. They observed the ultimate strength capacities received by numerical analysis, testing and standards being close to each other, when fully penetrated joints with different filler metals were used. In fully penetrated weld joints the weld metal penetrates through the full thickness of the base metal. The tested cruciform joint with the weld is shown in Figure 20.

In their studies, it was assumed that the ultimate load capacity using matched consumables was reached when the tensile part yielded through the whole cross-section (Figure 21).

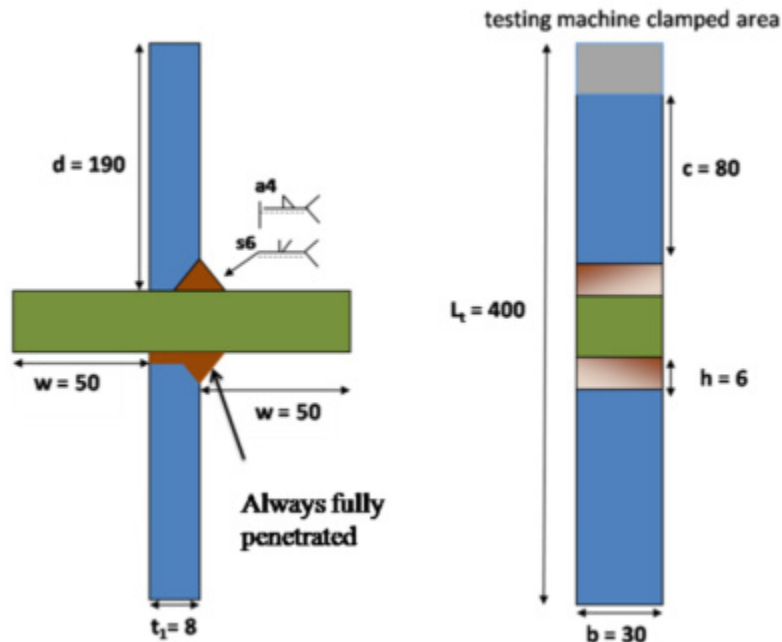


Figure 20: Front and side views of cruciform test specimen, dimensions are in mm. (Khursid and Mumtaz 2011)

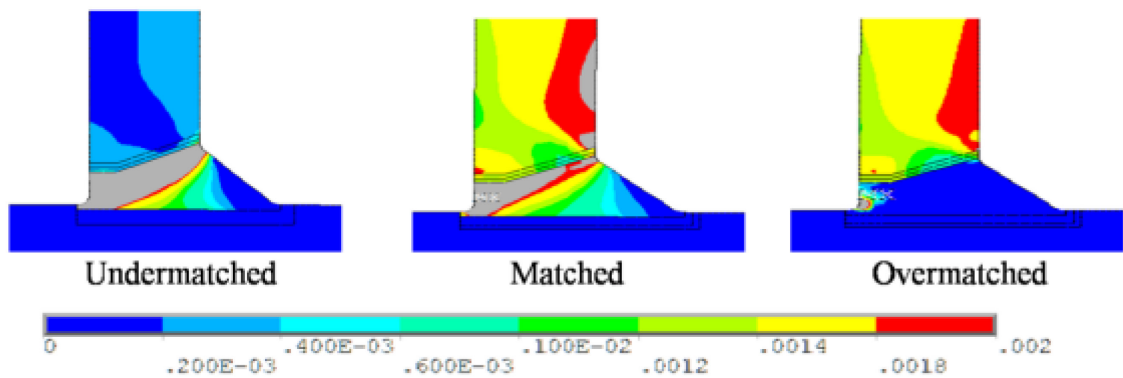


Figure 21: Plastic strain plots of full penetration joints with different consumables. (Khursid and Mumtaz 2011)

Several studies about K-joints (Crockett 1994; Dexter & Lee 1999; van der Vegte et al. 2002; Wardenier 1982) present the peak load of the load-deformation curve as one possible failure criterion for K-joints.

SFS-EN 1993-1-5 Annex C (2006) states that a limiting value of the principal membrane strain should be attained for the ultimate limit state criteria for regions

subjective to tensile stresses. A value of 5 % is recommended. For structures susceptible to buckling, the maximum load should be used as the ultimate state criterion.

Hendy et al. (2010) have given a background to the development of the National Annex to BS EN 1993-1-5. They justify using 5 % as the maximum principal strain by showing that for steel grades S235 and S355 the bi-linear model and the true stress and true strain model in BR EN 1993-1-5 fit the testing curves well up to a strain of 5 %. At higher strain values they become non-conservative. Therefore, the 5 % principal strain limit is taken for regions subjected to tensile stresses, regardless of the stress-strain model used. According to this justification, it is necessary to compare the material model d) from Figure 9 with the stress-strain curve from the tests. In this way, it can be defined whether or not the 5 % plastic strain limit is still applicable for higher steel grades.

The 5 % strain limit is considered to be applicable also for steel grades S460 and S550, because SFS-EN 1993-1-12 (2007) states that ‘the standard [EN 1993-1-5] is applicable to steels with grades greater than S460 up to S700 without further additional rules.’

The background documents for EN 1993-1-5 (Johansson et al. 2007) discuss the background of the rules, their reliability basis, and explanations on how the rules are to be used. It is mentioned that the rules in EN 1993-1-5 Annex C are the first attempt to codify the non linear FE modelling for design purposes. Therefore, the rules are not as developed as the rules found in the main text of the standard. This is why it is essential to validate FE analysis results with full scale testing.

Det Norske Veritas (DNV) (2013) published the recommended practice for establishing the structural resistance by use of non-linear FE methods. They imply that the recommendations are to be used in cases where the characteristic resistance is not directly covered by codes or standards. Table 7 gives recommended values for critical local maximum principal plastic strain. For the critical local value of the maximum principal plastic strain under uniaxial stress states, DNV defined a value of 9 % for steel grade S460. Steels with higher strengths were not studied.

Table 7: Critical local maximum principal plastic strain for uniaxial stress states. (DNV 2013)

	Maximum principal plastic critical strain			
	S235	S355	S420	S460
Critical local yield strain	0.15	0.12	0.10	0.09

Figure 22 shows the curve from the data of the steel grade and respective critical local yield strain from Table 7. It can be seen that the relation between steel grade and critical strain is nearly linear. For comparison, extrapolating the curve to include steel grade S550 gives 6.5 % for the local critical value of the maximum principal plastic strain. However, such extrapolation may not give reliable results and should not be used in structural design.

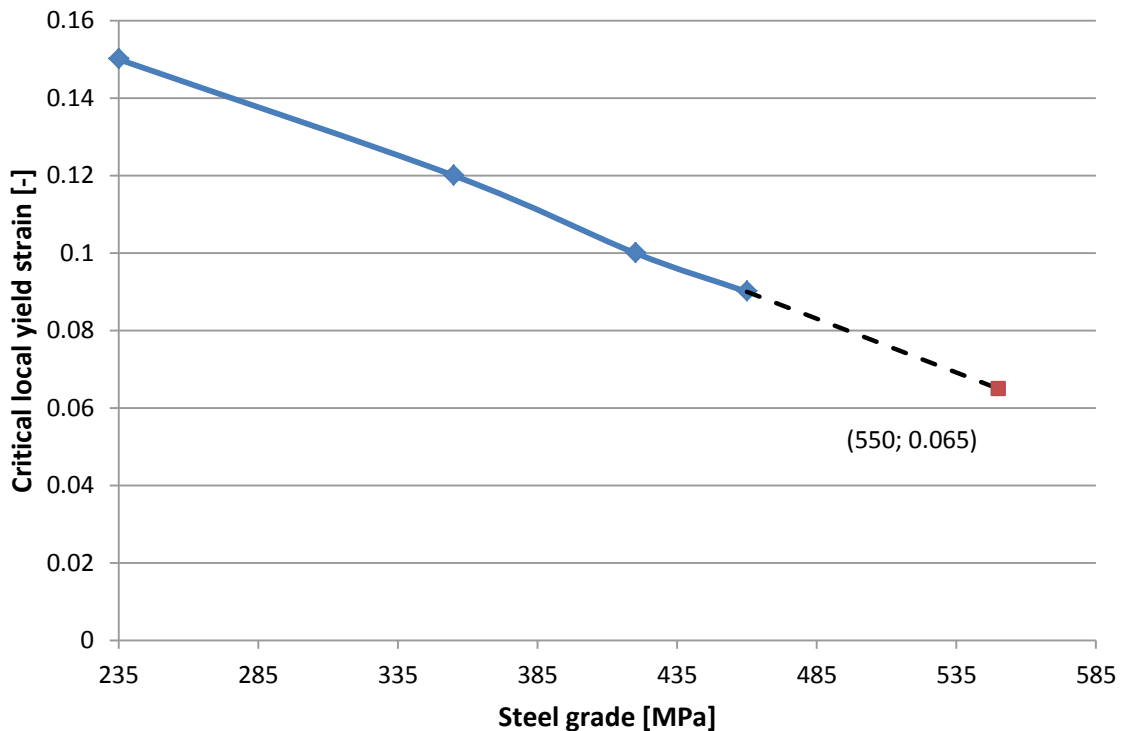


Figure 22: Critical local yield strains for different steel grades. (Based on data from DNV 2013)

Both SFS-EN 1993-1-5 and DNV base their recommendations on plate structures, and possible behaviour and interactions in the joint are not considered. The size of the local region for extracting the maximum plastic strain value was not defined in either source.

As a criterion a strain limit of 20 % has been proposed by Dexter & Lee (1999) and van der Vegte et al. (2002) in their studies about K-joints. In both studies, K-joints consist of circular hollow section (CHS) tubes. According to the criterion, cracking was assumed to have occurred when 20 % tensile strain was attained at any location of the joint. Dexter & Lee noticed in their study (1999) that the failure of overlapped joints was generally associated with high plastic strains visible in the joint. van Vegte et al. (2002) also observed large tensile strains in the chord wall at the weld toe of the tension brace. However, van Vegte et al. mention that the value of 20 % is arbitrary and is meant to enable a comparison among the different K-joints. In conclusion, it can be said that no clear theoretical base for defining the plastic strain limit for this type of joint made of high-strength steel has been established.

2.3 Previous studies

Jurmu (2011) studied the same type of joint with steel grades S355 and S420. Jurmu mentions that the limiting factor for the joint capacity, when a hollow section member is used as a lower chord, is the failure of the chord side wall. To avoid this failure criterion for the joint, a steel plate is used as the chord. According to his study, in models with the bracing angle of 45 or 60 degrees, the resistance of the tensile bracing member was higher when the thickness of the lower chord was increased. Jurmu also noticed that the utilisation ratio of the bracing member at the failure point of the joint was at its highest when a thicker division plate was used.

3 Finite element modelling

This part consists of modelling and analyzing the numerical model using a commercial software Abaqus/CAE and Abaqus/Standard versions 6.12. The geometry of the truss was modelled similarly to Jurmu's FE model (2011).

3.1 Geometrical model

The studied joint area was modelled with solid elements, as shown in Figure 23 (a). Welds were modelled as rigidly attached to bracing members, as shown in Figure 23 (b). Table 8 shows the throat thickness of welds for various steel grades, which are calculated based on equation (8) by assuming that the welds have the same yielding strength as the base material. In each variation of the model, only one bracing member is first modelled, and it is then mirrored to the other side of the stiffening plate to complete the joint assembly. To account for global effects of the truss on the behaviours of joint, the truss surrounding the joint was also modelled. In this way, for instance, bracing member rotations caused by bending of the truss can be taken into account in joint analysis. The rest of the truss was modelled with beam elements, as demonstrated in the Figure 24 which shows the completed assembly of the truss.

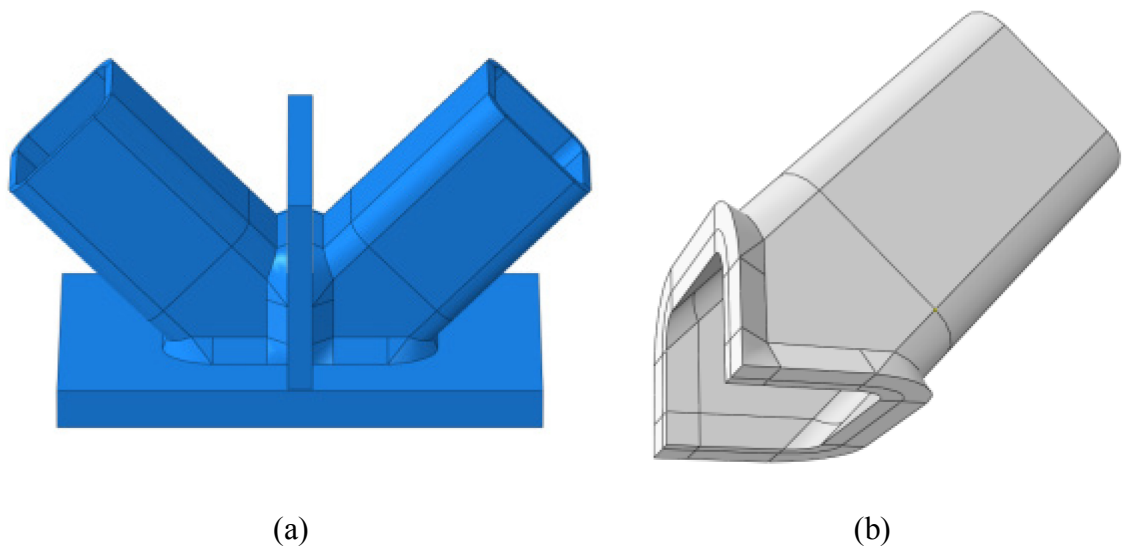


Figure 23: (a) FE model of the joint, (b) Bracing member of the joint with attached welds.

Table 8: Minimal throat thickness for steel grades S460 and S550.

Steel grade	chord thickness [mm]	bracing thickness [mm]	a [mm]
S460	40	10	14.3
S550	40	10	15.2
taken value			15.5

In order to simplify the creation of multiple variations of the FE model, only one throat thickness was used in FE modelling. The throat thickness of the weld was chosen to be 15.5 mm, which is motivated by the fact that it would be on the safe side for both steel grades.

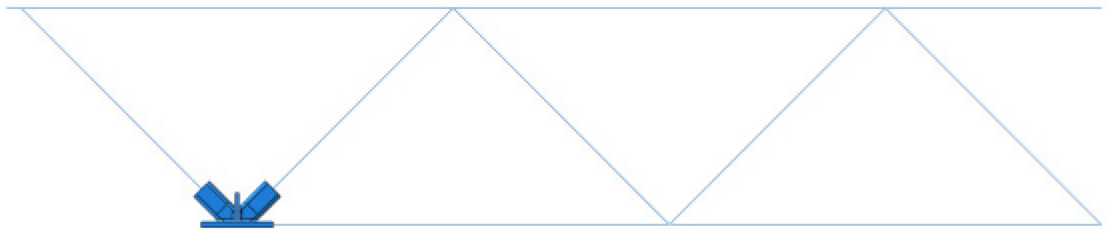


Figure 24: Completed truss assembly.

3.2 FE Meshes

Hexahedral elements provide solutions of equivalent accuracy with tetrahedral elements at less computational cost (Dassault Systèmes 2012). Therefore, these elements should be used if possible. Curved weld regions, however, are too complex geometries to mesh with hexahedral elements without resulting in numerous distorted elements. Both first- and second-order hexahedral elements become less accurate when their initial shape is distorted and therefore may lead to unreliable results.

Second-order elements capture stress concentrations more effectively, and they can be used to model a curved surface with fewer elements. Computational costs can be cut by using reduced-integration elements, which use lower-order integration to form the element stiffness. (Dassault Systèmes 2012)

First-order tetrahedral elements should be avoided in stress analysis problems whenever possible. They are considered to be poor elements because of their poor convergence rate; they typically require very fine meshes to produce reliable results. Therefore, these elements should only be used as fillers far from regions with stress concentrations, or

from areas where accurate results are needed (Dassault Systèmes 2012.) As seen in previous studies (Khursid and Mumtaz 2011, Jurmu 2011), in this type of joints the stress concentrations are near the welds or other areas with a geometrical discontinuity.

Curved weld regions were meshed with second-order tetrahedral elements C3D10I. These elements are suitable for modelling metal plasticity (Dassault Systèmes 2012). Before the analysis, the model was checked for distorted elements. If there were distorted elements in the regions of expected high stress concentrations, the hexahedral elements were replaced with tetrahedral elements. This phenomenon was observed in models with bracing angles 30° and 60° , where some straight weld regions were finally meshed with C3D10I elements to avoid distorted brick elements. For better connectivity between different element types, second-order brick elements C3D20R (Figure 25) were chosen instead of first-order elements to mesh the rest of the welds and the bracing tube near the areas meshed with second-order tetrahedral elements. The rest of the areas in bracing members were meshed computationally less costly with first-order brick elements C3D8R. This was done assuming that there are no critical stress concentrations on areas far from welds. The element types for the bracing member are shown in Figure 26, where second-order tetrahedral elements are marked in white. Second order (C3D20R) and first order (C3D8R) brick elements with reduced integration are marked in red and green, respectively.

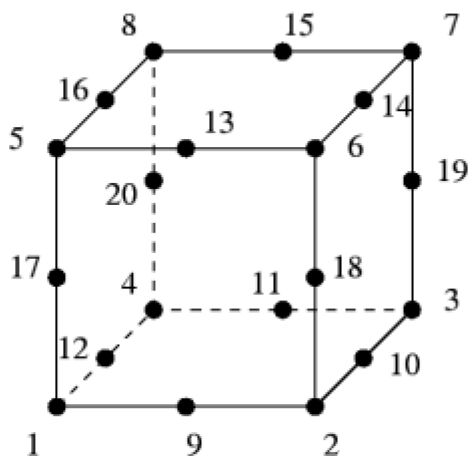


Figure 25: 20-node brick element (Dhondt 2011)

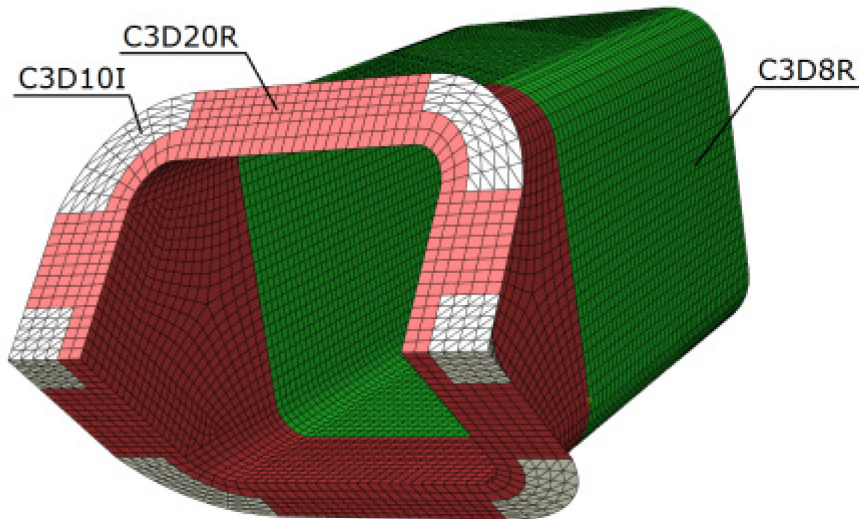


Figure 26: Element types for bracing member.

For the compressed bracing member, it is important to define the surface-to-surface contact interaction at the interfaces when bracing member comes into contact with the division plate and lower chord, respectively. This is to ensure that bracing members cannot penetrate into the stiffening plate or lower chord, which can lead to unreliable results. The areas in question are marked in red in Figure 27.

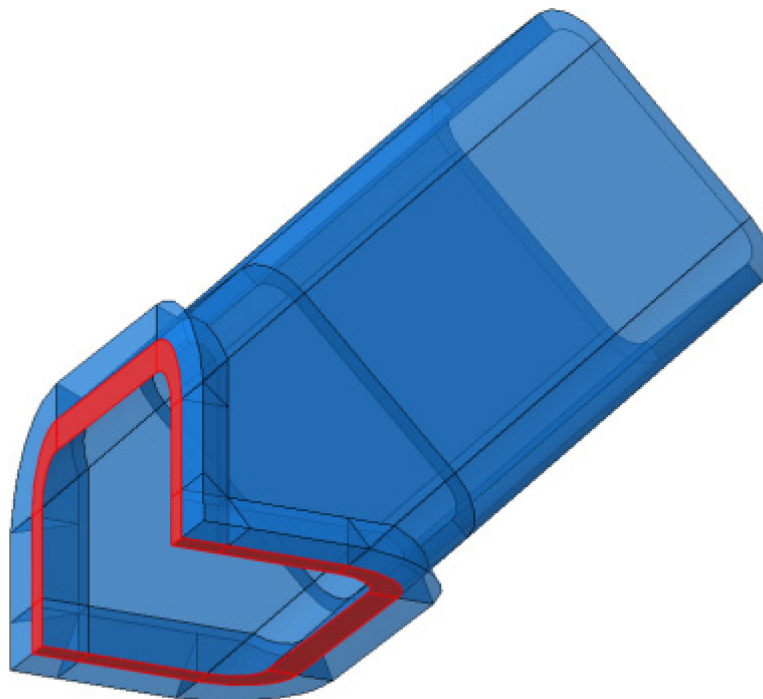


Figure 27: Areas requiring contact interaction properties.

For the division plate and bottom chord of the joint, second order brick elements C3D20R were chosen. Because the numerical analysis model was created using separate parts, links were needed to be created between each connected part. The division plate, bottom chord plate and welds were attached using Tie-command, which connects parts as they would have been modelled as one part. The bracing member part consisted of the RHS tube and welds, so that no separate connection needed to be created between the welds and bracing member. This made it faster to create different variations of the model. Beam elements B31 were used to mesh the lower chord, bracing members, and upper chord outside the joint area. Coupling-command was used to connect the beam elements of the truss with solid elements of the joint. Coupling is used for transferring the loads from the reference node of the 2D beam element to the surface of the 3D bracing member, as shown in Figure 28.

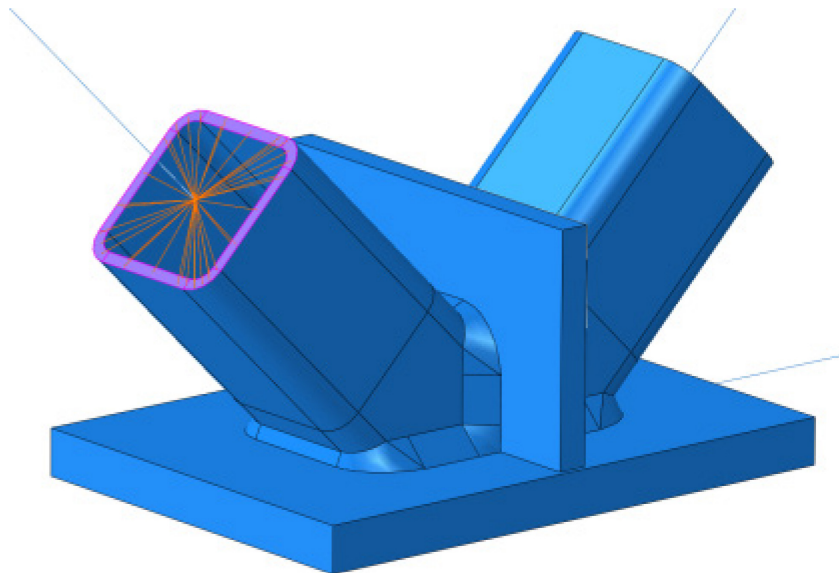


Figure 28: Coupling of 2D and 3D parts of the bracing member.

3.3 Material properties

Two material models with strain hardening were compared: the elastic-plastic material model with linear strain hardening and the true stress-strain curve from real tensile tests. The intention of the comparison was to see, whether or not it is justified to use the stress-strain curve from the tests, which should be avoided if not necessary as it makes the FE analysis computationally more expensive.

In FE analysis, true stress and strain values need to be used for defining plasticity instead of engineering values (Abaqus 2011). True stress and strain values are also used in the tri-linear material model, because that material model can be thought as a

simplification of the real material curve. For both material models the steel density $\rho = 7850 \text{ kg/m}^3$ was used, the modulus of elasticity was set to $E = 210 \text{ GPa}$ and Poisson's ratio was taken as $\nu = 0.3$.

3.3.1 Elastic-plastic model with linear strain hardening

The elastic-plastic model with linear strain hardening (Figure 29) was constructed so that the material behaviour is elastic until reaching the yielding stress f_y . After that, the material is plastic with linear strain hardening until reaching the nominal ultimate limit stress f_u . After this, the material becomes fully plastic. In this thesis, the elastic-plastic material model with a linear strain hardening is further referred to as the tri-linear material model.

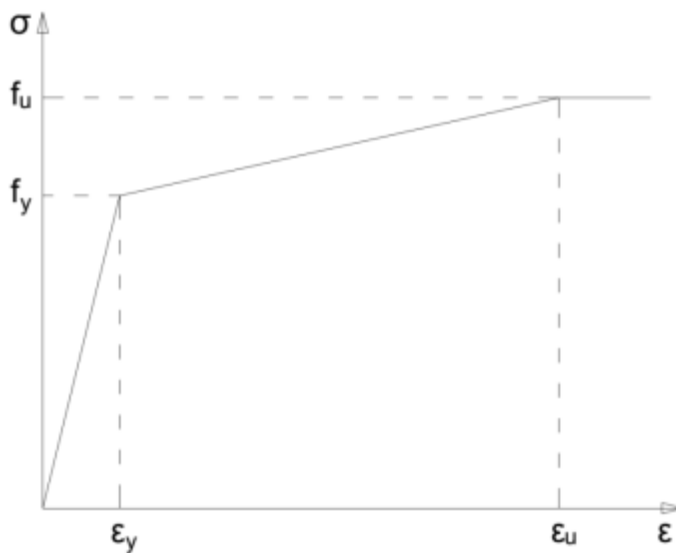


Figure 29: Elastic-plastic material model with linear strain hardening.

Table 8 shows the nominal and true yield and ultimate stresses with their corresponding strains for steel grades S460 and S550. Nominal stress values are taken from (Ongelin & Valkonen 2010). The tri-linear material models for steel grade S460 and S550 are shown in Figure 30.

Table 9: Nominal and true stresses and strains for steel grades S460 and S550.

Steel grade	f_y [MPa]	ϵ_y [-]	f_u [MPa]	ϵ_u [-]	$f_{y\text{-true}}$ [MPa]	$\epsilon_{y\text{-true}}$ [-]	$f_{u\text{-true}}$ [MPa]	$\epsilon_{u\text{-true}}$ [-]
S460	460	0.00219	570	0.05238	461	0.00219	600	0.05106
S550	550	0.00262	640	0.04286	551	0.00262	667	0.04196

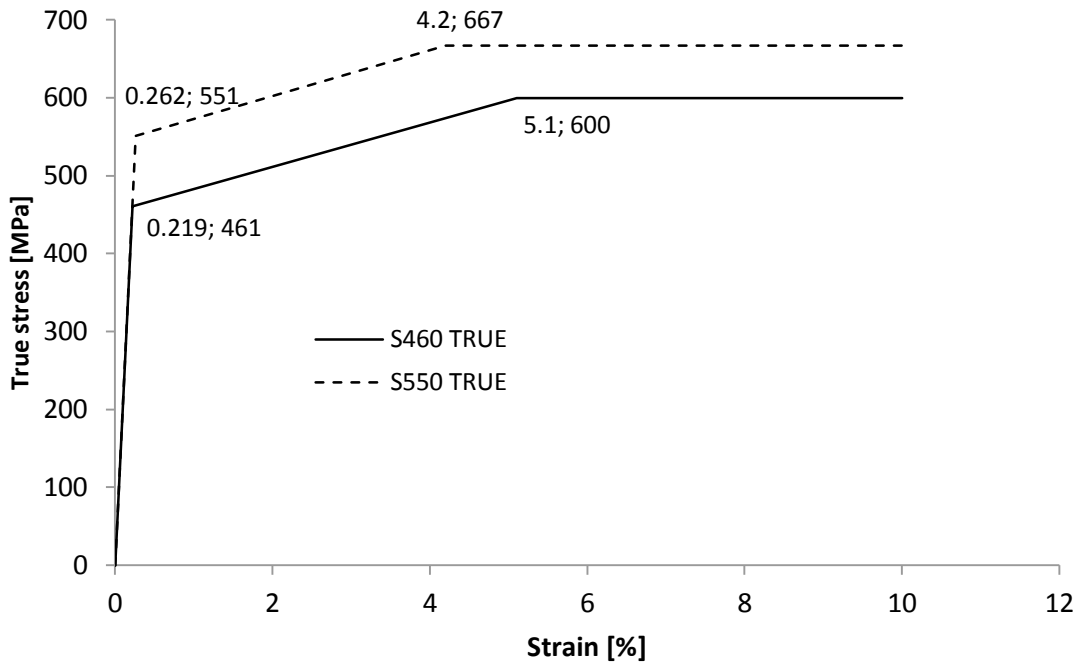


Figure 30: Tri-linear material models with true stress and strain for steel grades S460 and S550.

3.3.2 Simplified stress-strain curve

For the comparison of the material model, stress-strain curves from tensile tests of rectangular hollow sections were provided by Rautaruukki Oyj. Figure 31 shows the material curve from the tension test compared to the tri-linear material model with steel grade S460. It can be seen that the tri-linear material model is more conservative compared to the test-based material model in the region where the strain values are under 5 %. Figure 32 shows the material curve from the tension test compared to the tri-linear material model with steel grade S550. It was noticed that the tri-linear model was not on the safe side compared to the test-based model when the plastic strain exceeded 2.5 %.

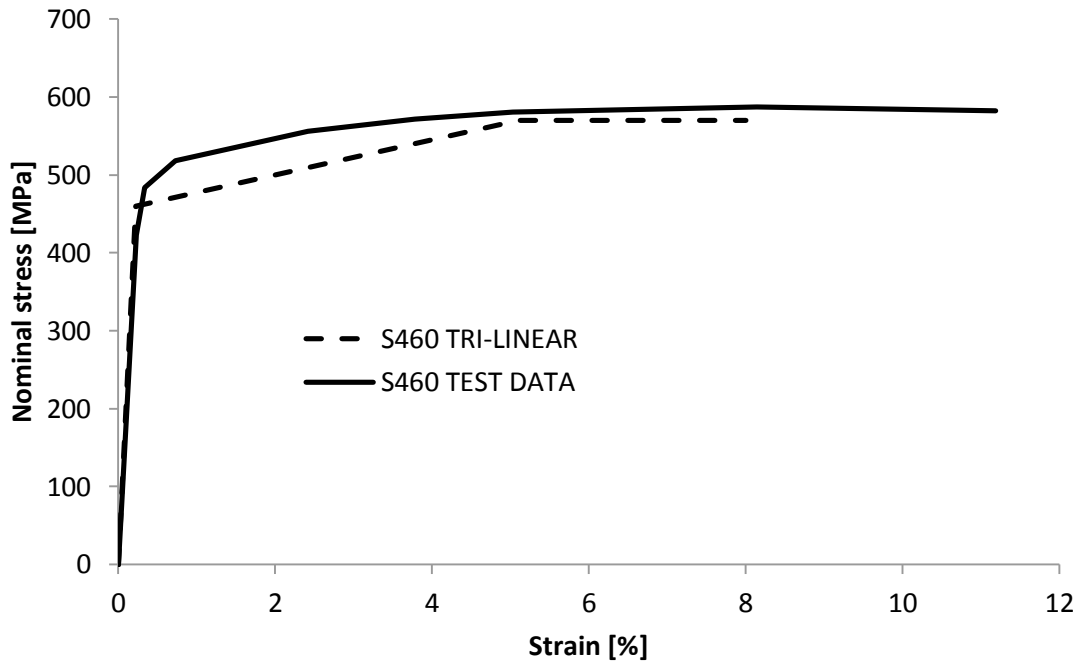


Figure 31: Tri-linear and test data based material models for steel grade S460.

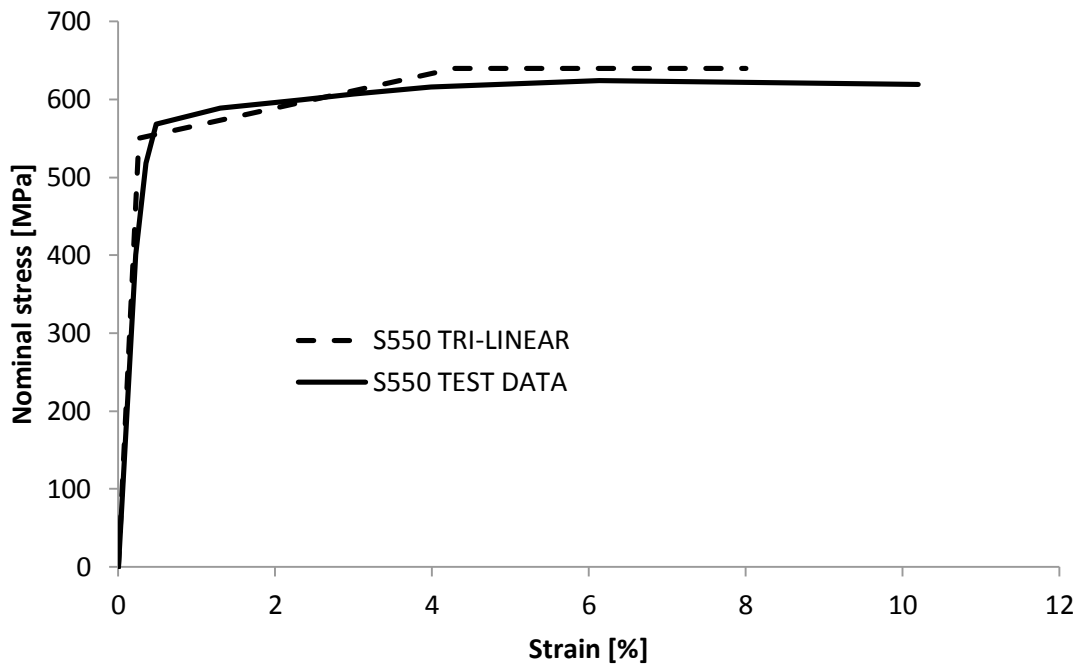


Figure 32: Tri-linear and test data based material models for steel grade S550.

3.4 Boundary conditions

The truss was pre-dimensioned using Finnmap Consulting Oy's spreadsheet for analysing WQ trusses with the steel plate as a lower chord. In both pre-dimensioning and numerical analysis, the load was assumed to originate from the equally distributed load of the hollow core slabs and imposed load affecting the floor levels.

Only half of the truss was modelled because of symmetry. On the right side of the modelled truss, a symmetry condition was set as a boundary condition in Abaqus/CAE. The symmetry condition in the x-direction implies that displacements and rotations around y and z axis are zero. At the support of the truss only the displacements in the x direction and rotations around y and z directions are allowed. Also, the displacement perpendicular to the span direction of the upper chord is set to zero. Boundary conditions and loads of the truss are shown in Figure 33.

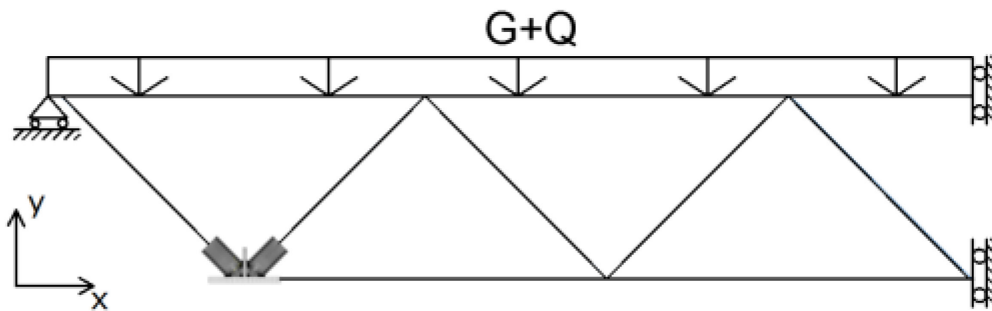


Figure 33: Boundary conditions and loads of the truss.

3.5 Analysis step

Riks method was used in the FE analysis. A load-deflection (Riks) analysis must be performed if there is a concern about material nonlinearity, geometric nonlinearity prior to buckling, or unstable post-buckling response (Dassault Systèmes 2012). It is suitable for solving limit load problems. The method is also used to solve non-linear problems in Johansson et al.'s study (2007).

In Riks method, the load magnitude is assumed to vary with a single scalar parameter. The load in every increment in an analysis step is always proportional in respect of the reference load. The current load magnitude P_{total} is defined as:

$$P_{total} = P_0 + \lambda(P_{ref} - P_0) \quad (9)$$

where P_0 is the load existing at the beginning of the calculation step [-]
 P_{ref} is the reference load vector [-]
 λ is the load proportionality factor (LPF) [-]

The reference load P_{ref} represents the whole load defined in the Riks step. The prescribed load is ramped from the initial load value to the value of the reference load. In current analysis, there are no any loads at the beginning of the step, therefore the dead load is taken as zero. The continuous loading on the top chord between 400 kN/m ... 600kN/m depending on the model is defined as the reference load. The Nlgeom-function of Abaqus was used to take into account large deflections and geometrical non-linearity.

The amount of increments was limited to 60, the minimum increment size was $1 \cdot 10^{-10}$, and the maximum 0.05. The initial increment size was set to 0.05. If a too small initial load was set, the analysis job could not be completed within the previously set amount of increments because of the maximum increment size. However, if large enough, the initial load does not affect the final result, because in analysis the loading starts from zero, and is being increased step by step. It can be seen later that the analyses were terminated after one of the failure criteria was met.

4 Validation and analysis of results

4.1 Geometries of joint

The geometries of the joint for validating the FE model are shown in Table 10. The joint of the validation model consists of bracing members of 150×150×10, steel plate as the lower chord with the thickness of 40 mm, and a division plate with the thickness of 35 mm. The model matches one of the models studied by Jurmu (2011).

Table 10: Geometries of the joint.

<i>Part</i>	<i>Cross-section [mm]</i>
Lower chord	Steel plate 40×350
Tensile bracing member	RHS 150×150×10
Compressive bracing member	RHS 150×150×10
Division plate	Steel plate 35×200

4.2 Convergence tests

In numerical analysis, a convergence test is needed to find the balance between modelling accuracy required and reliability of results. Very coarse mesh leads to unreliable results, and very fine mesh causes high computational costs.

Mesh convergence was carried out by comparing plastic strains of constant volume using different mesh densities at the same load step. The volume location was chosen to be near the area where the initial plastic strains developed during the continuous loading. Four different mesh densities were used to carry out the convergence test. Reference volumes and their average plastic strains of respective meshes are shown in Table 11.

Table 11: Convergency tests with various mesh densities.

Mesh number	Element size [m]	Reference volume V [m ³]	Average equivalent plastic strain ϵ [-]	ϵ/V
1	0.006	3.29E-6	1.52E-2	4620
2	0.005	2.93E-6	1.65E-2	5631
3	0.0045	3.05E-6	1.52E-2	4984
4	0.004	2.97E-6	1.53E-2	5152

Due to different mesh densities, it was not possible to extract exactly the same volume for each density. ϵ/V value was used to ignore the effects of small differences of reference volumes to average plastic strain values. It was calculated as the average plastic strain divided by the reference volume.

From Figure 34 it can be seen that the case number 3 provides sufficiently accurate results, as the difference of the ϵ/V value between meshes 3 and 4 is only about 3%.

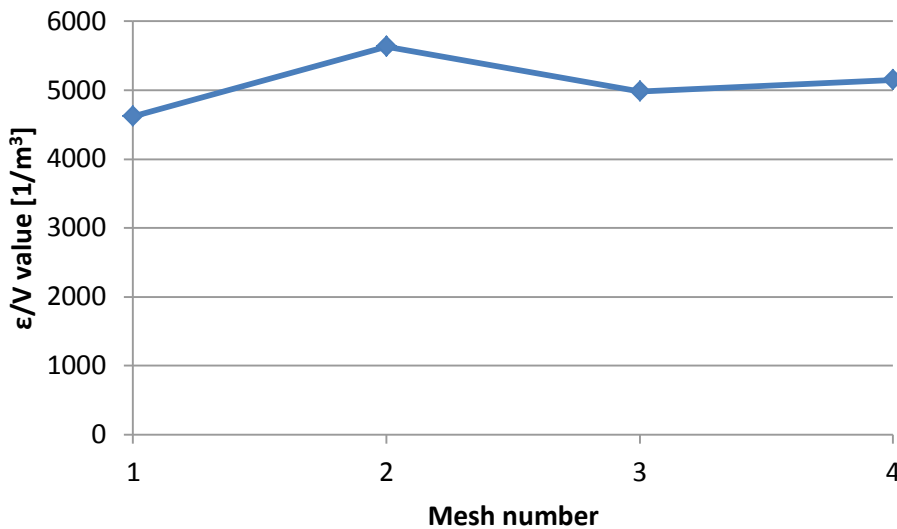


Figure 34: ϵ/V values for different mesh densities.

In the final FE model, the mesh density for bracing members was set to 0.0045. This is the same density that was used by Jurmu (2011) for bracing members.

For other members, the same mesh density as in Jurmu's thesis (2011) was used. Table 12 shows the element densities for different parts of the joint.

Table 12: Element densities for joint parts.

<i>Part</i>	<i>Element size</i>
Bracing members with welds	0.0045
Division plate	0.01
Bottom chord	0.015

4.3 Criteria to determine the limit load

In order to obtain the limit load, the load was applied on the top chord of the truss and increased until the plastic strains measured from element centroids in the joint exceeded the given plastic strain limit. The last loading step resulting in average plastic strain under the defined limit was taken as the critical loading step. The normal force of the bracing members and lower chord were then taken as limit loads at the loading steps when previous criteria were met.

Criteria to determine the limit load of the joint was studied. Failure criteria compared were limit loads and displacements respective to three different plastic strain limits and the peak of the load-deformation curve of the bracing member. The strain limit criteria defined for a joint with two different steel grades are shown in Table 13. The 5 % of plastic strain limit is recommended by the EN 1993-1-5. DNV recommends using 9 % of local plastic strain limit for steel grade S460. The 7 % plastic strain limit for S550 is obtained by extrapolation as discussed earlier. 20 % strain limit is included according to studies made by Dexter & Lee (1999) and van der Vegte et al. (2002). Due to the reasons discussed in Section 3.3.2, also the 2.5 % plastic strain limit was checked for steel grade S550.

Table 13: Limits to determine the limit load for S460 and S550.

S460	S550
	2.5 % plastic strain limit
5 % plastic strain limit	5 % plastic strain limit
9 % plastic strain limit	7 % plastic strain limit
20 % plastic strain limit	20 % plastic strain limit
peak load	peak load

Load-displacement curves for the compression and tension bracing members of the joint were output during the analysis. Data locations for load-displacement curves are shown

with circles in Figure 35. The data was taken from the nodes where the beam element of the bracing member is coupled with solid elements on the tension and compression sides of the joint (A and B, respectively). To neglect the global displacement of the joint, a reference displacement point was chosen at the intersection of bracing member axes (C). The deflection direction follows the direction of the tensile bracing member ($C \rightarrow A$) or the compression bracing member ($C \rightarrow B$). To obtain the displacements of the tension or compression bracing member only, the reference displacement was subtracted from the displacement of the brace ends. This methodology to extract relative displacements of the joint members has also been used in previous studies by Crockett (1994) and Chen et al. (2008).

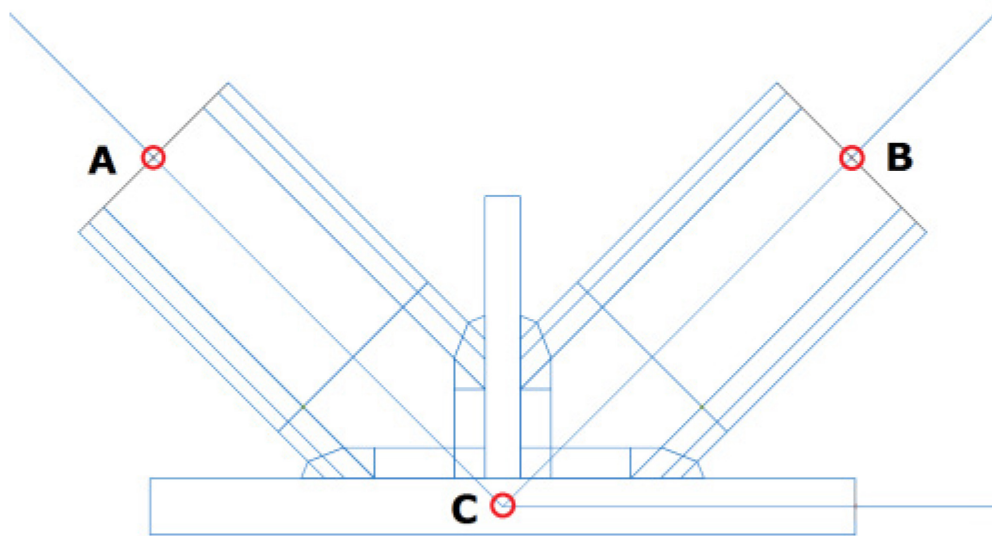


Figure 35: Location of the reference points for load-deflection curves.

According to Jurmu (2011), the moment in the joint caused by eccentricity of joint parts can be neglected. Figure 36 shows the load components on the joint members when the validation model has reached its peak load. It can be seen that the shear force on the lower chord (64 kN) is much smaller than the normal force (3808 kN). The magnitude of the shear force is only $\sim 1.5\%$ of the normal force. Figure 37 shows the development of the shear force versus the development of the normal force on the lower chord when the load on the truss is increased. The shear force starts increasing rapidly only when the joint is about to reach its peak load. Before this phase, the shear force accounts for even smaller portion of the normal force of the lower chord. Therefore, the effect of shear will be neglected in the analysis.

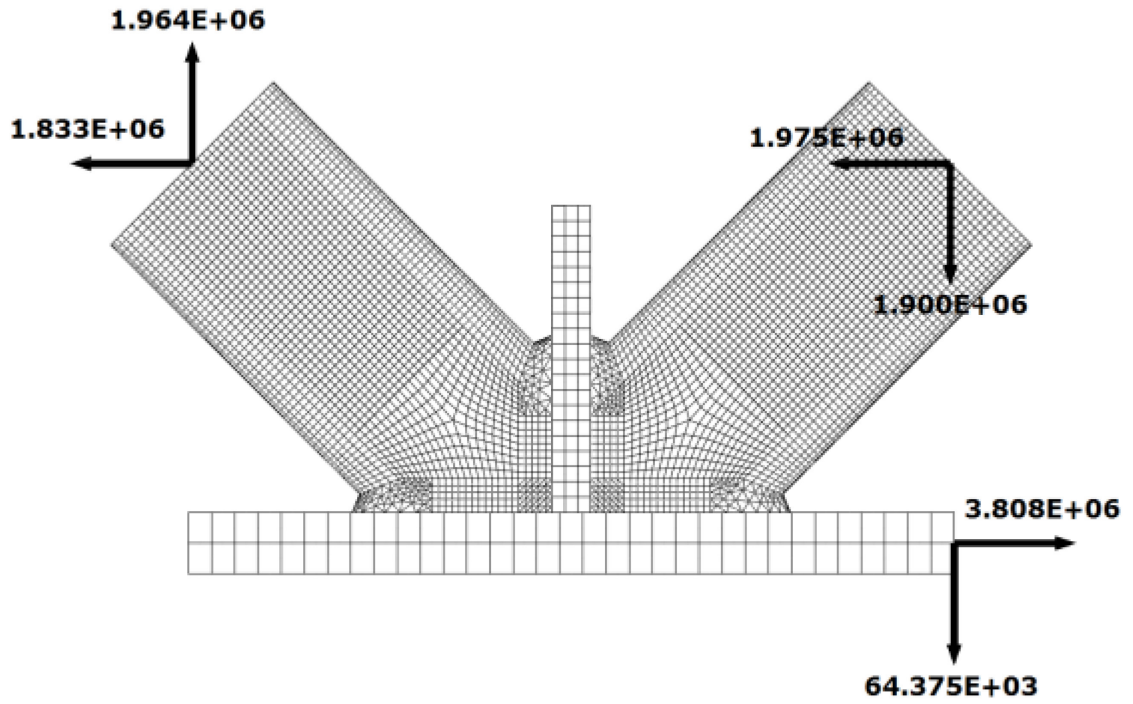


Figure 36: Load components of validation model members when the peak load has been reached.

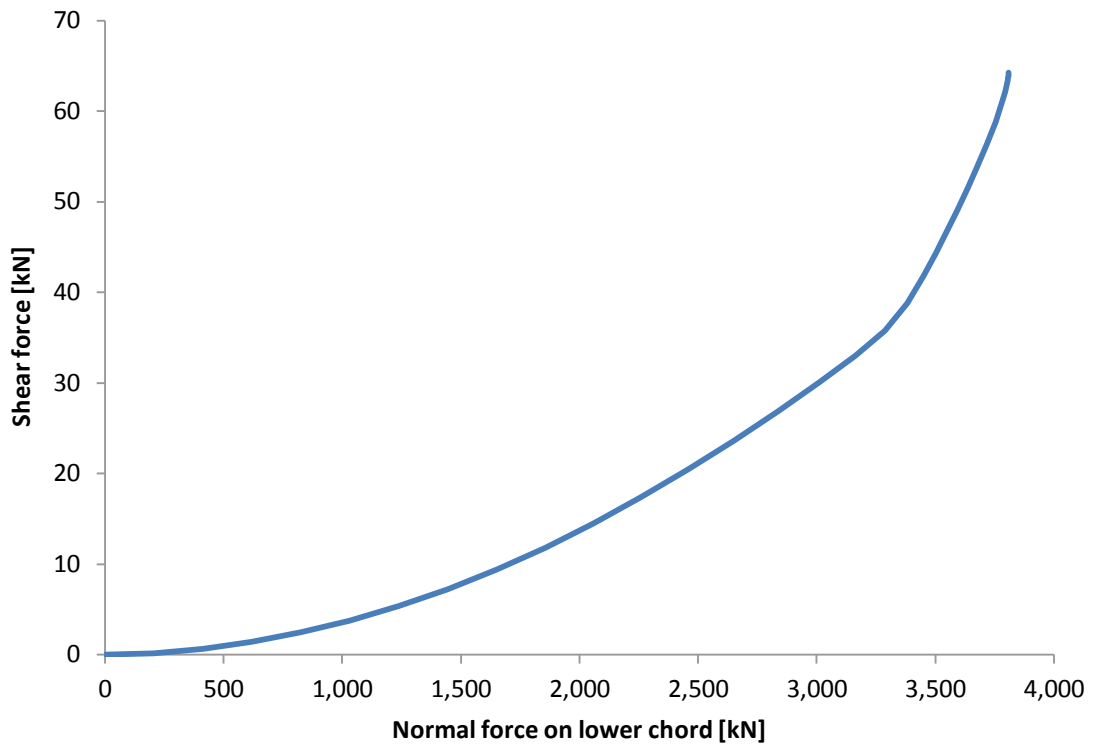


Figure 37: Shear force versus normal force on the lower chord when the load of the truss is being increased.

Load-displacement curves for compression and tension bracing members of the validation model with steel grade S460 are shown in Figure 38. The curves for both compression and tension bracing members showed very similar load-displacement behaviour until the peak load was reached. At the beginning, the curve is linear. This implies the elastic behaviour of the joint before the yielding has started. After the elastic part of the curve, the slope of the curve begins to change because yielding takes place in the joint. Even when the regions in the joint have yielded, the tangent slope of the curve will not become horizontal. This is caused by the strain hardening defined in the material model. When the load is being further increased, the compression bracing member will reach its peak load. This is the load at which the buckling of the bracing member occurs. The meeting points of the 2.5 %, 5 % and 9 % strain criteria are marked in curve with diamond, cross and triangle, respectively. The peak load was reached before regions with plastic strains of 20 % were observed in the joint.

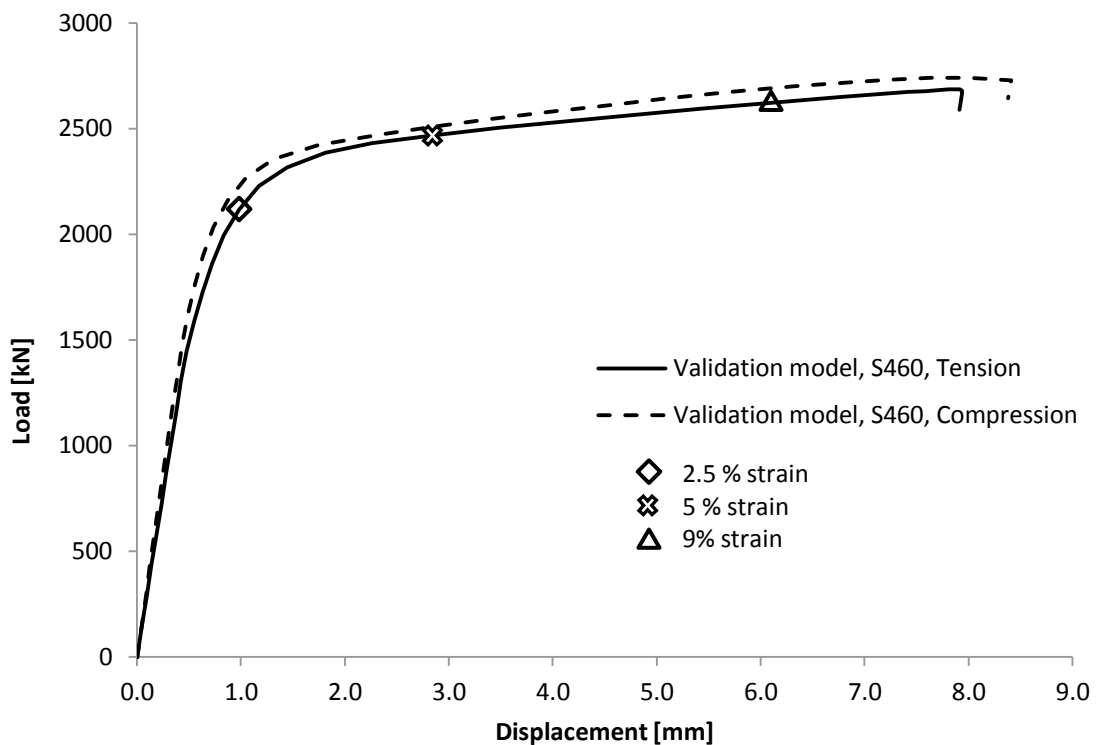


Figure 38: Load-displacement curves for compression and tension bracing members for steel grade S460.

Figure 39 shows the deformations of the joint immediately after the peak load has been reached in the compression bracing member. In the figure, the deformation scale factor is set to 10 for the purpose of better visualisation. At this stage, large deformations are

observed in the bracing member when the load on the top chord of the truss is even slightly increased.

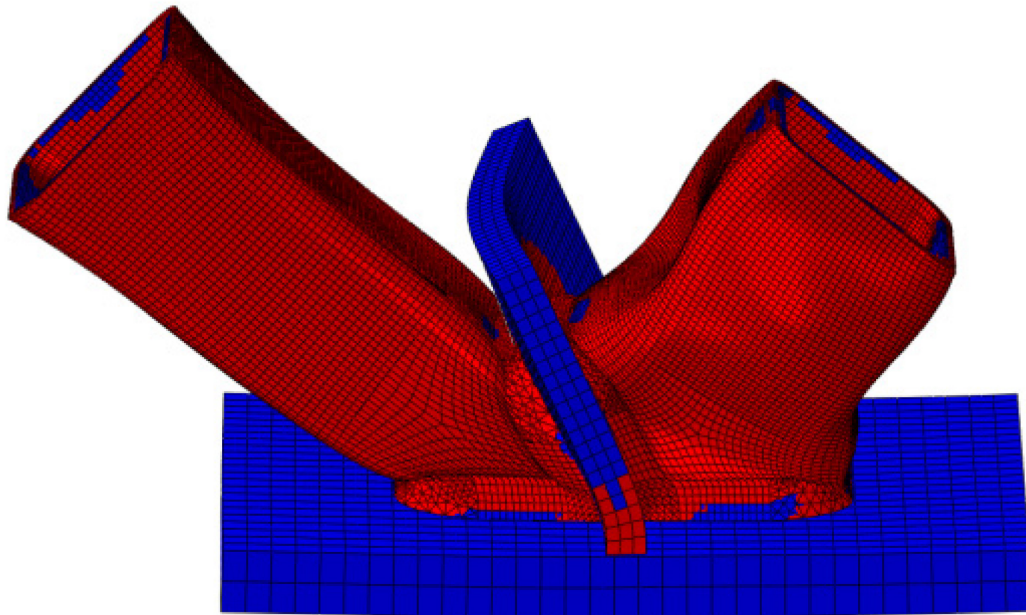


Figure 39: Member deformations in the joint after the peak load has been reached in the compression bracing member.

Table 14 shows limit loads and their respective displacements according to different limit criteria for steel grade S460. Limit load according to member failure as the limit criterion matches well with the limit load according to 5 % equivalent plastic strain criterion. The load on the tensile bracing member according to the 5 % plastic strain limit is 2469 kN. This load is ~94 % of the limit load according to 9 % strain limit (2622 kN). The peak load (2686 kN) is similar to the load according to 9 strain limit. Peak load occurred before any regions with strains of 20 % were observed. The limit load according to 2.5 % strain limit is ~85 % of the load based on the 5 % strain limit.

Table 15 lists the limit loads and their respective displacements for steel grade S550. Similar behaviour as with steel grade S460 can be seen. The limit load according to 5 % strain criterion is 2824 kN. Larger relative difference is seen between the 7 % strain limit and the peak compared to the steel grade S460, where the 9 % strain limit was very similar with the peak load. This is obviously caused by larger strains allowed for steel grade S460 according to DNV (2013). Similarly to the validation model with steel grade S460, the peak load occurred before regions with equivalent plastic strains of 20 % were observed.

Table 14: Limit loads and respective displacements according to different limit criteria for steel grade S460.

Limit criterion	Equivalent plastic strain limit				Peak load
	2.5 %	5 %	9 %	20 %	
Limit load [kN]	2118	2469	2622	N/A	2686
Displacement [mm]	1.0	2.8	6.1	N/A	7.9

Table 15: Limit loads and respective displacements according to different limit criteria for steel grade S550.

Limit criterion	Equivalent plastic strain limit				Peak load
	2.5 %	5 %	7 %	20 %	
Limit load [kN]	2420	2824	2957	N/A	3101
Displacement [mm]	1.0	2.0	3.5	N/A	7.2

No studies are found justifying the use of the 2.5 % plastic strain limit as the limiting criterion in K-joints. The 5 % plastic strain limit is taken as the limiting strain criterion, as it results in limit loads close to loads based on 9 % and 7 % strain limits respectively for steel grades S460 and S550 while still being more conservative. The 5 % plastic strain limit has also been used to determine the limit loads in Jurmu's work (2011) and is also recommended by SFS EN 1993-1-5 (2006) for regions subjected to tensile stresses. The failure location was defined as the location where the failure criterion was first met.

4.4 Effect of the material model on limit loads

Two material models were compared in the validation model. Figure 40 shows the load-displacement curves for two material models for steel grade S460. The normal forces at the tensile member show a significant variance when two material models for steel grade S460 are compared. For the test-based material model for steel grade and the 5 % strain criterion, the normal force of the tensile bracing member at the failure load is 2611 kN. For the elastic-plastic model with linear strain hardening with the same strain criterion, the respective load is 2469 kN. Also, for 2.5 % plastic strain criterion, the limit loads for test-based material model and tri-linear material model show a significant difference. The use of the test-based material model results in the limit load of 2263 kN, which is 107 % of the limit load obtained when using the tri-linear material model.

Figure 41 shows similar curves for steel grade S550. It can be seen that the limit loads on tensile members from two different material models are practically equal.

The limit loads for 2.5 % and 5 % equivalent plastic strain criteria for steel grades S460 and S550 are shown in Table 16.

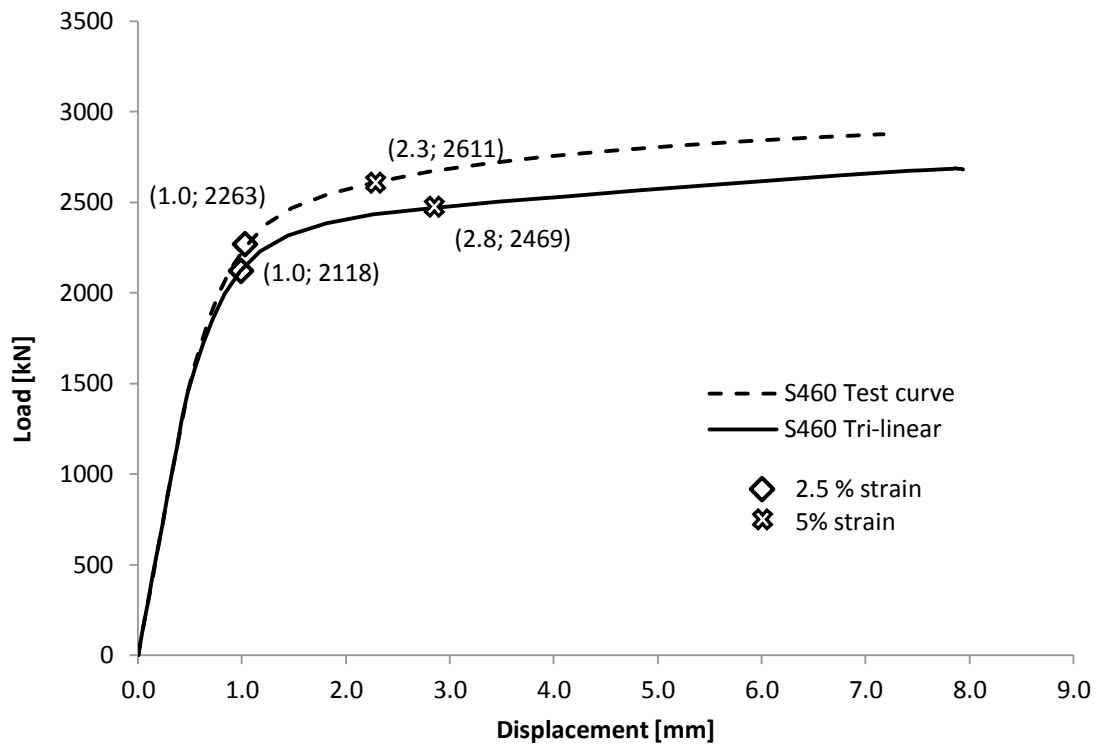


Figure 40: Load-displacement curves for the tension bracing member of the Model 2-1 with different material models for steel grade S460. Diamonds mark the points where 2.5 % equivalent plastic strain criterion is met. Crosses mark the meeting of the 5 % criterion.

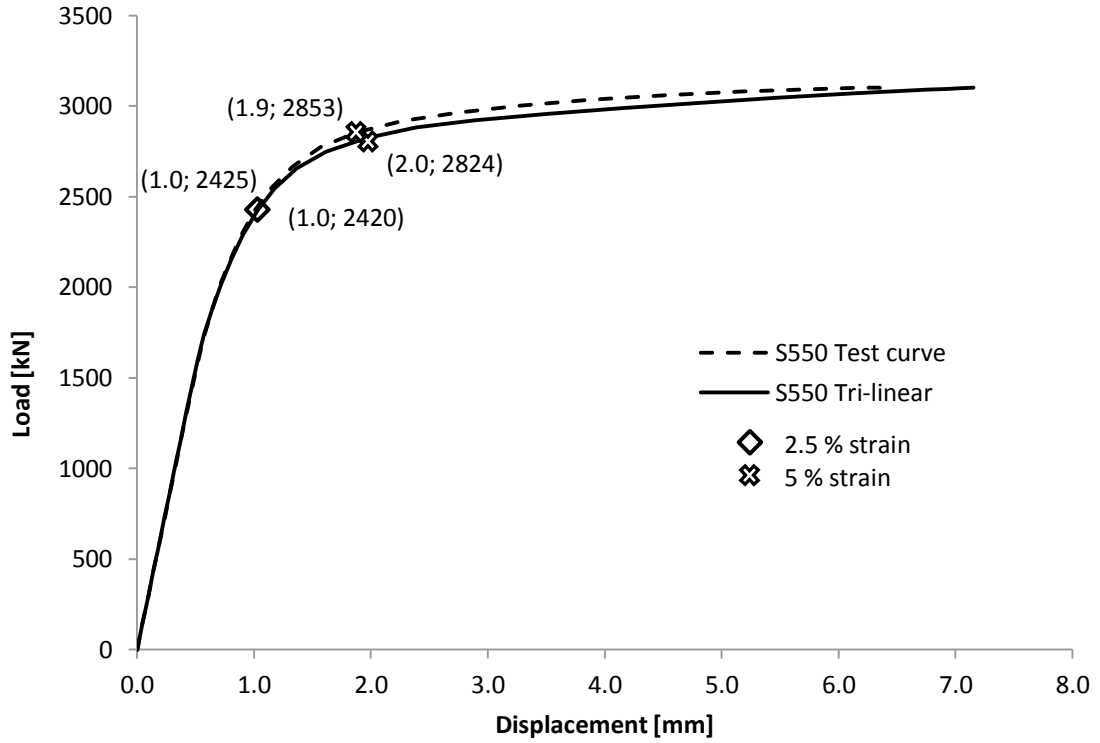


Figure 41: Load-displacement curves for the tension bracing member of the Model 2-1 with different material models for steel grade S550. Diamonds mark the points where 2.5 % equivalent plastic strain criterion is met. Crosses mark the meeting of the 5 % criterion.

Table 16: Limit loads comparison for tensile bracing with different material models and equivalent strain limits for steel grades S460 and S550.

Steel grade	Material model	Limit load for tensile bracing member [kN]	
		2.5 %	5 %
S460	Tri-linear	2118	2469
	Test curve	2263	2611
S550	Tri-linear	2420	2824
	Test curve	2425	2853

Table 17 lists the limit loads with various equivalent plastic strain criteria and design weld capacities $F_{w.Rd}$. Also, the yield strength of the bracing tube member is shown. Test-based material model is used in the numerical analysis. The weld capacity of the joint $F_{w.Rd,j}$ is obtained from the equation (5) by multiplying the design weld resistance per unit length $F_{w.Rd}$ with the total length of the weld l :

$$F_{w.Rd,j} = f_{vw} \cdot d \cdot a \cdot l \quad (10)$$

where $f_{vw,d}$ and a are defined in Section 2.3.2
 l is the total length of the weld [mm]

The yielding capacity of the tubular bracing member $F_{tube,y}$ is similar to the calculated weld capacity $F_{w,Rd}$. The yielding capacity of the bracing member is 98 % of the calculated weld capacity for both steel grades. The similarity can be explained by the fact that the throat thickness of the weld was chosen so that that the welds have the same yielding strength as the base material. Changing the correlation factor from $\beta_w = 1.0$ to $\beta_w = 0.85$ results in 18 % higher weld capacities that do not match any capacities obtained using previously mentioned limit criteria. In Finland, the correlation factor for steels from grade S460 up to S700 should be taken as $\beta_w = 1.0$, according to SFS-EN 1993-1-8 and SFS-EN 1993-1-12.

Table 18 lists the limit loads with different equivalent plastic strain criteria and design weld capacities. Also, the yield strength of the bracing tube member is shown. The tri-linear material model is used in the numerical analysis. Correlation can be seen between the weld capacity (with $\beta_w = 1.0$), yielding capacity of the bracing member and joint capacity according to 5 % strain limit. These capacities for steel grade S460 are 2474 kN, 2418 kN and 2428 kN, respectively. Similar correlation can be seen with steel grade S550.

Table 17: Design weld capacities for tensile member with correlation factor values $\beta_w = 1.0$ and $\beta_w = 0.85$ compared to yielding capacity of the tube and limit capacities due to equivalent plastic strain limits using test-based curve as a material model, and $l = 640$ mm.

<i>Steel grade</i>	β_w	$F_{w,Rd,j}$ [kN]	$F_{tube,y}$ [kN]	$F_{FE,2.5\%}$ [kN]	$F_{FE,5\%}$ [kN]
S460	1.0	2474	2418	2356	2616
	0.85	2911			
S550	1.0	2932	2891	2532	2856
	0.85	3450			

Table 18: Design weld capacities for tensile member with correlation factor values $\beta_w = 1.0$ and $\beta_w = 0.85$ compared to the yielding capacity of the tube and limit capacities due to equivalent plastic strain limits using tri-linear curve as material model, and $l = 640$ mm.

Steel grade	β_w	$F_{w,Rd,j}$ [kN]	$F_{tube,y}$ [kN]	$F_{FE,2.5\%}$ [kN]	$F_{FE,5\%}$ [kN]
S460	1.0	2474	2418	2117	2428
	0.85	2911			
S550	1.0	2932	2891	2543	2882
	0.85	3450			

As explained in Figure 40, the nominal ultimate strength in the tri-linear material model is lower than that in the test-based material model. This explains a higher joint capacity in FE analysis when the test-based material model is used. Regardless of the material model and steel grade used, 2.5 % equivalent plastic strain criterion results in joint capacity that is ca. 90 % of the capacity obtained by the 5 % limit.

The test-based stress-strain curve was provided according to the testing result of only one specimen. Therefore, the material model based on the tensile test cannot be considered to be reliable enough. To obtain a more reliable material curve, larger amount of tests and averaging of the results are needed.

Günther, Hildebrand, et al. (2009) found in their report that the ultimate load is predicted with a good accuracy when the multi-linear material model is used. In further analyses, the tri-linear material model is used.

4.5 Comparison with previous studies

A similar FE model as in Jurmu's thesis (2011) was created to compare and validate the new model with previously accepted results. Therefore, it was easy to compare, how the high strength of steel affects the capacity of the joint. The main differences between the two models are element types used. In the current model, true stress and strain were used in the material plasticity definition. The normal force on tensile bracing was compared with two models loaded until their defined limit criteria were reached. Jurmu stated that the limit criterion has been reached when the plastic strains exceeded 5 % over the area of 300-400 mm².

Using the 5 % criteria to define the limit state for the new model, the normal force on the tensile bracing member at the failure point was 2026 kN (Figure 42). Compared to Jurmu's work (2011) the load obtained was very similar. The normal force on the tensile bracing member at the failure point in Jurmu's FE model was 2074 kN.

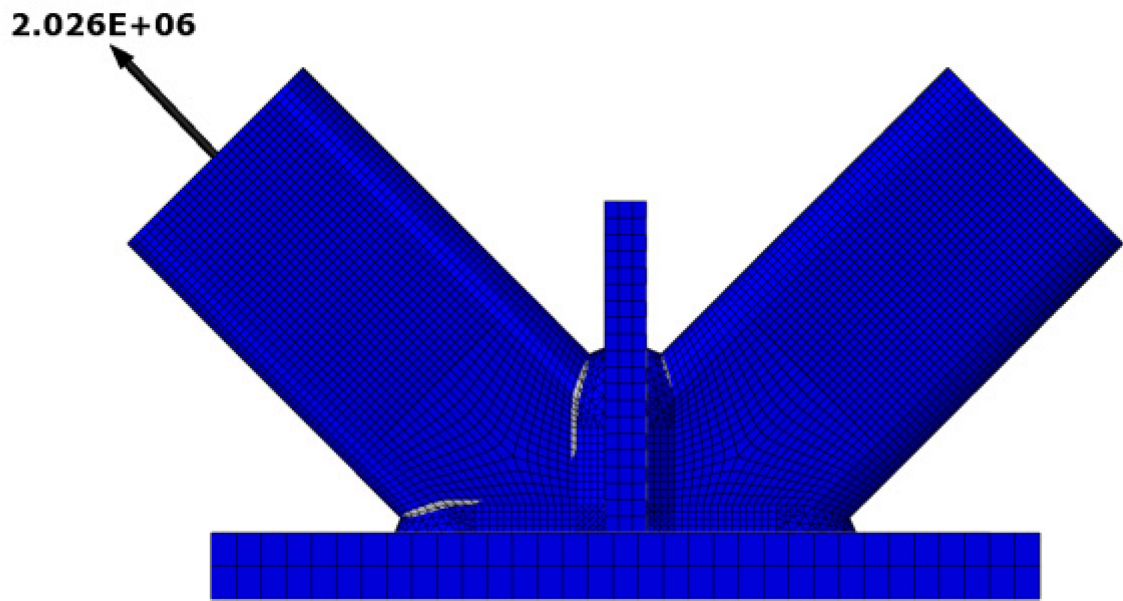


Figure 42: Normal force at the failure point on the tensile bracing member of the validation model for steel grade S420. Areas where the equivalent plastic strains exceed 5 % are marked with light grey colour.

5 Parametric studies

15 different FE models were created and analysed with two steel grades leading to 30 analyses. The parts in the models are shown in Table 19. Variables in the models were angles and dimensions of the rectangular hollow sections, thickness of the lower chord and division plate, as well as material strength of the steel. The cross-section of the lower chord was changed among models with the same bracing angle so that the area of the cross-section remained the same. The parts of the joint were kept the same as in Jurmu's thesis (2011). The locations of normal forces extracted from the joint are shown in Figure 43.

Table 19: Joint assemblies of FE models.

Model name	Bracing angle [°]	Bracing member [mm]	Lower chord [mm]	Division plate [mm]
1-1	30	150×150×10	40×350	25×340
1-2	30	150×150×10	20×700	25×690
1-3	30	150×150×10	40×350	35×340
2-1	45	150×150×10	40×350	25×340
2-2	45	150×150×10	20×700	25×690
2-3	45	150×150×10	40×350	35×340
3-1	60	150×150×10	40×300	25×290
3-2	60	150×150×10	20×600	25×590
4-1	30	250×150×10	40×450	25×440
4-2	30	250×150×10	20×900	25×440
4-3	30	250×150×10	40×450	35×440
5-1	45	250×150×10	40×450	25×440
5-2	45	250×150×10	20×900	25×440
6-1	60	250×150×10	40×400	25×290
6-2	60	250×150×10	20×800	25×290

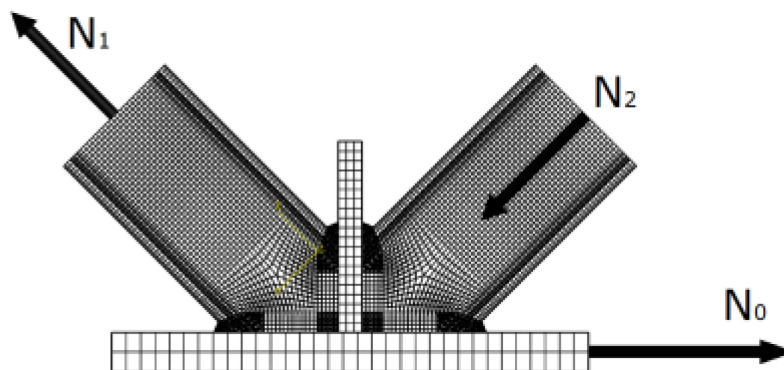


Figure 43: Normal forces in the joint.

Only one failure criterion was found in the analysis: the local yielding of the tension bracing member. However, the location where this failure was observed varied in different models.

Three potential failure criteria were considered and checked for each joint variation.

The criteria checked were:

- Peak load on the brace load-displacement plot
- Exceeding of the tensile strain limit

5.1 Models with $\theta = 30^\circ$ and $150 \times 150 \times 10$ bracing members

5.1.1 Model 1-1: $t_0 = 40$ mm, $t_p = 25$ mm

For steel grade S460, the initial yielding becomes visible at the corners of the tensile bracing member close to the weld, when the normal force applied to the bracing member is 1673 kN. Regions with equivalent plastic strains exceeding 5 % are marked with an arrow in Figure 44. The normal force applied to the tensile bracing member at this point is 2613 kN, exceeding the yielding capacity of the tension bracing member. Therefore, the failure criterion for the joint Model 1-1 with steel grade S460 is the local yielding of the bracing member or possible yielding failure of the tension bracing member in the truss.

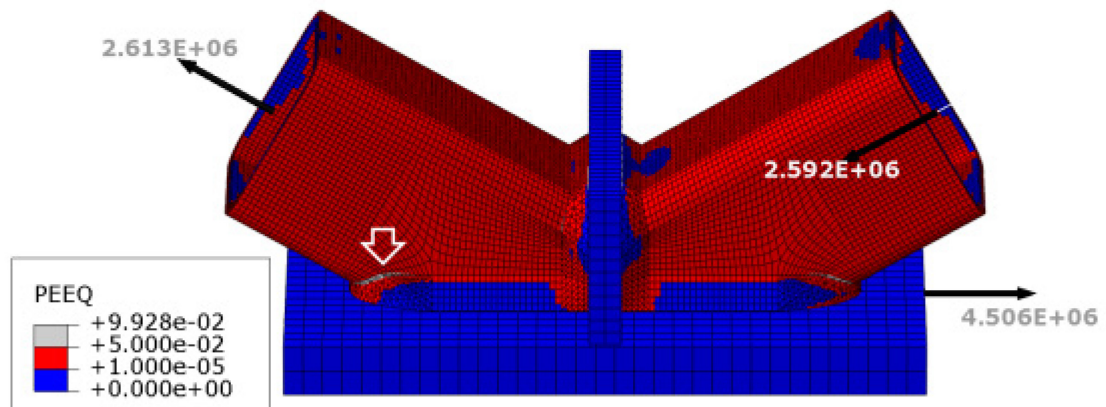


Figure 44: Equivalent plastic strains of Model 1-1 with steel grade S460.

5.1.2 Model 1-2: $t_0 = 20$ mm, $t_p = 25$ mm

In this model, the thickness of the lower chord is reduced from $t_0 = 40$ mm to $t_0 = 20$ mm. The normal force applied to the tensile bracing member is 2489 kN when the 5 % limit strain has been reached. This value is only slightly larger than the tension yielding capacity of the bracing member. Therefore, the failure criterion is either local yielding of the bracing member in the joint or the possible yielding failure of the tension bracing member in the truss. Regions with equivalent plastic strains exceeding 5 % are marked with an arrow in Figure 45.

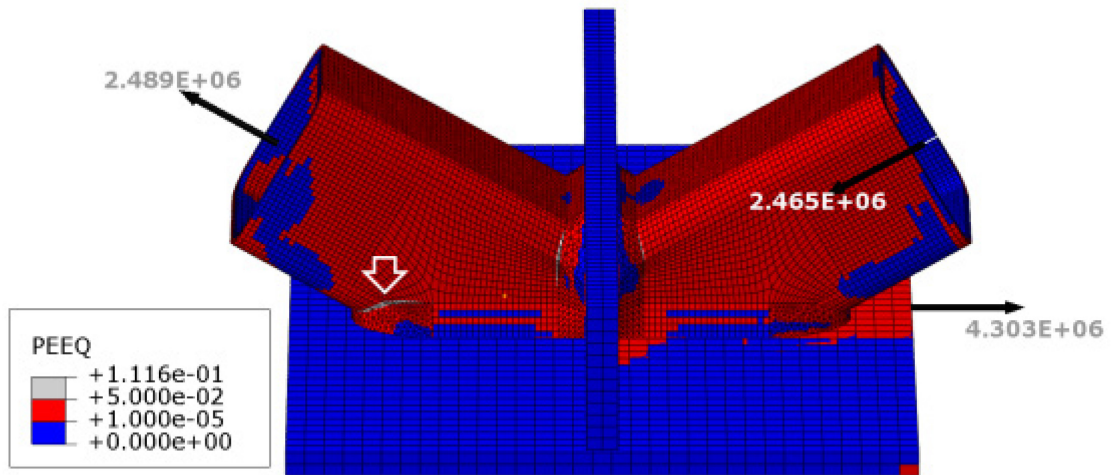


Figure 45: Equivalent plastic strains of Model 1-2 with steel grade S460.

5.1.3 Model 1-3: $t_0 = 40$ mm, $t_p = 35$ mm

In Model 1-3, the thickness of the division plate was increased from $t_0 = 25$ mm to $t_0 = 35$ mm. For steel grade S460, the initial yielding areas on the tensile side are seen at the corners of the bracing member. They occur when the normal force on the tensile member is 1431 kN. The normal force applied to the tensile bracing member is 2489 kN when the 5 % limit strain has been reached. However, at this point, the yielding capacity of the tension bracing member has already been exceeded. Regions with equivalent plastic strains exceeding 5 % are marked with an arrow in Figure 46. The failure criterion for this joint is the local yielding of the bracing member or the possible yielding failure of the bracing member. No significant change in the limit load or failure criterion resulting from increasing the thickness of the division plate is seen.

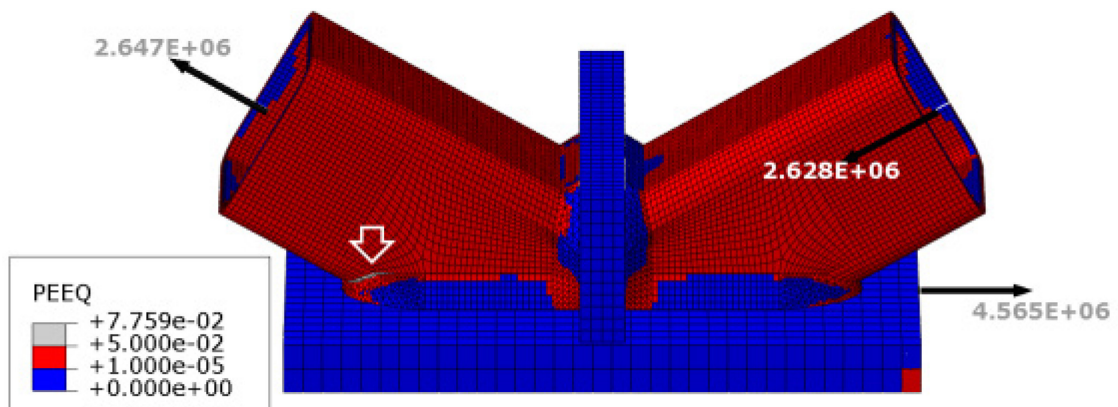


Figure 46: Equivalent plastic strains of Model 1-3 with steel grade S460.

5.1.4 Conclusion of models with $\theta = 30^\circ$ and $150 \times 150 \times 10$ bracing members

Tension load-displacement (TLD) curves of Models 1-1, 1-2, and 1-3 are shown in Figure 47, respectively. In the legend, first two numbers (21 = Model 2-1) stand for the model number and last three numbers stand for steel grade (460 = S460). Crosses mark the normal force applied on bracing members and their respective displacements when the 5 % equivalent plastic strain criterion has been reached. In Model 1-1, the yielding capacity of the bracing member is exceeded before the strain limit. Reducing the thickness of the lower chord results in more ductile behaviour of the joint, also the strain limit is reached nearly at the same time with the yielding capacity of the bracing member. Increasing the thickness of the division plate in Model 1-3 results in very similar load-displacement behaviour compared to the one of Model 1-1. For models with $\theta = 30^\circ$ and $150 \times 150 \times 10$ bracing members, no significant changes in displacements respective to 5 % limit loads were found regardless of division plate and lower chord thicknesses.

Compression load-displacement curves (CLD) of three models are shown in Figure 48. As seen in the figure, the strain criterion is reached earlier than the peak loads for compression members in every model.

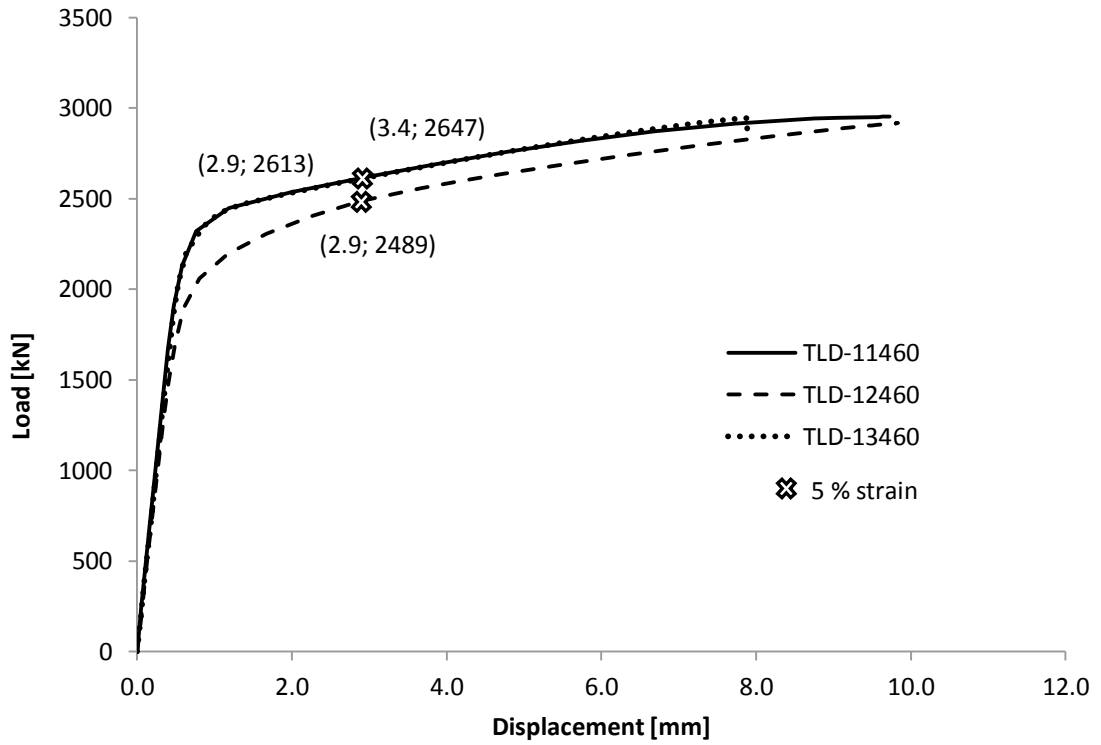


Figure 47: Load-displacement behaviour of tension bracing member in FE models 1-1, 1-2, and 1-3 with steel grade S460.

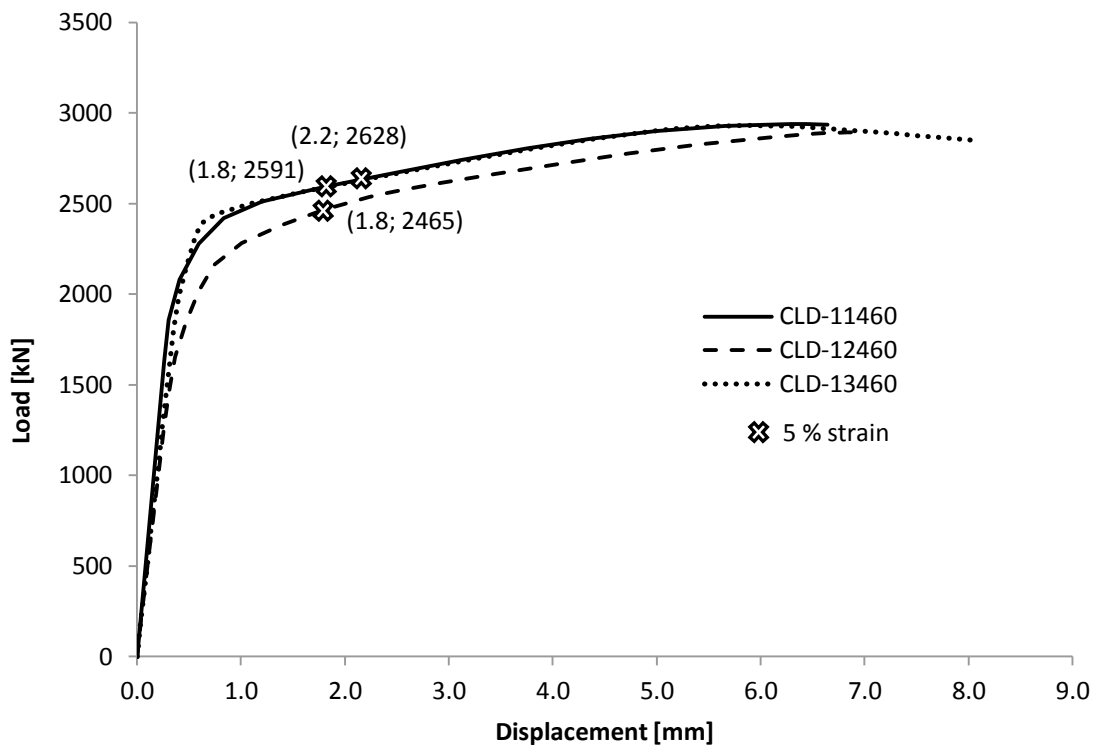


Figure 48: Load-displacement behaviour of compression bracing member in FE models 1-1, 1-2, and 1-3 with steel grade S460.

5.2 Models with $\theta = 45^\circ$ and $150 \times 150 \times 10$ bracing members

5.2.1 Model 2-1: $t_0 = 40$ mm, $t_p = 25$ mm

For steel grade S460, the initial yielding becomes visible at the corners of the tensile bracing member close to the weld, when the normal force applied to the bracing member is 1447 kN. Regions with equivalent plastic strains exceeding 5 % are marked with an arrow in Figure 49. When the 5 % strain criterion is met at the corners of the bracing member, the normal force is applied to the tension bracing member is 2469 kN. This value is only slightly larger than the tension yielding capacity of the bracing member. Therefore, the failure criterion is either local yielding of the bracing member in the joint or the possible yielding failure of the tension bracing member.

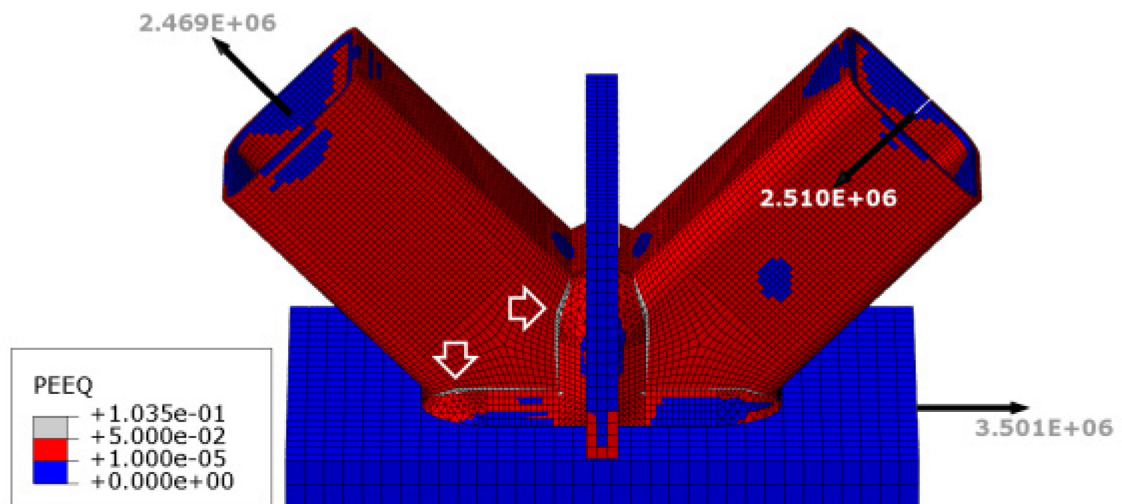


Figure 49: Equivalent plastic strains of Model 2-1 with steel grade S460.

5.2.2 Model 2-2: $t_0 = 20$ mm, $t_p = 25$ mm

For steel grade S460, the initial yielding becomes visible at the corners of the tensile bracing member close to the weld, when the normal force on the brace member is 1282 kN. When the 5 % strain criterion is met at the corners of the bracing member, the normal force is 2324 kN. Regions where equivalent plastic strains exceed 5 % are marked with an arrow in Figure 50. Local yielding of the bracing member in the joint can be taken as the failure criterion. Compared to the Model 2-1, yielded areas are now concentrated on the upper chord of bracing members. This is caused by the division plate having higher stiffness compared to the lower chord, leading to forces in the model transferring through the division plate rather than the lower chord. Same phenomenon occurred in Jurmu's thesis (2011).

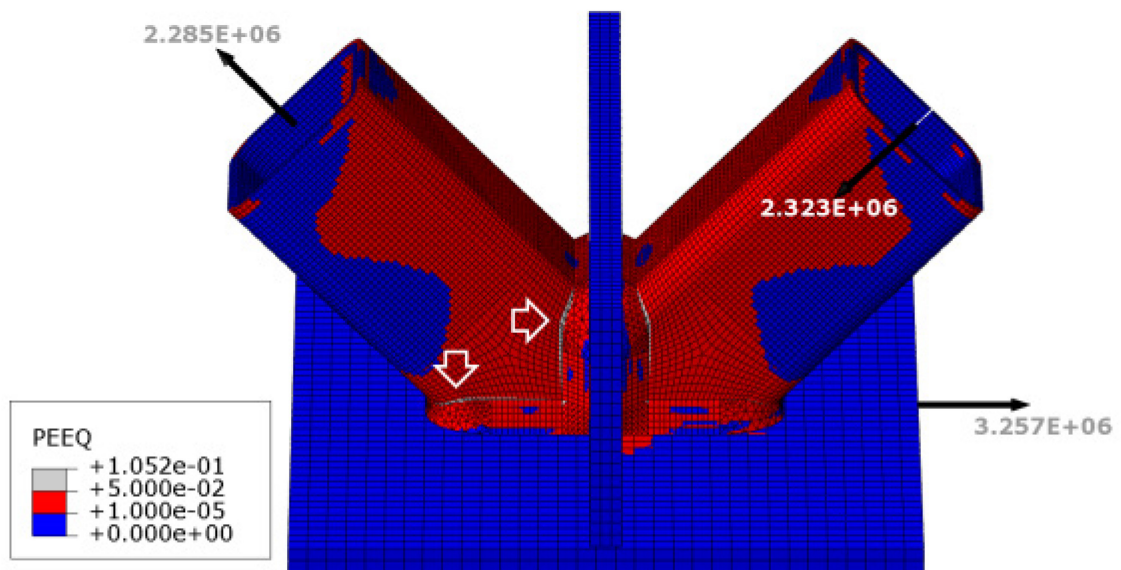


Figure 50: Equivalent plastic strains of Model 2-2 with steel grade S460.

5.2.3 Model 2-3: $t_0 = 40$ mm, $t_p = 35$ mm

For steel grade S460, the initial yielding becomes visible at the corners of the tensile bracing member close to the weld, when the normal force applied to the bracing member is 1546 kN. Regions with equivalent plastic strains exceeding 5 % are marked with arrows in Figure 51. When the 5 % strain criterion is reached at the corners of the bracing member, the normal force applied to the tension bracing member is 2701 kN. The failure criterion is either local yielding of the bracing member in the joint or the possible yielding failure of the tension bracing member. Compared to the Model 2-1, yielded areas are now concentrated on the upper chords of bracing members. This is caused by division plate now having relatively higher stiffness compared to the lower chord, leading to forces in the model transferring through the division palte rather than through the lower chord.

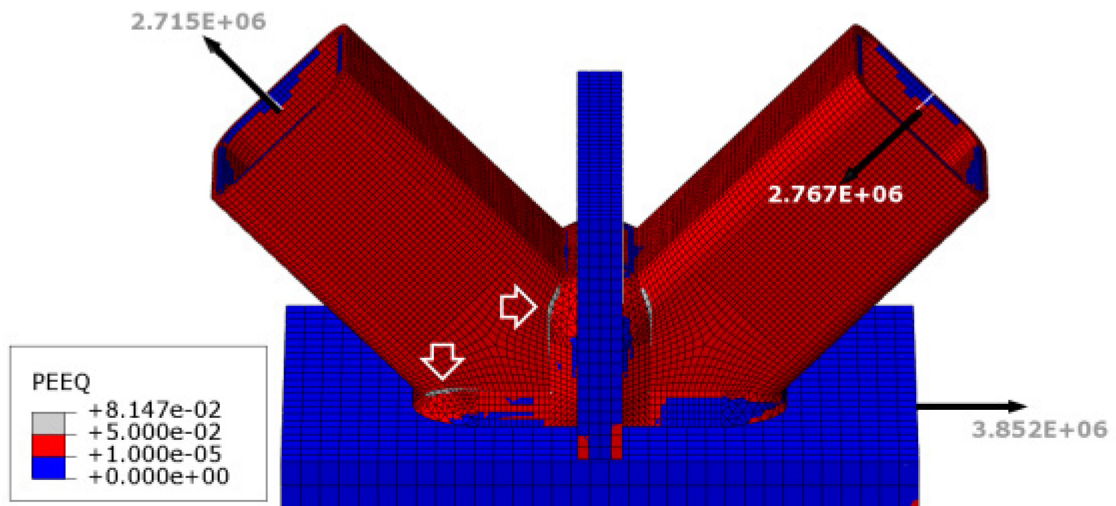


Figure 51: Equivalent plastic strains of Model 2-3 with steel grade S460.

5.2.4 Conclusion of models with $\theta = 45^\circ$ and $150 \times 150 \times 10$ bracing members

Tension load-displacement (TLD) curves of three models are shown in Figure 52, respectively. Crosses mark the normal force applied on bracing members and their respective displacements when the 5 % equivalent plastic strain criterion has been reached. In Model 2-1, the 5 % equivalent plastic strain criterion is reached at the same time with the yielding capacity of the bracing member. The same criterion is met with lower loads in the Model 2-2. The stiffness of the joint is reduced, when thinner lower chord is used. In the Model 2-3, the thickness of the division plate was increased from 25 mm to 35 mm. This causes the joint to be stiffer compared to the Model 2-1 and the 5 % strain criterion to be met in the joint with significantly larger deformations of the bracing member. However, the yielding resistance of the bracing member is exceeded before the 5 % criterion is met, leading to possible yielding failure of the bracing member in the truss.

Compression load-displacement curves (CLD) of three models are shown in Figure 53. As seen in Figure 46, the 5 % equivalent strain criteria are reached earlier than the peak loads for compression members.

The region where the strain limit is met stays the same regardless of the lower chord and division plate thickness in Models 2-1, 2-2, and 2-3.

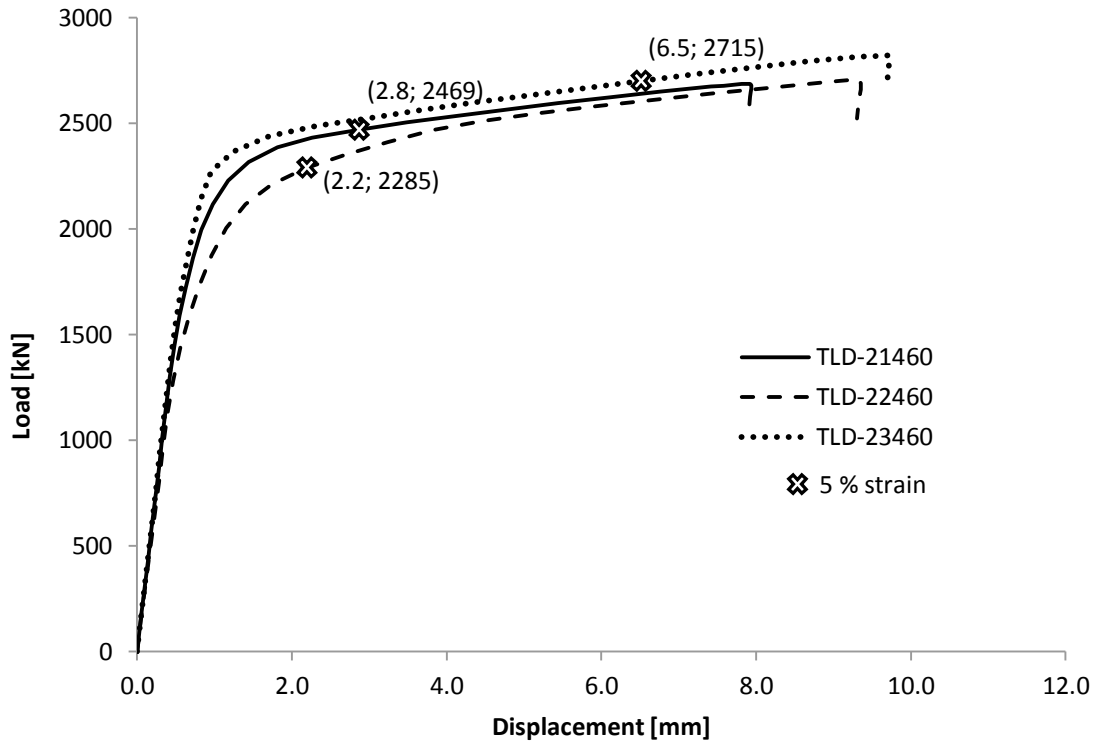


Figure 52: Load-displacement behaviour of tension bracing member in FE models 2-1, 2-2, and 2-3 with steel grade S460.

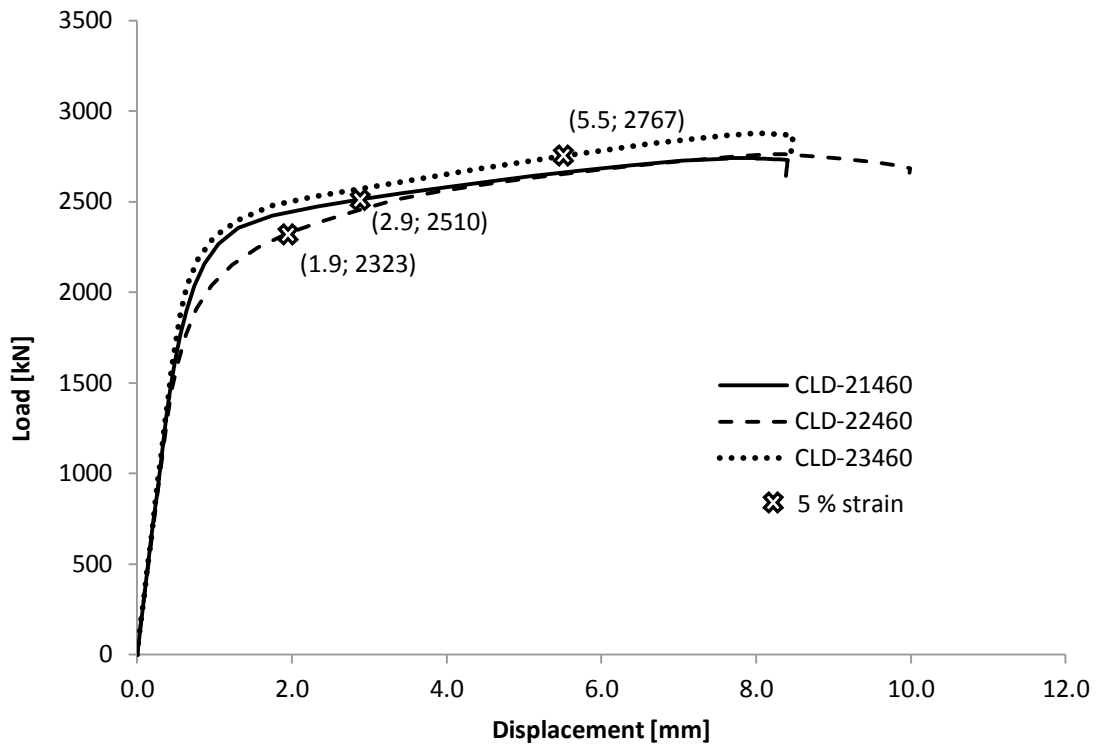


Figure 53: Load-displacement behaviour of compression bracing member in FE models 2-1, 2-2, and 2-3 with steel grade S460.

5.3 Models with $\theta = 60^\circ$ and $150 \times 150 \times 10$ bracing members

5.3.1 Model 3-1: $t_0 = 40$ mm, $t_p = 25$ mm

For steel grade S460, the initial yielding becomes visible at the corners of the tensile bracing member close to the weld, when the normal force applied to the bracing member is 1436 kN. Regions with equivalent plastic strains exceeding 5 % are marked with an arrow in Figure 54. When the 5 % strain criterion is met at the corners of the bracing member, the normal force applied to the tension bracing member is 2558 kN. This value is larger than the tension yielding capacity of the bracing member. The failure criterion is either local yielding of the bracing member in the joint or the possible yielding failure of the tension bracing member.

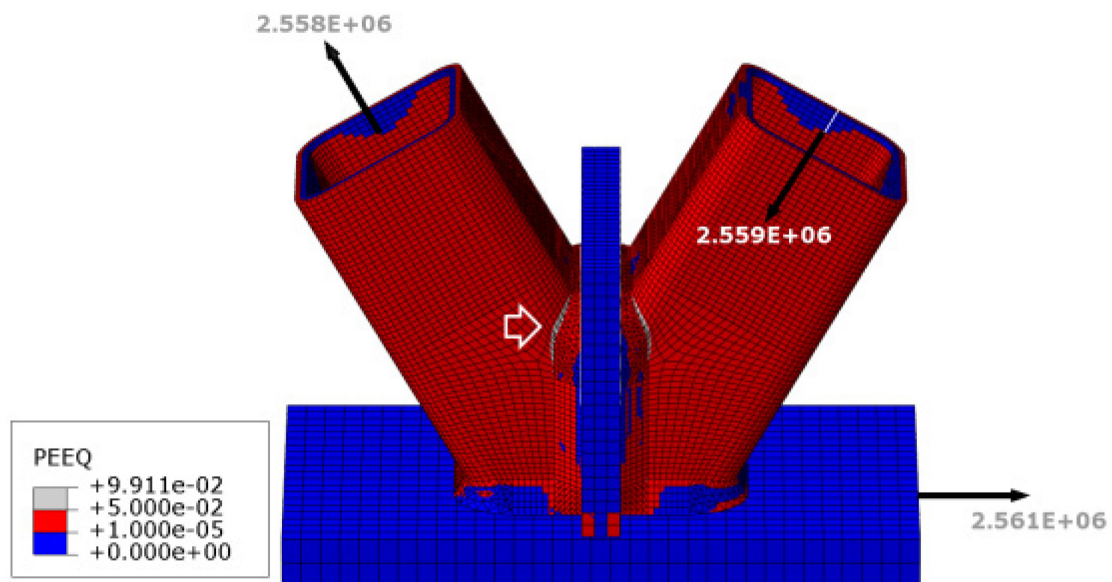


Figure 54: Equivalent plastic strains of Model 3-1 with steel grade S460.

5.3.2 Model 3-2: $t_0 = 20$ mm, $t_p = 25$ mm

For steel grade S460, the initial yielding becomes visible at the corners of the tensile bracing member close to the weld, when the normal force applied to the bracing member is 1436 kN. Regions with equivalent plastic strains exceeding 5 % are marked with an arrow in Figure 55. When the 5 % strain criterion is met at the corners of the bracing member, the normal force applied to the tension bracing member is 2404 kN. This value is nearly equal to the tension yielding capacity of the bracing member. Therefore, the failure criterion for this joint is either local yielding of the bracing member in the joint or the yielding failure of the tension bracing member.

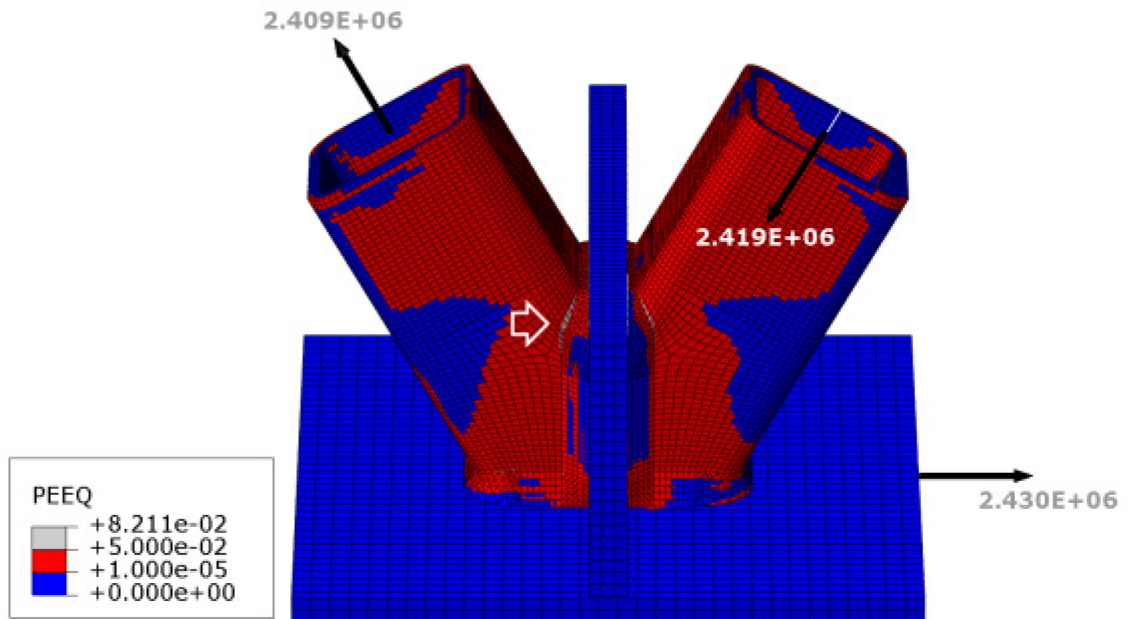


Figure 55: Equivalent plastic strains of Model 3-2 with steel grade S460.

5.3.3 Conclusion of models with $\theta = 60^\circ$ and $150 \times 150 \times 10$ bracing members

Tension load-displacement curves for models 3-1 and 3-2 are shown in Figure 56. Compression load-displacement curves are shown in Figure 57, respectively.

Reducing the lower chord thickness in the Model 3-2 causes the forces in the joint to transfer through a relatively stiffer division plate. Therefore, the equivalent plastic strain limit is reached with smaller loads and deformations than in the stiffer joint (Model 3-1). However, the location of the region where the strain criterion has been met stays the same regardless of the lower chord thickness.

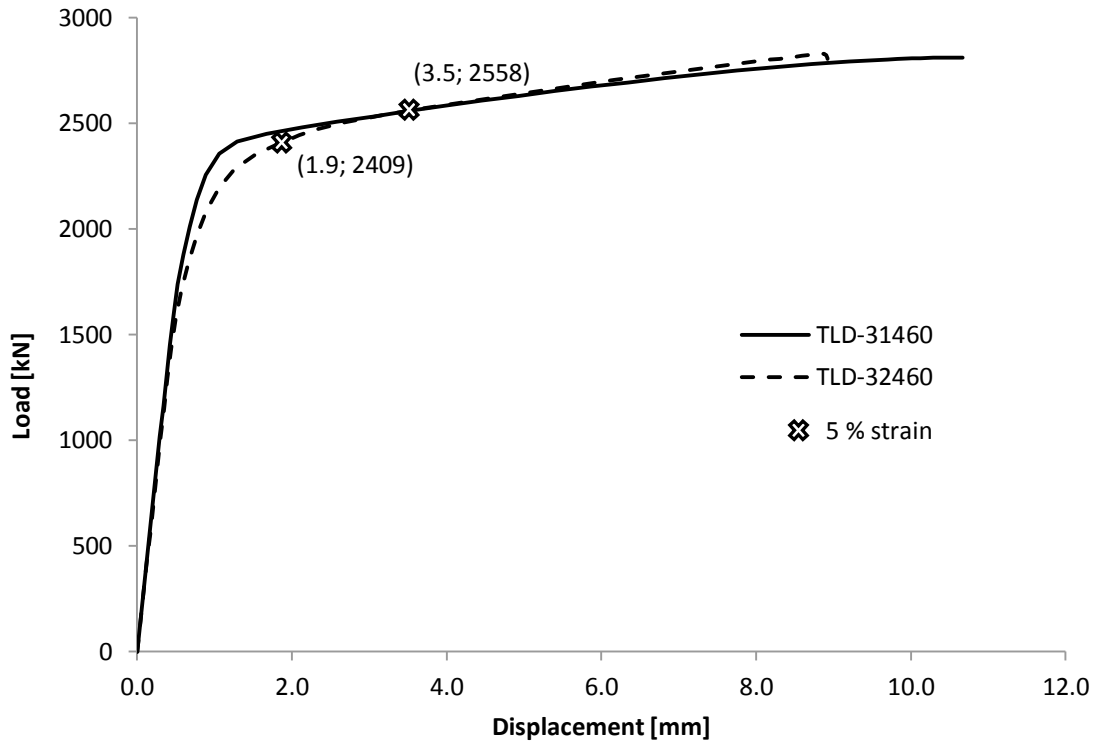


Figure 56: Load-displacement behaviour of tension bracing member in FE models 3-1 and 3-2 with steel grade S460.

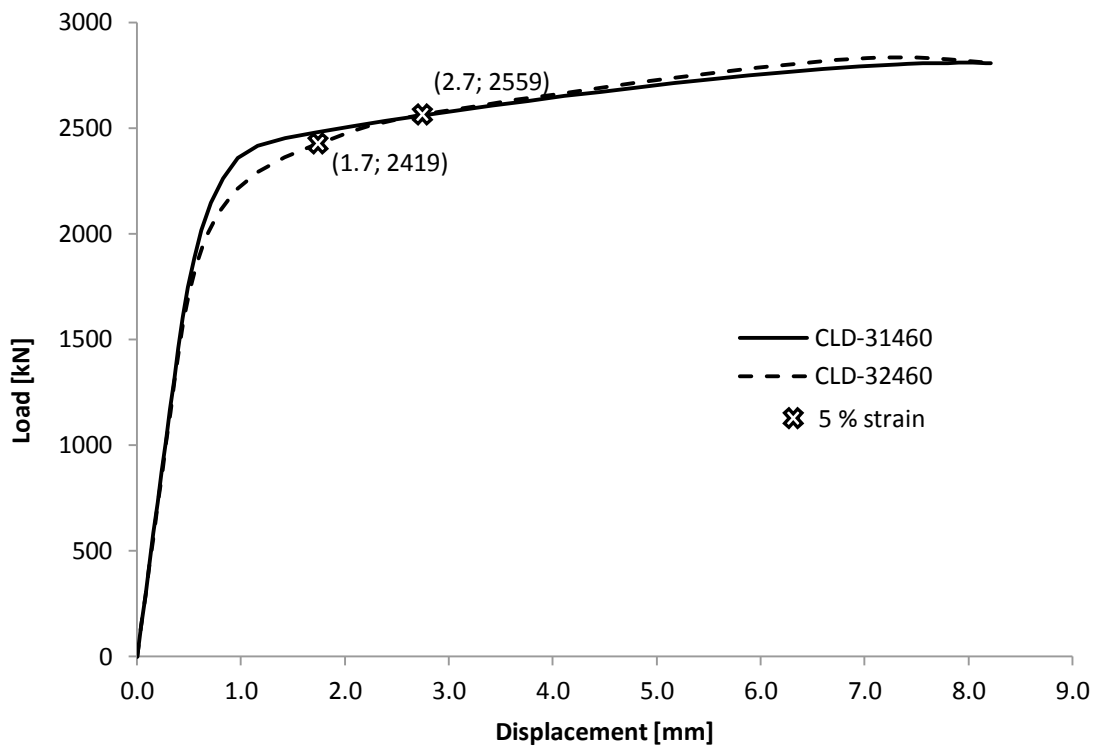


Figure 57: Load-displacement behaviour of compression bracing member in FE models 3-1 and 3-2 with steel grade S460.

5.4 Models with $\theta = 30^\circ$ and $250 \times 150 \times 10$ bracing members

5.4.1 Model 4-1: $t_0 = 40$ mm, $t_p = 25$ mm

For steel grade S460, the initial yielding becomes visible at the corners of the tensile bracing member when the normal force applied to the tensile bracing member is 1759 kN. The location of these initial yield regions are in the corners of the bracing member and close to the welds. Regions with equivalent plastic strains exceeding 5 % are marked with arrows in Figure 58. When the 5 % strain criterion is met at the corners of the bracing member, the normal force applied to the tension bracing member is 3279 KN. This value is less than the yielding capacity of the tension bracing member. Therefore, the failure criterion for Model 4-1 with steel grade S460 is the local yielding of the tension bracing member.

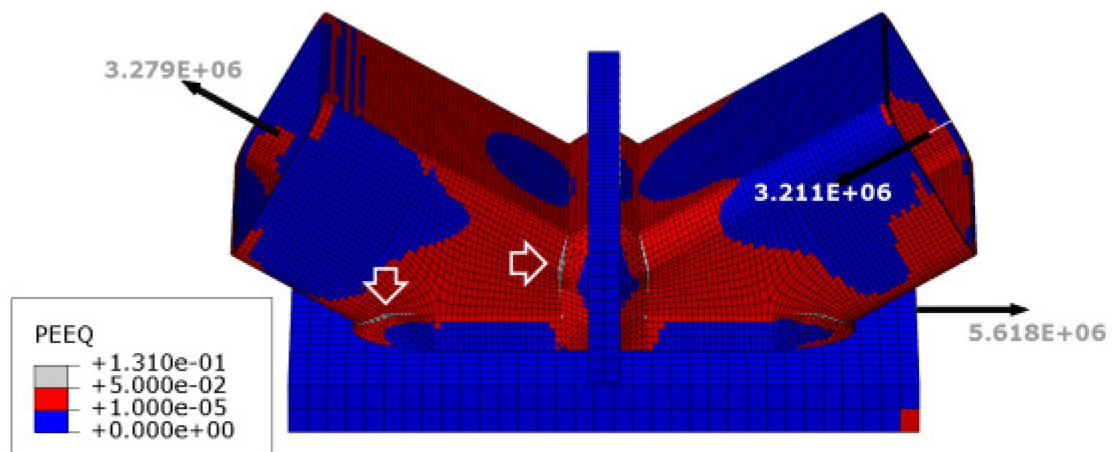


Figure 58: Equivalent plastic strains of Model 4-1 with steel grade S460.

5.4.2 Model 4-2: $t_0 = 20$ mm, $t_p = 25$ mm

When the thickness of the lower chord is reduced, the force transfer in the joint is concentrated through the division plate, as this is a stiffer part compared to the lower chord. The initial yielding occurs when the normal force applied on the tensile bracing member is 1340 kN. The location of the initial yielding regions is in the corners of the bracing member near the areas where the weld intersects with the bracing member. Regions with equivalent plastic strains exceeding 5 % are marked with arrows in Figure 59. Because of the reduced stiffness of the joint, the strain criterion is met earlier than in the previous model. However, the location of the areas where the strain criterion has first been reached is the same.

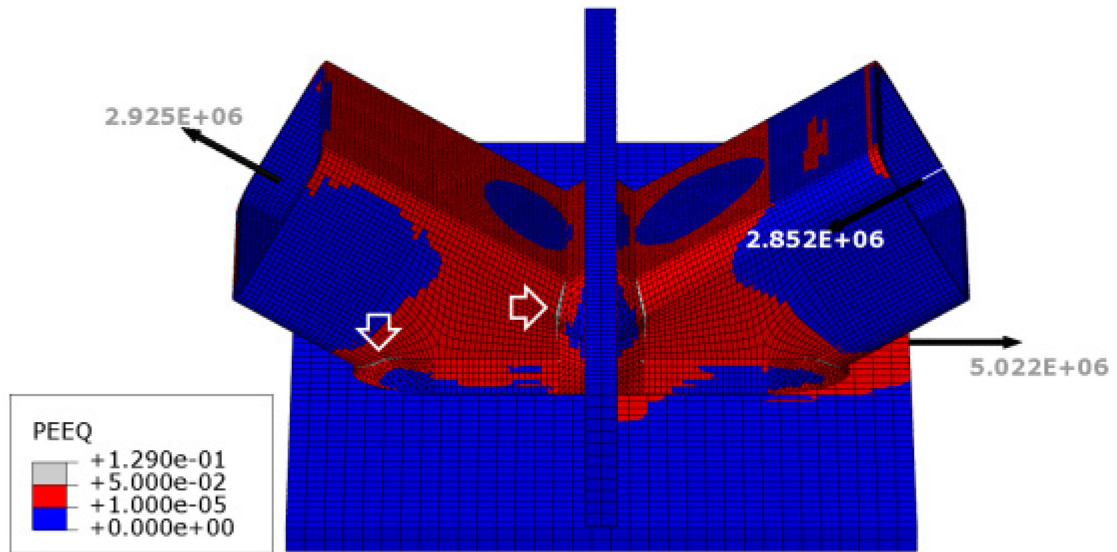


Figure 59: Equivalent plastic strains of Model 4-2 with steel grade S460.

5.4.3 Model 4-3: $t_0 = 40 \text{ mm}$, $t_p = 35 \text{ mm}$

The initial yielding occurs when the normal force applied on the tensile bracing member is 1761 kN. The region with equivalent plastic strains exceeding 5 % is marked with an arrow in Figure 60. When the 5 % strain criterion is met at the corners of the bracing member, the normal force applied to the tension bracing member is 3523 kN. The failure criterion for this joint is either local yielding of the bracing member in the joint or possible yielding failure of the tension bracing member.

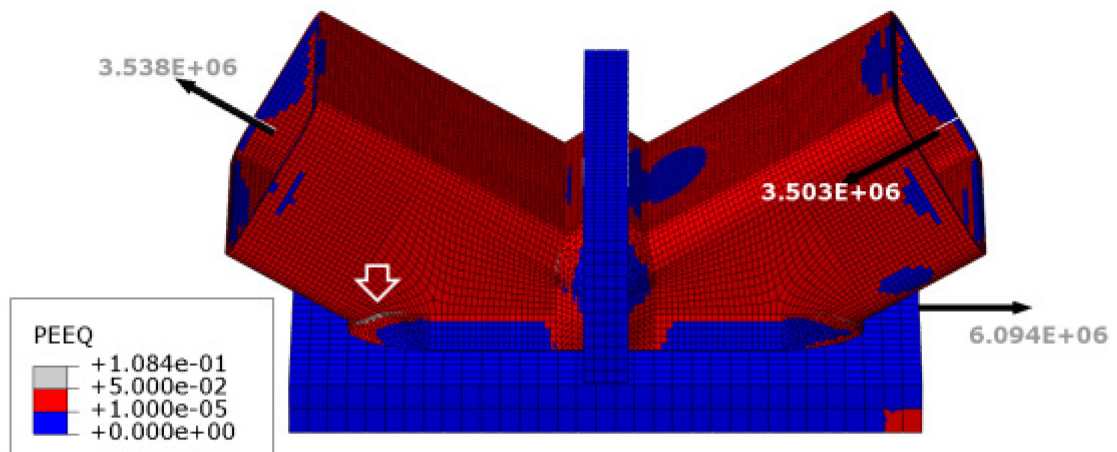


Figure 60: Equivalent plastic strains of Model 4-3 with steel grade S460.

5.4.4 Conclusion of models with $\theta = 30^\circ$ and 250×150×10 bracing members

Tension load-displacement (TLD) curves of three models are shown in Figure 61, respectively. Crosses mark the normal force applied on bracing members and their respective displacements when the 5 % equivalent plastic strain criterion has been met. In Models 4-1 and 4-2, the 5 % equivalent plastic strain criterion is met earlier than the yielding capacity of bracing members. In Model 4-3, the thickness of the division plate was increased from 25 mm to 35 mm. This causes the joint to be stiffer compared to the Model 2-1 and the 5 % strain criterion was met in the joint with significantly larger bracing member deformations. However, the yielding resistance of the bracing member is exceeded before the 5 % criterion is met, leading to possible yielding failure of the bracing member in the truss.

Compression load-displacement curves (CLD) of three models are shown in Figure 62. As seen in the figure, the 5 % equivalent strain criteria are reached earlier than the peak loads for compression bracing members. The region where the strain limit is met depends on the division plate thickness.

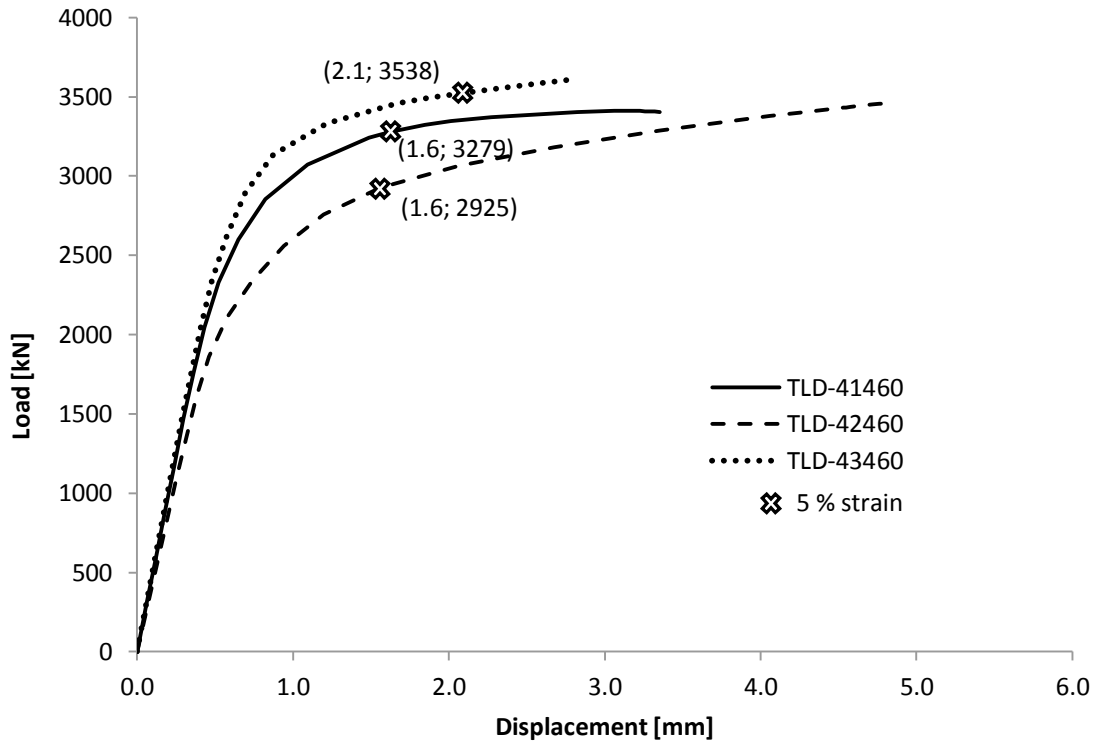


Figure 61: Load-displacement behaviour of tension bracing member in FE models 4-1, 4-2, and 4-3 with steel grade S460.

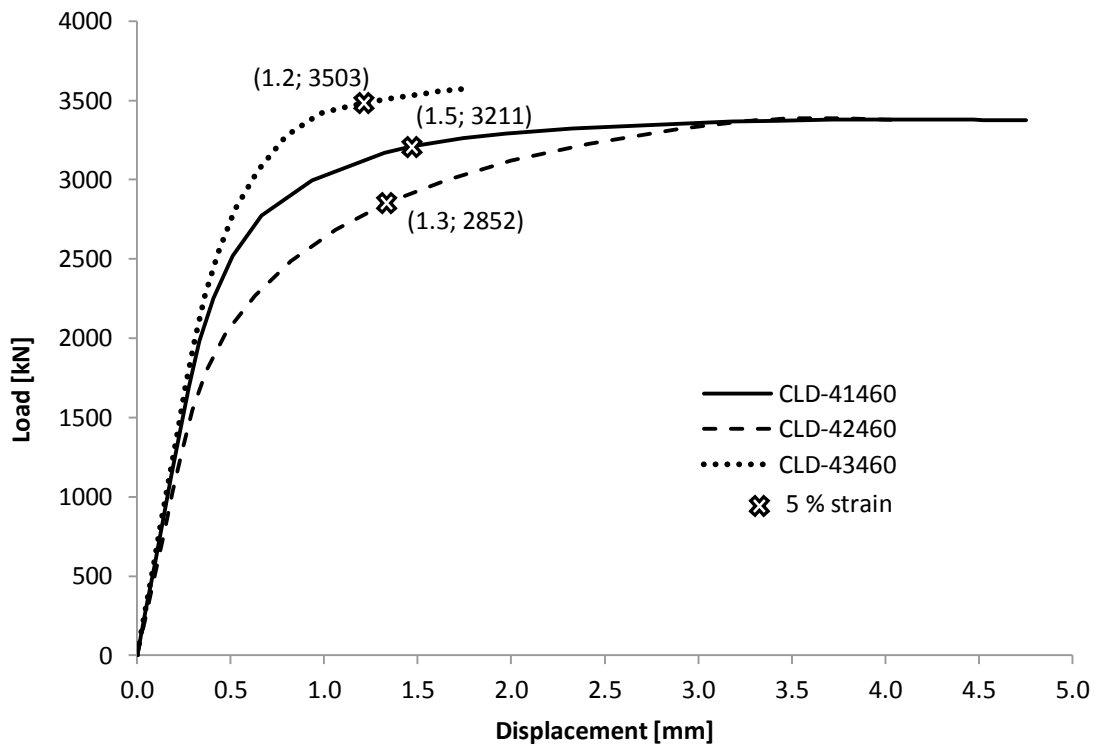


Figure 62: Load-displacement behaviour of compression bracing member in FE models 4-1, 4-2, and 4-3 with steel grade S460.

5.5 Models with $\theta = 45^\circ$ and $250 \times 150 \times 10$ bracing members

5.5.1 Model 5-1: $t_0 = 40$ mm, $t_p = 25$ mm

The initial yielding occurs near the welds at corners of the bracing member, when the normal force applied to the bracing member is 1645 kN. The region with equivalent plastic strains exceeding 5 % is marked with an arrow in Figure 63. When the strain criterion is met at the corners of the bracing member, the normal force applied to the tension bracing member is 2753 kN. This value is significantly smaller than the tension yielding capacity of the bracing member. Therefore, the failure criterion for this joint is the local yielding of the bracing member in the region marked with an arrow in Figure 63.

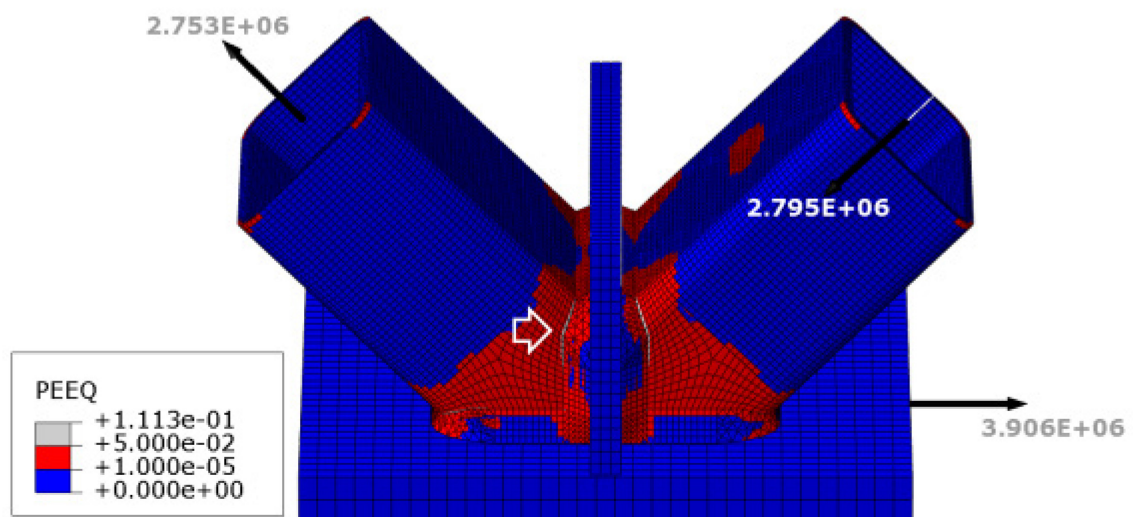


Figure 63: Equivalent plastic strains of Model 5-1 with steel grade S460.

5.5.2 Model 5-2: $t_0 = 20$ mm, $t_p = 25$ mm

The initial yielding takes place near the welds at corners of the bracing member, when the normal force applied to the bracing member is 1338 kN. The region with equivalent plastic strains exceeding 5 % is marked with an arrow in Figure 64. When the strain criterion is met at the corners of the bracing member, the normal force applied to the tension bracing member is 2496 kN. This value is significantly smaller than the tension yielding capacity of the bracing member. Therefore, the failure criterion for this joint is the local yielding of the bracing member in the region marked with an arrow in Figure 64.

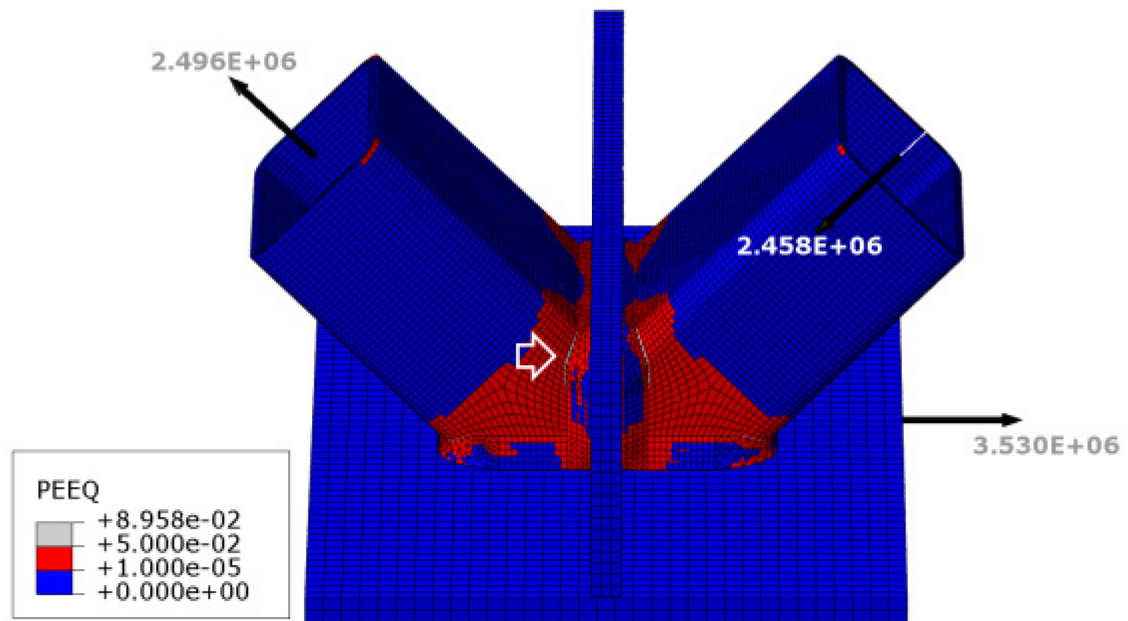


Figure 64: Equivalent plastic strains of Model 5-2 with steel grade S460.

5.5.3 Conclusion of models with $\theta = 45^\circ$ and $250 \times 150 \times 10$ bracing members

Tension load-displacement (TLD) curves of two models are shown in Figure 65, respectively. Crosses mark the normal force applied on bracing members and their respective displacements when the 5 % equivalent plastic strain criterion has been met. In the Model 5-2, the strain criterion is met with lower normal force applied to the tension bracing member. The stiffness of the joint is reduced, when thinner lower chord compared to Model 5-1 is used.

Compression load-displacement curves (CLD) of two models are shown in Figure 66. The 5 % equivalent strain criteria are reached earlier than the peak loads for compression members.

The region where the strain criterion is met stays the same regardless of the lower chord thickness in Models 5-1 and 5-2. Also, there is no difference in the deformation of the bracing members at the 5 % limit load.

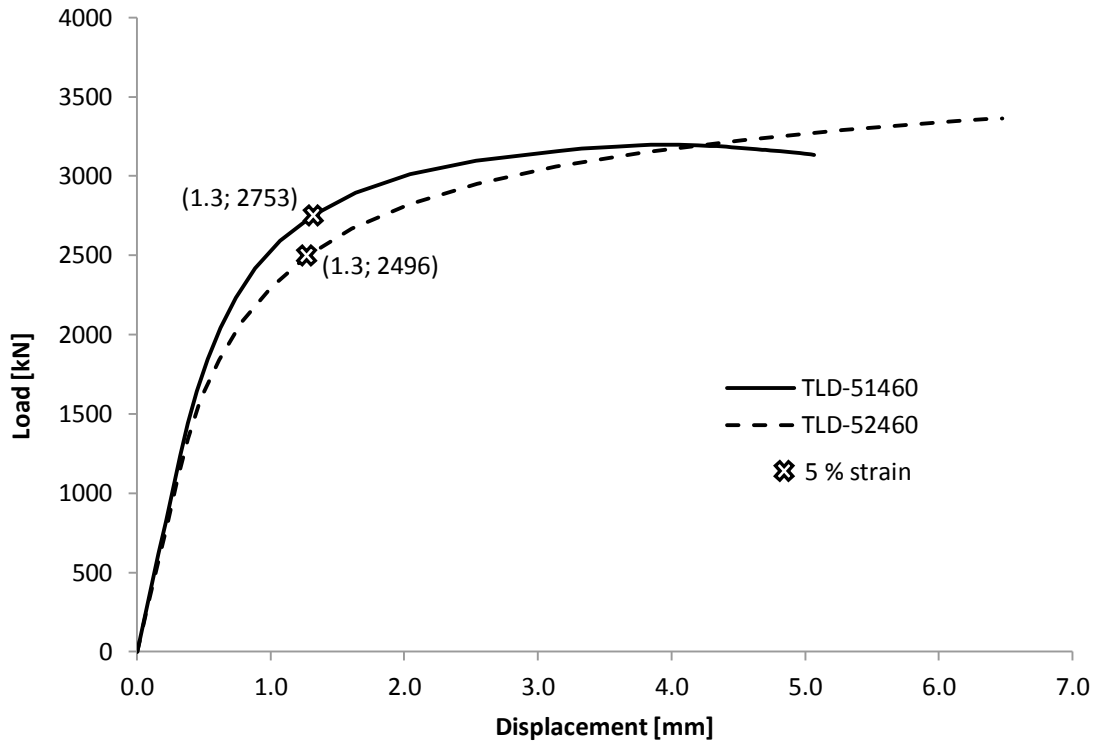


Figure 65: Load-displacement behaviour of tension bracing member in FE models 5-1 and 5-2 with steel grade S460.

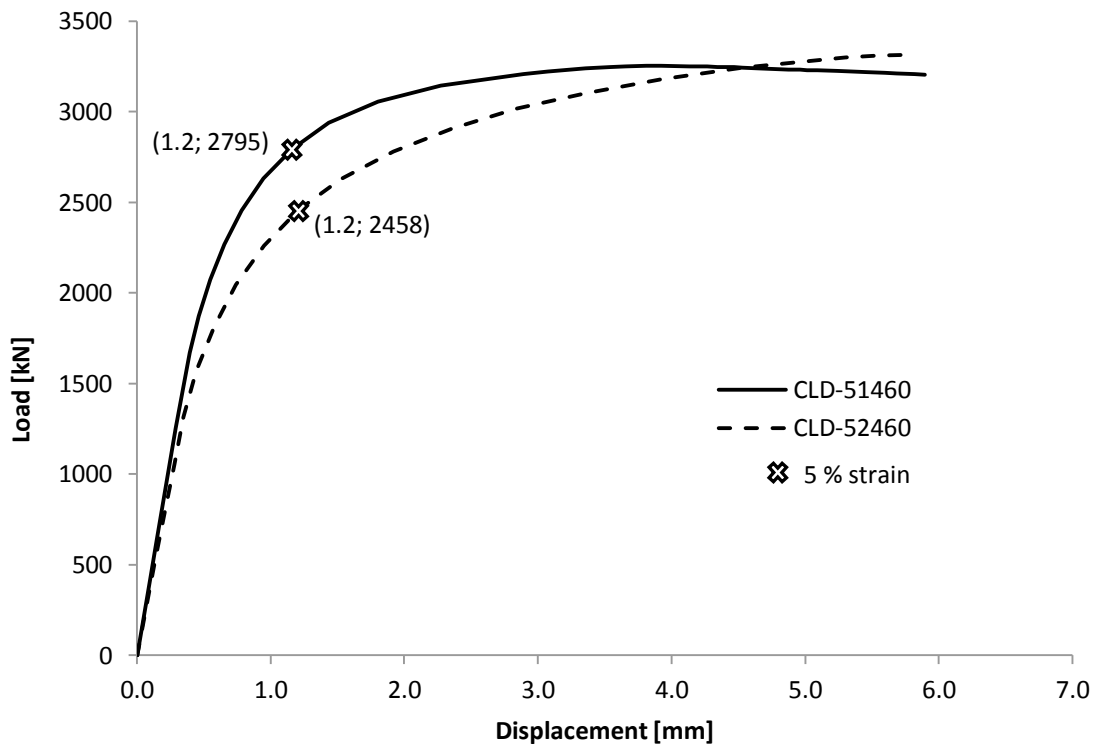


Figure 66: Load-displacement behaviour of compression bracing member in FE models 5-1 and 5-2 with steel grade S460.

5.6 Models with $\theta = 60^\circ$ and $250 \times 150 \times 10$ bracing members

5.6.1 Model 6-1: $t_0 = 40$ mm, $t_p = 25$ mm

The initial yielding occurs near the welds at the corners of the bracing member, when the normal force applied to the bracing member is 1846 kN. The region with equivalent plastic strains exceeding 5 % is marked with an arrow in Figure 67. When the strain criterion is met at the corners of the bracing member, the normal force applied to the tension bracing member is 3316 kN. This value is only slightly smaller than the tension yielding capacity of the bracing member. Therefore, the failure criterion for this joint is the local yielding of the bracing member, but one possible failure criterion to consider is also the yielding failure of the tension bracing member.

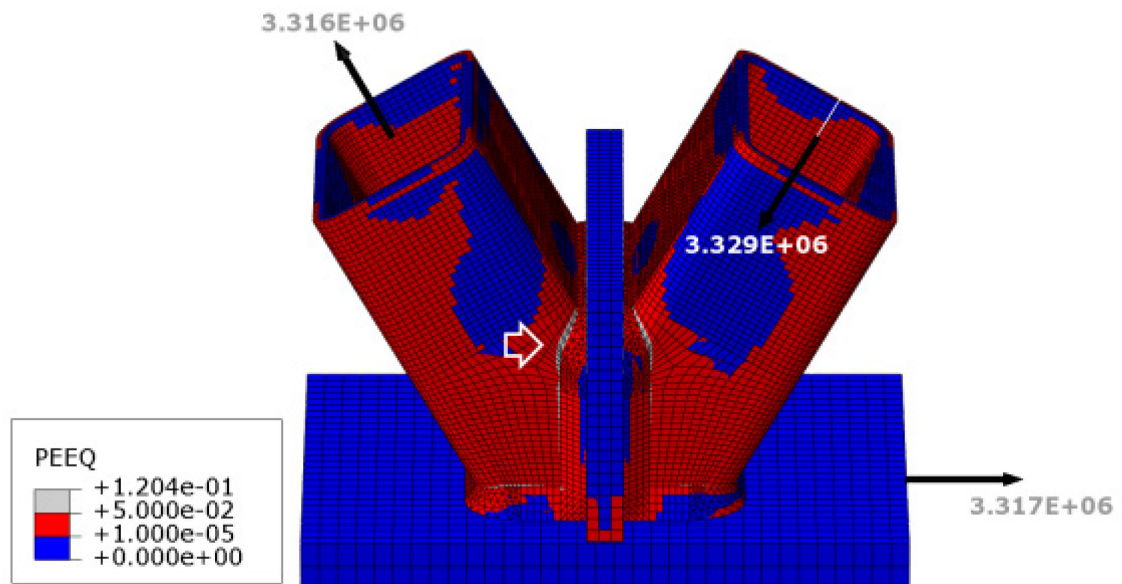


Figure 67: Equivalent plastic strains of Model 6-1 with steel grade S460.

5.6.2 Model 6-1: $t_0 = 20$ mm, $t_p = 25$ mm

The initial yielding occurs near the welds at the corners of the bracing member, when the normal force applied to the bracing member is 1714 kN. The region with equivalent plastic strains exceeding 5 % is marked with an arrow in Figure 68. When the strain criterion is met at the corners of the bracing member, the normal force applied to the tension bracing member is 3125 kN. This value is smaller than the tension yielding capacity of the bracing member. Therefore, the failure criterion for this joint is the local yielding of the bracing member.

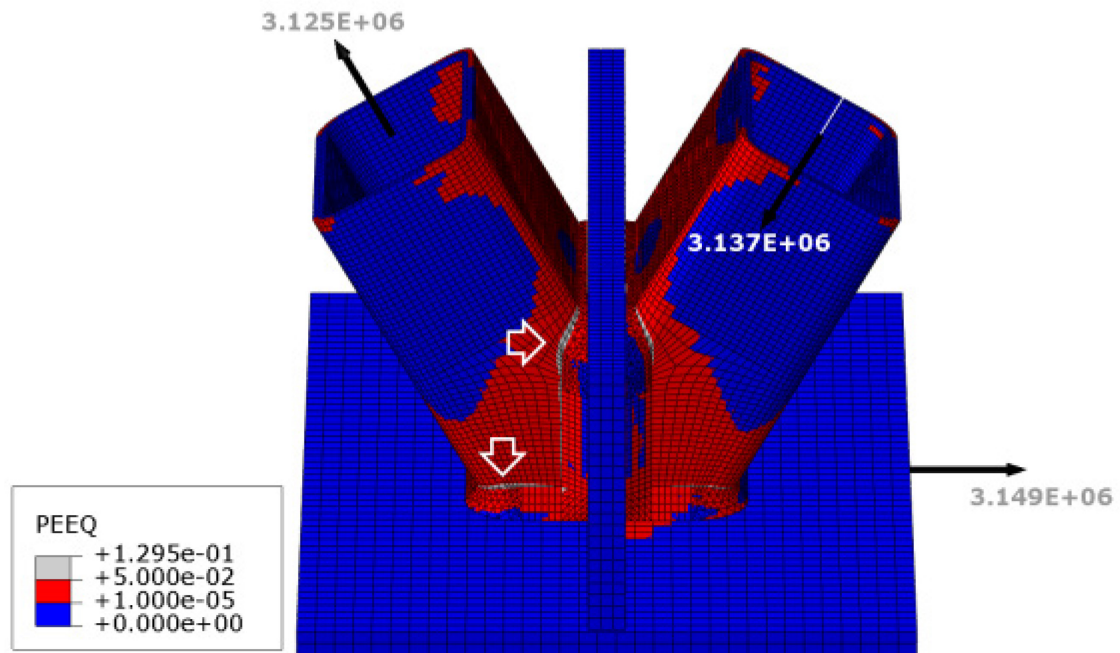


Figure 68: Equivalent plastic strains of Model 6-2 with steel grade S460.

5.6.3 Conclusion of models with $\theta = 60^\circ$ and $250 \times 150 \times 10$ bracing members

Tension load-displacement (TLD) curves of two models are shown in Figure 69, respectively. Crosses mark the normal force applied on bracing members and their respective displacements when the 5 % equivalent plastic strain criterion has been met. In the Model 6-2, the strain criterion is met with lower normal force applied to the tension bracing member. The stiffness of the joint is reduced, when a thinner lower chord compared to Model 6-1 is used.

Compression load-displacement curves (CLD) of two models are shown in Figure 70. The 5 % equivalent strain criteria are reached earlier than the peak loads for compression members.

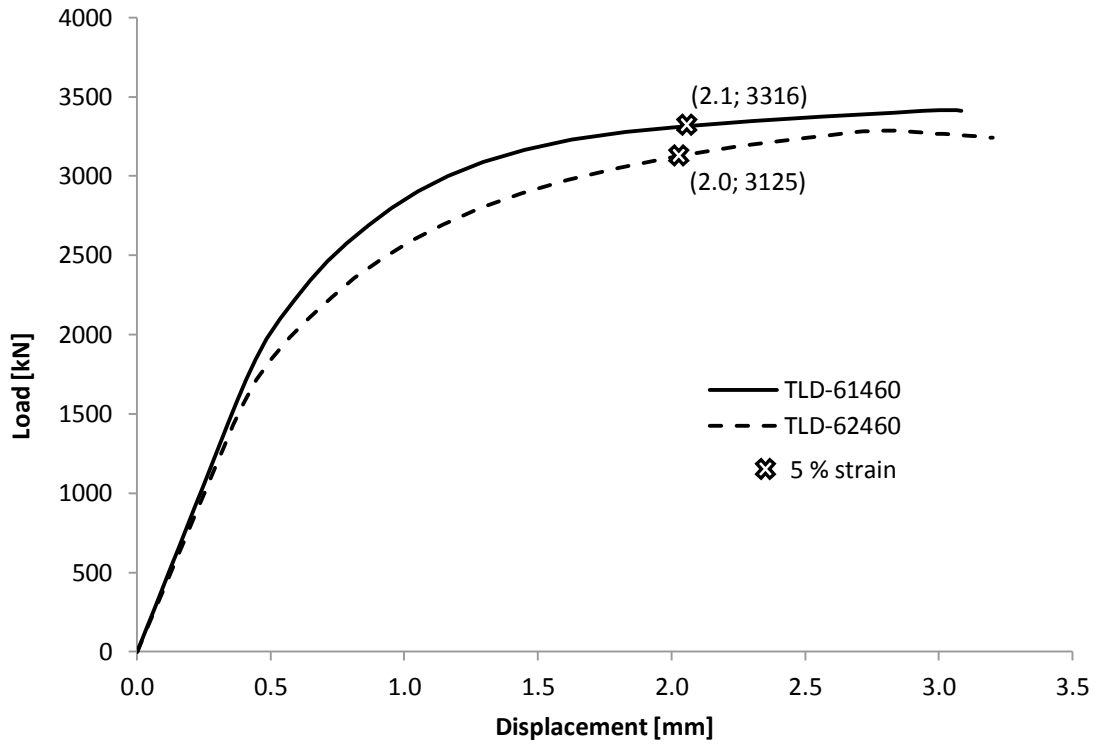


Figure 69: Load-displacement behaviour of tension bracing member in FE models 6-1 and 6-2 with steel grade S550.

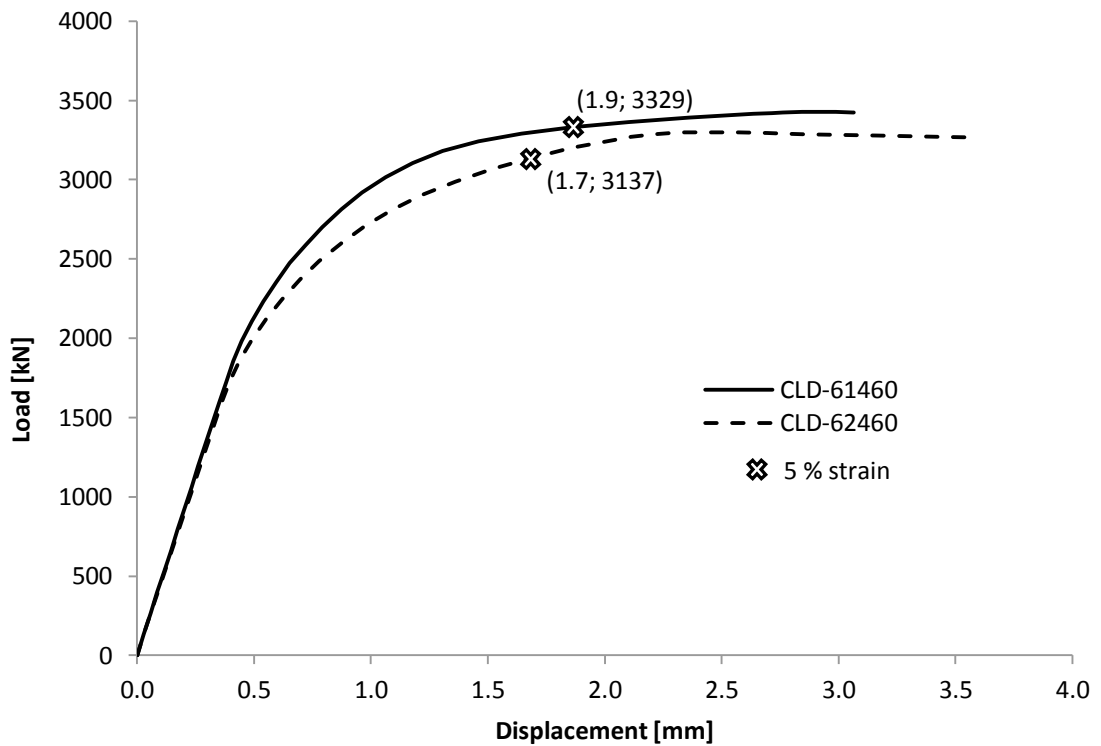


Figure 70: Load-displacement behaviour of compression bracing member in FE models 6-1 and 6-2 with steel grade S460.

5.7 Comparison of brace inclination angles

Figure 71-77 show the load-displacement curves for the end of the tension bracing member in the joint when only the inclination angle of bracing members is varied in the models.

It is seen that for models with 150×150×10 bracing members, varying of the inclination angle of bracing member is more sensitive in models with lower chord thickness $t_0 = 20$ mm causing larger variation of displacement capacity compared to models with $t_0 = 40$ mm. In both cases, the inclination angle $\theta = 30^\circ$ leads to slightly higher limit loads compared to models with $\theta = 45^\circ$ or $\theta = 60^\circ$. The limit load with the inclination angle $\theta = 30^\circ$ is ~6 % higher than the limit load with $\theta = 45^\circ$ in models where $t_0 = 40$ mm. In models with $t_0 = 20$ mm the difference is even larger (~9 %). The inclination angle $\theta = 45^\circ$ leads to smallest limit loads in both cases where $t_0 = 20$ mm and $t_0 = 40$ mm.

For models with 250×150×10 bracing members, the deformations respective to limit loads do not show practically any variance when the inclination angle is kept constant and the lower chord thickness is reduced from $t_0 = 40$ mm to $t_0 = 20$ mm. However, compared to models with 150×150×10 bracing members, wider bracing members cause a higher variation for limit loads when the inclination angle is changed. The inclination angle $\theta = 60^\circ$ leads to slightly higher limit loads compared to models with $\theta = 30^\circ$ or $\theta = 45^\circ$ regardless of lower chord thickness. The limit load with the inclination angle $\theta = 60^\circ$ is ~20 % higher than the limit load with $\theta = 45^\circ$ in models where $t_0 = 40$ mm. In models with $t_0 = 20$ mm the difference is even larger (~25 %). The inclination angle $\theta = 45^\circ$ leads to smallest limit loads and deformations in both cases where $t_0 = 20$ mm and $t_0 = 40$ mm.

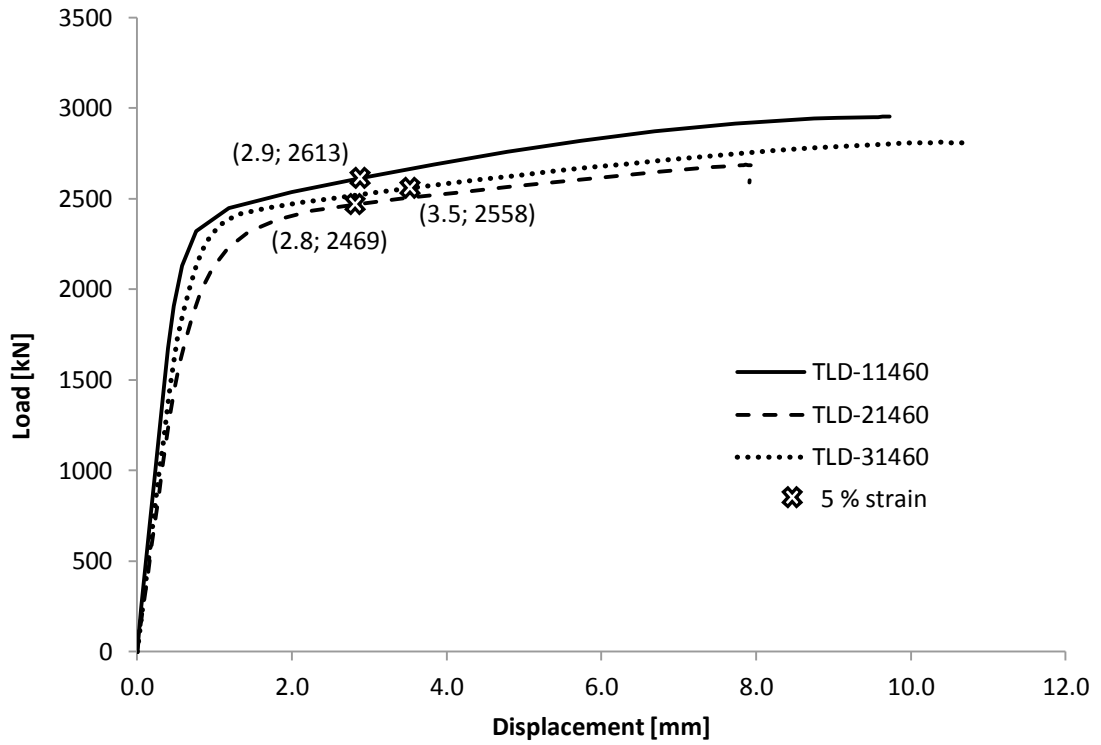


Figure 71: Comparison of load-displacement curves from models with different bracing inclination angles. Bracing members: $150 \times 150 \times 10$, $t_0 = 40$ mm, $t_p = 25$ mm.

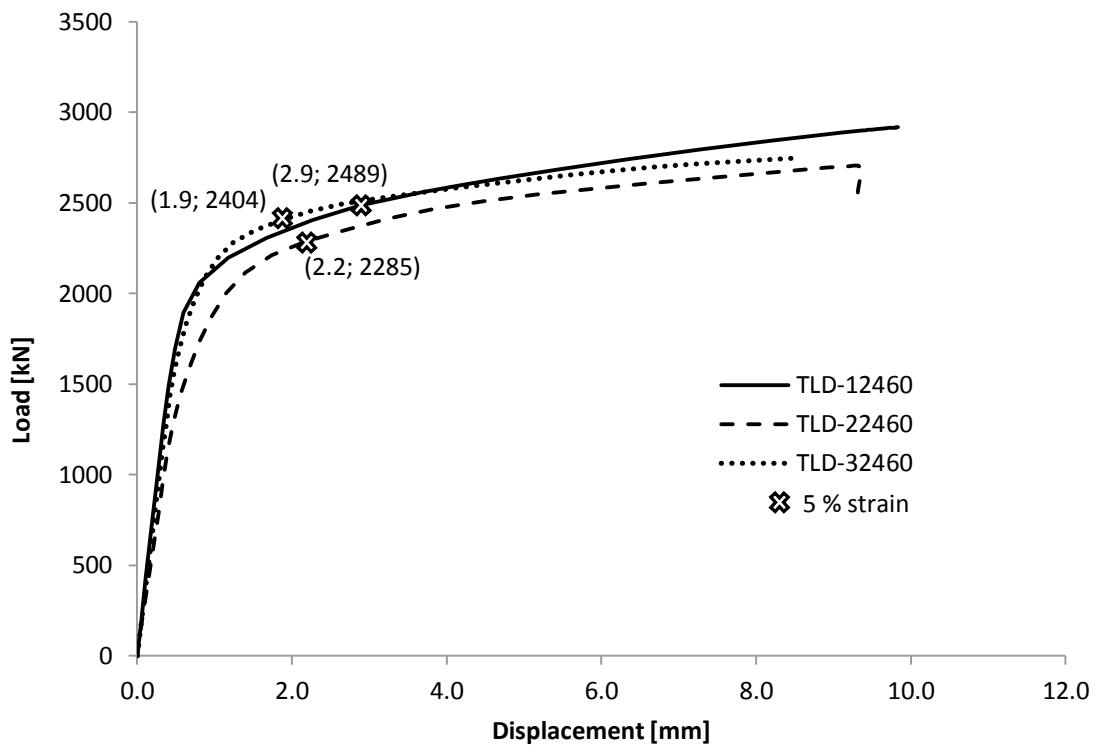


Figure 72: Comparison of load-displacement curves from models with different bracing inclination angles. Bracing members: $150 \times 150 \times 10$, $t_0 = 20$ mm, $t_p = 25$ mm.

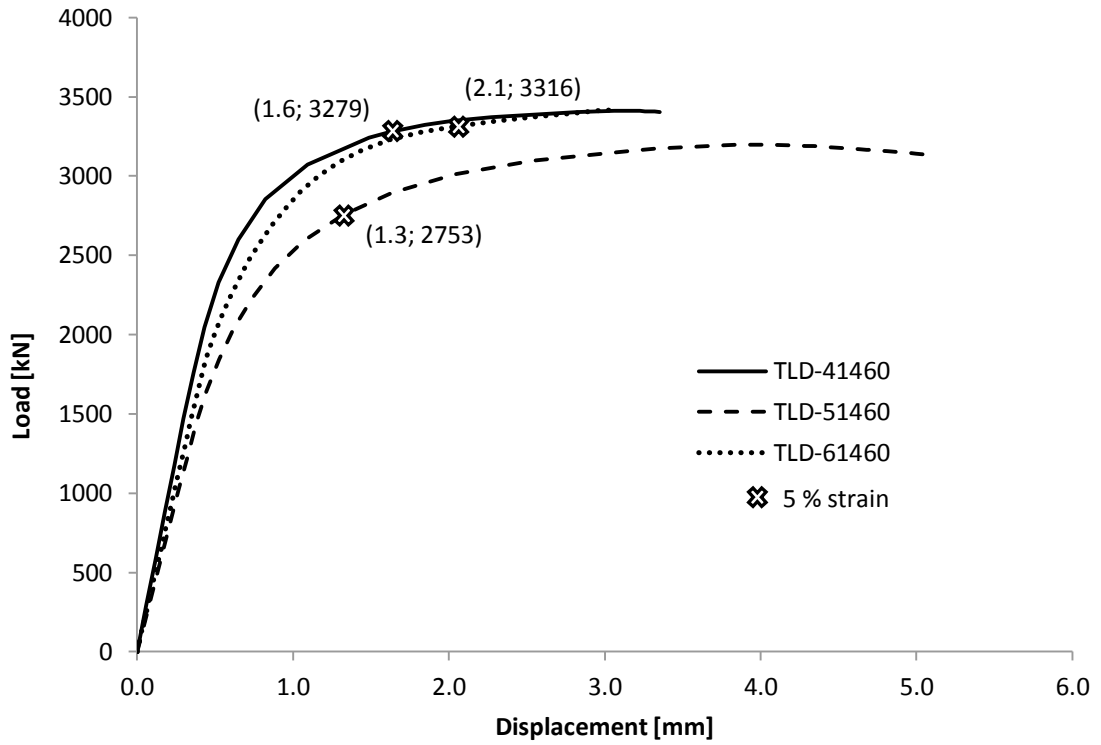


Figure 73: Comparison of load-displacement curves from models with different bracing inclination angles. Bracing members: $250 \times 150 \times 10$, $t_0 = 40$ mm, $t_p = 25$ mm.

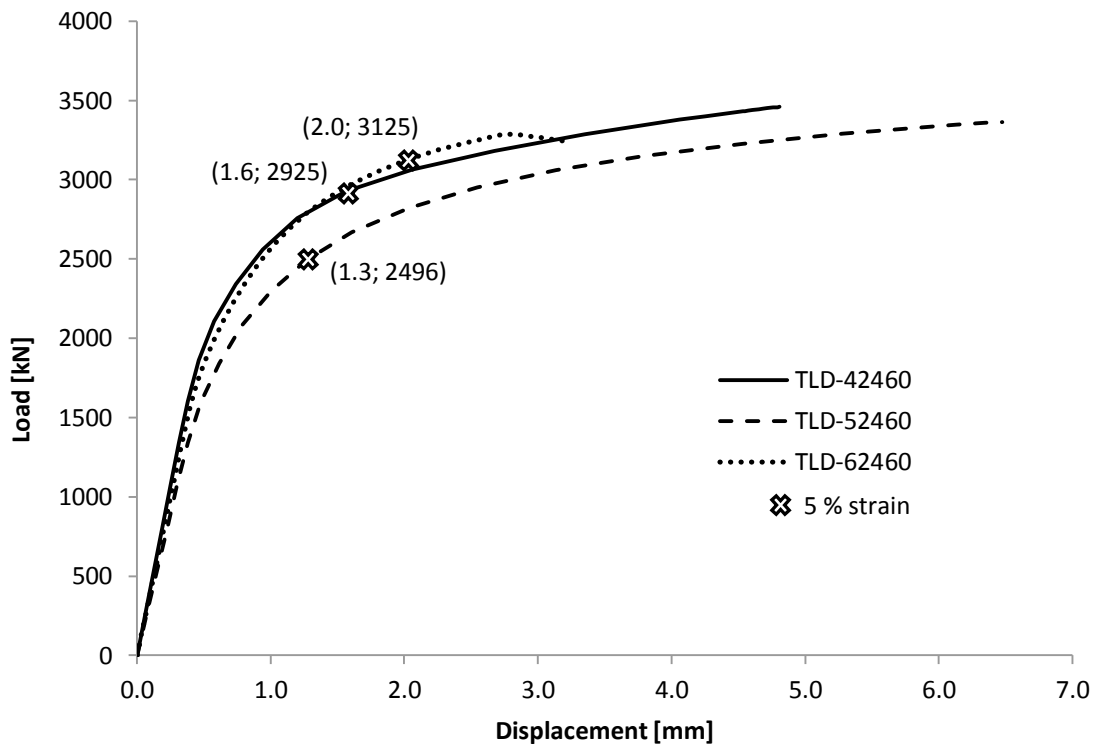


Figure 74: Comparison of load-displacement curves from models with different bracing inclination angles. Bracing members: $250 \times 150 \times 10$, $t_0 = 20$ mm, $t_p = 25$ mm.

5.8 Comparison with EN 1993-1-8

The comparison of joint resistances according to FE analysis and EN 1993-1-8 are shown in Figure 75-78. It can be seen that for this type of joint EN 1993-1-8 gives conservative results when bracing members of $150 \times 150 \times 10$ are being used. The same phenomenon is seen with $250 \times 150 \times 10$ bracing members used together with the lower chord having a thickness of 20 mm. However, for models with a thicker lower chord, EN 1993-1-8 might even slightly over-estimate the joint resistance. The equations also do not take into account the inclination angles of the bracing members. Hence, the equations given in current Eurocode to obtain the design resistance for joints between square or circular hollow sections or the design resistance of the reinforced welded K and N joints between RHS or CHS brace members and RHS chords are not valid to be used in the joint, where the steel plate acts as a lower chord.

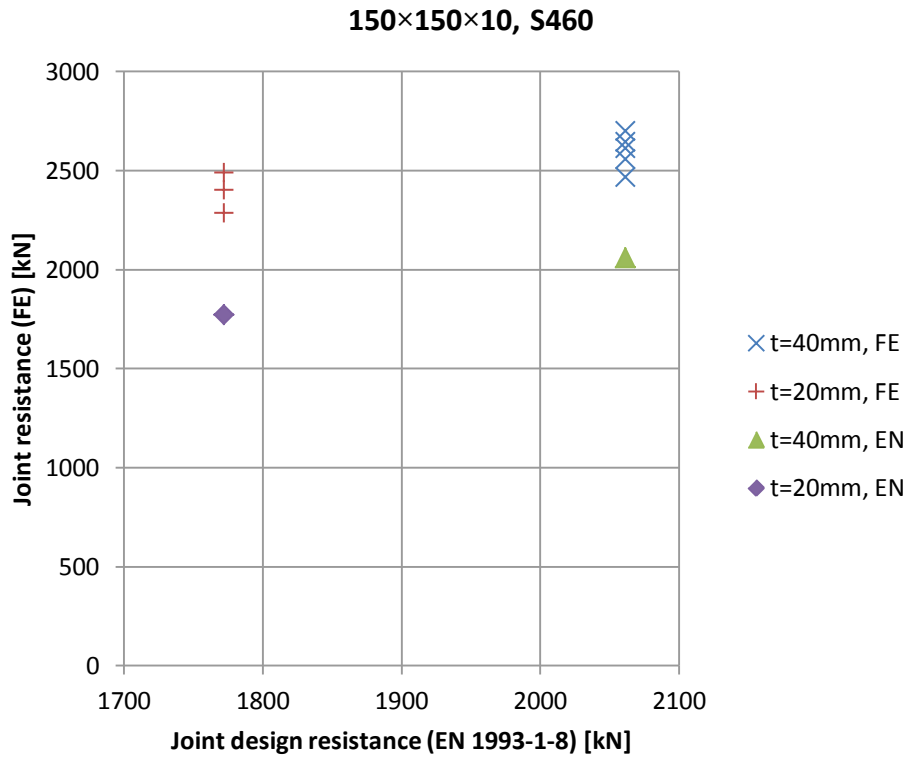


Figure 75: Joint resistances according to FE analysis and EN 1993-1-8 for models with 150×150×10 bracing members, steel grade S460 and two different lower chord thicknesses.

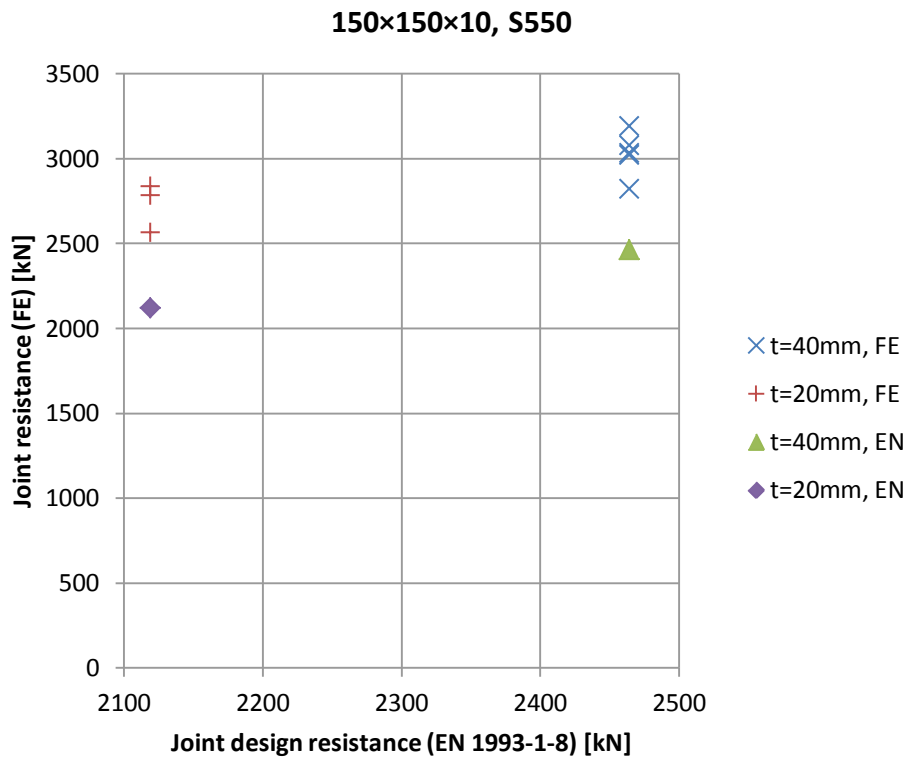


Figure 76: Joint resistances according to FE analysis and EN 1993-1-8 for models with 150×150×10 bracing members, steel grade S550 and two different lower chord thicknesses.

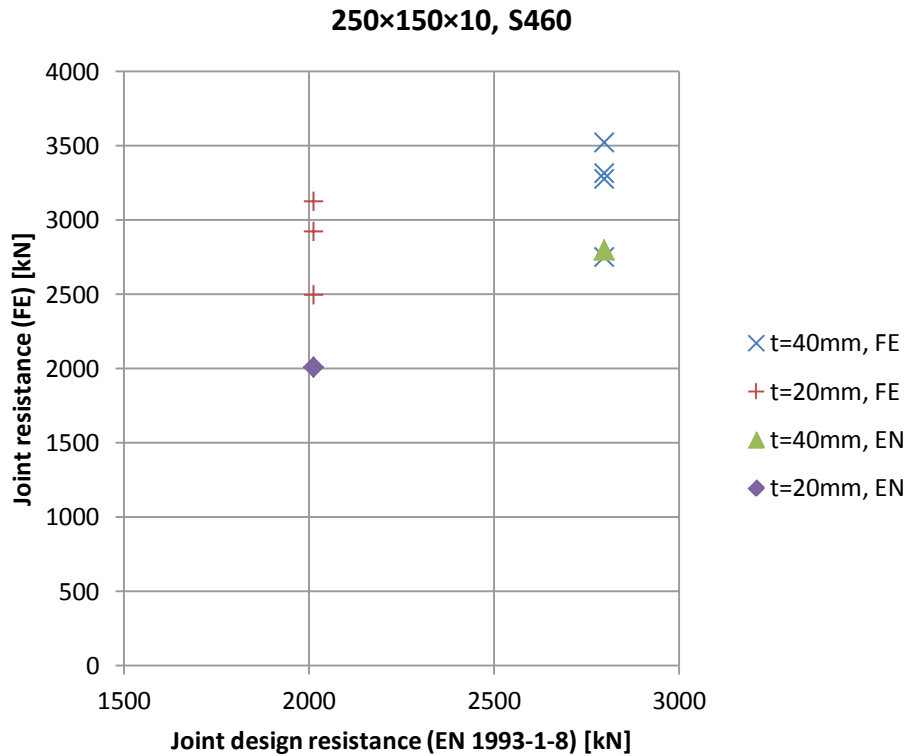


Figure 77: Joint resistances according to FE analysis and EN 1993-1-8 for models with 250×150×10 bracing members, steel grade S460 and two different lower chord thicknesses.

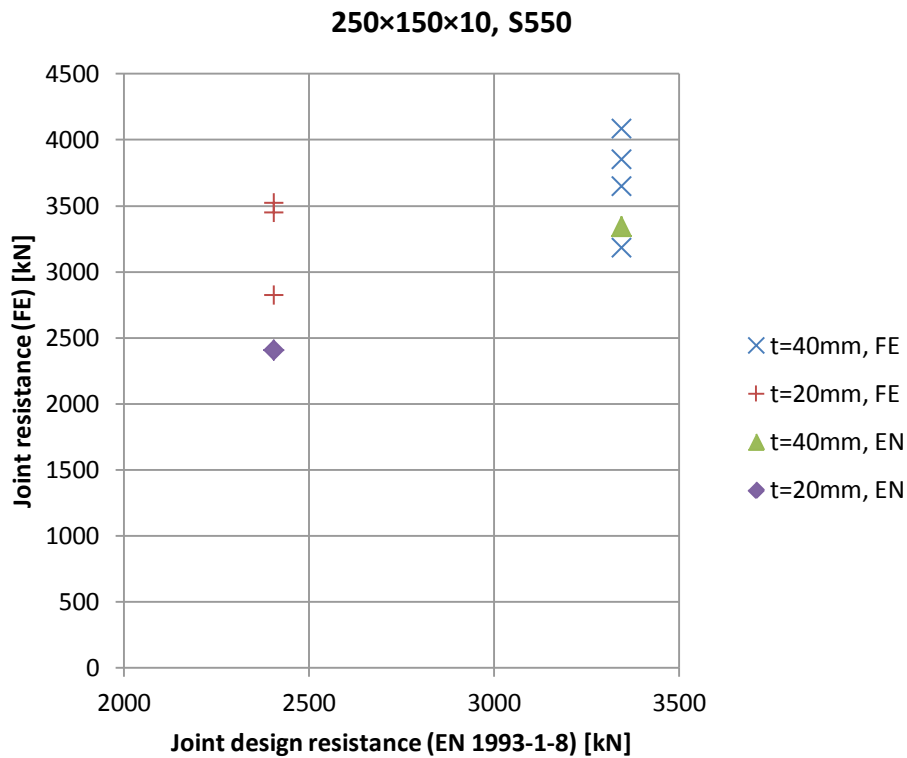


Figure 78: Joint resistances according to FE analysis and EN 1993-1-8 for models with 250×150×10 bracing members, steel grade S550 and two different lower chord thicknesses.

6 Conclusions

The joint failure was determined when the normal force applied on bracing members caused 5 % equivalent plastic strains in the joint. Figure 79 shows possible failure locations in the joint. The only failure criterion for all joint variations was found to be local yielding of the bracing member. This criterion always occurred on the tension side of the joint. Normal forces applied to the joint members at the point where the equivalent plastic strain criterion has been reached are shown in Table 16. The table also shows the respective displacements of the bracing end and failure locations in the joint. Two locations for failure were identified. The 5 % plastic strain limit was first exceeded either in the tension bracing member corners close to the lower chord (LC), or tension bracing member corners close to the division plate (DP). In some models, the strain limit was seen to be reached simultaneously in both regions.

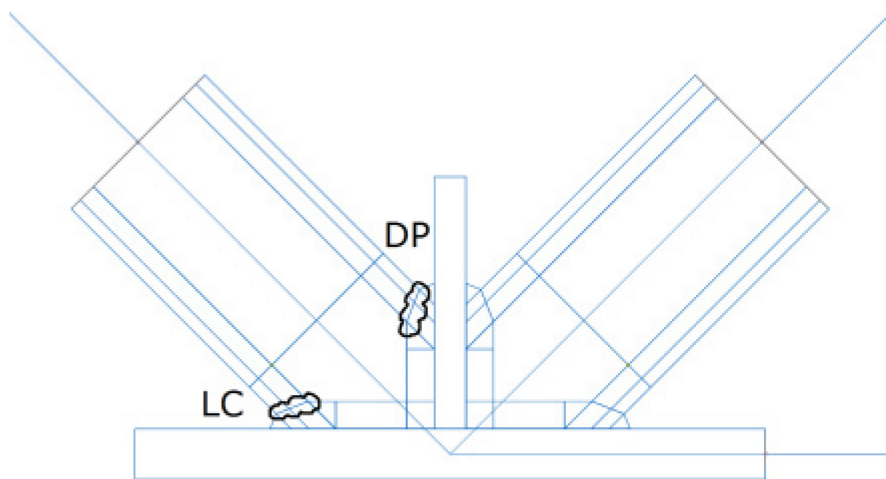


Figure 79: Failure locations in the joint.

Table 20 shows the normal forces on the joint members, tension bracing member displacements and failure locations in the joint when the 5 % equivalent plastic strain criterion has been reached. Smaller relative displacements occur at the limit load when the steel grade is increased, although no clear rule can be observed. Depending on the model, the relative displacement for steel grade S550 is 71...108 % of the displacement of steel grade S460. Increasing the steel grade from S460 to S550 results in the increase of the joint capacity of 12...19 % depending on the model. No clear reasons for the variation can be observed.

In truss design, it is safer to use thicker steel plate as a lower chord, which leads to the situation that yielding capacity of the tension bracing member in the truss is reached before the local yielding of the bracing member occurs in the joint.

High stress concentrations such as folds in weld geometry were seen in regions with a geometrical discontinuity. In those regions, the equivalent plastic strain limits were first met, especially in models with $\theta_1 = \theta_2 = 60^\circ$. Smoother geometry modelling would reduce these stress concentrations. This would possibly lead to equivalent plastic strain limit to be reached with slightly higher normal forces applied to bracing members.

The current standard 1993-1-8 does not give valid methods to define the capacity of this type of K joint. Equations for defining the load capacity for K type overlap joint with a division plate lead to conservative results with $150 \times 150 \times 10$ bracing members. However, for the joints with $250 \times 150 \times 10$ bracing members these equations can even lead to non-conservative results as was seen in cases where $t_0 = 40$ mm. A full-scale loading test should be performed to validate the FE model and failure locations in the joint against the true behaviour of the joint.

Table 20: Normal forces on the joint members, tension bracing member displacements and failure locations in the joint when the 5 % equivalent plastic strain criterion has been reached.

Model	Steel grade	Normal force [kN]			Displacement [mm]	Failure location
		N_1	N_2	N_0		
1-1	S460	2613	2592	4506	2.9	LC
	S550	3021	3001	5214	2.3	LC
1-2	S460	2489	2465	4303	2.9	LC
	S550	2839	2817	4913	2.4	LC
1-3	S460	2647	2628	4565	3.4	LC
	S550	3080	3064	5316	2.9	LC
2-1	S460	2469	2510	3501	2.8	DP, LC
	S550	2824	2871	4005	2.0	DP, LC
2-2	S460	2285	2323	3257	2.2	DP, LC
	S550	2565	2608	3658	1.8	DP
2-3	S460	2701	2752	3831	6.5	DP, LC
	S550	3193	3253	4528	6.6	DP
3-1	S460	2558	2559	2561	3.5	DP
	S550	3034	3034	3036	3.5	DP
3-2	S460	2404	2414	2425	1.9	DP
	S550	2786	2795	2807	1.7	DP
4-1	S460	3279	3211	5618	1.6	DP, LC
	S550	3647	3563	6243	1.3	LC
4-2	S460	2925	2852	5022	1.6	DP, LC
	S550	3451	3371	5928	1.7	DP, LC
4-3	S460	3523	3482	6064	2.1	LC
	S550	4085	4039	7033	1.7	LC
5-1	S460	2753	2795	3906	1.3	DP
	S550	3184	3234	4518	1.4	DP
5-2	S460	2496	2458	3530	1.3	DP
	S550	2825	2866	4025	1.4	DP
6-1	S460	3316	3329	3317	2.1	DP
	S550	3850	3865	3852	1.9	DP
6-2	S460	3125	3137	3149	2.0	DP, LC
	S550	3523	3537	3549	1.8	DP, LC

6.1 Recommendations for future studies

In future the effects of under and overmatched filler materials should be studied. The possibility to increase capacity by using reliable and averaged test results for defining material models should also be considered. Also, correct boundary conditions need to be defined for the joint, so that full scale testing to validate FE analysis results of the joint would be possible. After validating the FE model, more variations of the joint should be modelled and analysed to draw clearer conclusions from the joint behaviour. For the sake of computational cost, further mesh optimisation needs to be done.

References

Ballio, G., Mazzolani, F. M. 1983. Theory and Design of Steel Structures. Chapman and Hall. New York. ISBN: 0-412-23660-5.

Björk, T., Toivonen, J., Nykänen, T. 2010. Capacity of fillet welded joints made of ultra high strength steel. Lappeenranta University of Technology. Laboratory of Fatigue and Strength. Lappeenranta, Finland.

Chen, Y., Zhao, X., Chen, Y. 2008. Parametric analysis and design equation of ultimate capacity for unstiffened overlapped CHS K-joints. *Frontiers of Structural and Civil Engineering*, 2(2): 107-115. DOI: 10.1007/s11709-008-0014-x

Collin P., Johansson B., Design of welds in high strength steel, 4th European Conference on Steel and Composite Structures, Maastricht 2005.

Crockett, P. 1994. The basis of design of the WQ-lattice bottom chord joint. Doctoral thesis. University of Nottingham, Department of Civil Engineering. Nottingham. 309 p.

Dassault Systèmes. 2012. Abaqus 6.12 Online Documentation.

Dexter, E. M., Lee, M. M. K. 1999. Static Strength of Axially Loaded Tubular K-Joints. I: Behavior. *Journal of Structural Engineering*. 1999.125:194-201.

Dhondt, G. 2011. CalculiX CrunchiX User's Manual Version 2.4. [online] (05.12.2011) Available at: <http://web.mit.edu/calculix_v2.4/CalculiX/ccx_2.4/doc/ccx/ccx.html> [Accessed 10.01.2014].

DNV-RP-C208. 2013. Recommended practice. Determination of Structural Capacity by Non-linear FE analysis methods. Det Norske Veritas AS.

Günther, H.-P., Hildebrand, J., Rasche, C., Versch, C., Wudtke, I., Kuhlmann, U., Vormwald, M., Werner, F. 2009. Welded connections of high strength steels for the building industry. International Institute of Welding.

Hendy, C. et al. 2010. EN 1993-1-5: The UK NA for EN 1993-1-5. In *Bridge Design to Eurocodes: UK Implementation*. Institution of Civil Engineers, 22-23.11.2010 s.l.: ICE Publishing. 318–329. DOI: 10.1680/bdte.41509

Johansson, B., Maquoi, G., Sedlacek, G., Müller, C., Beg, D. 2007. Commentary and worked examples to EN 1993-1-5 "Plated structural elements". JRC – ECCS cooperation agreement for the evolution of Eurocode 3. ISSN 1018-5593.

Jurmu, A. 2011. The basis of design of the WQ-lattice bottom chord joint. Master's thesis. University of Oulu, Department of Mechanical Engineering. Oulu. 108 p.

Khursid, M., Mumtaz, N.A. 2011. Static and Fatigue Design of Load Carrying Welded Joints in High Strength Steels. Master's thesis. Royal Institute of Technology, Department of Aeronautical and Vehicle Engineering. Stockholm. 54 p.

Kuhlmann, U., Günther, H.-P. and Rasche, C. 2008. High-strength steel fillet welded connections. *Steel Construction*, 1(1): 77–84. [online], DOI: 10.1002/stco.200890013 [Accessed 13.01.2014].

Moffat, D. G., Hsieh, M. F., & Lynch, M. 2001. An assessment of ASME III and CEN TC54 methods of determining plastic and limit loads for pressure system components. *The Journal of Strain Analysis for Engineering Design*, 36(3): 301-312. DOI: 10.1243/0309324011514485

Ongelin, P., Valkonen, I. 2012. *Rakennepuutket EN 1993 –käsikirja*. Rautaruukki Oyj. ISBN 978-952-5010-51-0.

Packer, J.A., Wardenier, J., Zhao, X.-L., van der Vegte, G.J., and Kurobane, Y. 2009. Design guide for rectangular hollow section (RHS) joints under predominantly static loading. CIDECT. ISBN 978-3-938817-04-9.

Rasche, C., Kuhlmann, U. 2009. Investigations on longitudinal fillet weld lap joints of HSS. *Proceedings of Nordic Steel 2009 Construction Conference*: 462-469.

Rautaruukki Oyj. 2009. WQ-palkkijärjestelmä. [online] Available at:
<http://www.ruukki.fi/~media/Finland/Files/Rakentamisen-esitteet/Ruukki_WQ_liittopalkkijarjestelma.pdf> [Accessed 09.01.2014].

Sedlacek, G., Müller, C. 2001. High Strength Steels In Steel Construction. In International Symposium Niobium 2001. Orlando, Florida, USA, 2-5.12.2001. Bridgeville, Pennsylvania, USA: Niobium 2001 Ltd. 907-930.

SFS-EN 1993-1-1. 2006. Eurocode 3. Design of steel structures. Part 1-1: General rules and rules for buildings. Helsinki: Finnish Standards Association.

SFS-EN 1993-1-5. 2006. Eurocode 3. Design of steel structures. Part 1-5: Plated structural elements. Helsinki: Finnish Standards Association.

SFS-EN 1993-1-8. 2005. Eurocode 3. Design of steel structures. Part 1-8: Design of joints. Helsinki: Finnish Standards Association.

SFS-EN 1993-1-12. 2007. Eurocode 3. Design of steel structures. Part 1-12: Additional rules for the extension of EN 1993 up to steel grades S 700. Helsinki: Finnish Standards Association.

Sperle, J-O. 1997. High Strength Sheet Steels for Optimum Structural Performance. Available at: < http://www.sperle.se/referenser/pdf/artiklar/V2_JK250.pdf > [Accessed 09.01.2014]

van der Vegte, G.J., Makino, Y., Wardenier, J. 2002. The effect of chord pre-load on the static strength of uniplanar tubular K-joints. Proceedings of The Twelfth International Offshore and Polar Engineering Conference. Kitakyushu, Japan, May 26-31, 2002. ISBN 1-880653-58-3.

Wang, Y., Liu, M., Song, Y. 2011. Second Generation Models for Strain-Based Design. Report. Pipeline Research Council International, Inc.

Yu, Wei-Wen., LaBoube, Roger A. 2010. Cold-Formed Steel Design (4th Edition).
New York, USA: John Wiley & Sons. Available through: Aalto University Library
website <<http://lib.aalto.fi>> [Accessed 13.01.2014]

Appendix

Appendix 1. Results for models 1-1...6-2 with steel grade S550. 12 pages.

Appendix 1.

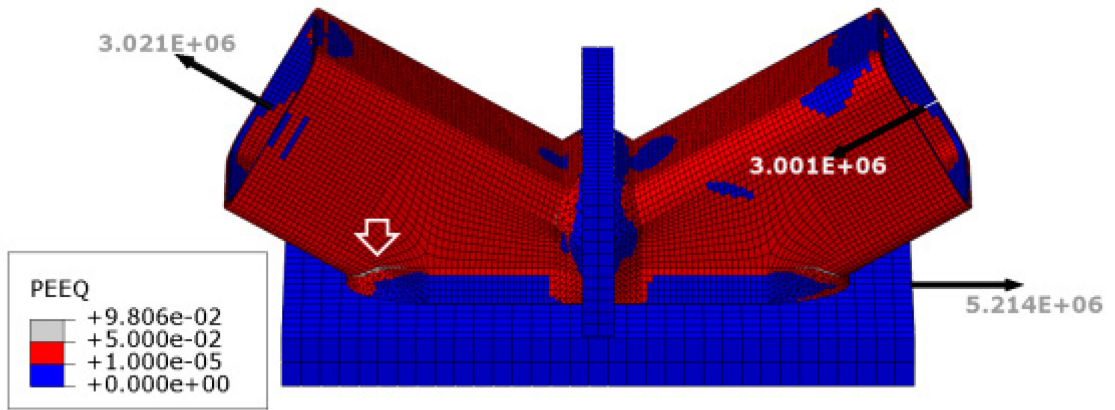


Figure A-1: Equivalent plastic strains of Model 1-1 with steel grade S550.

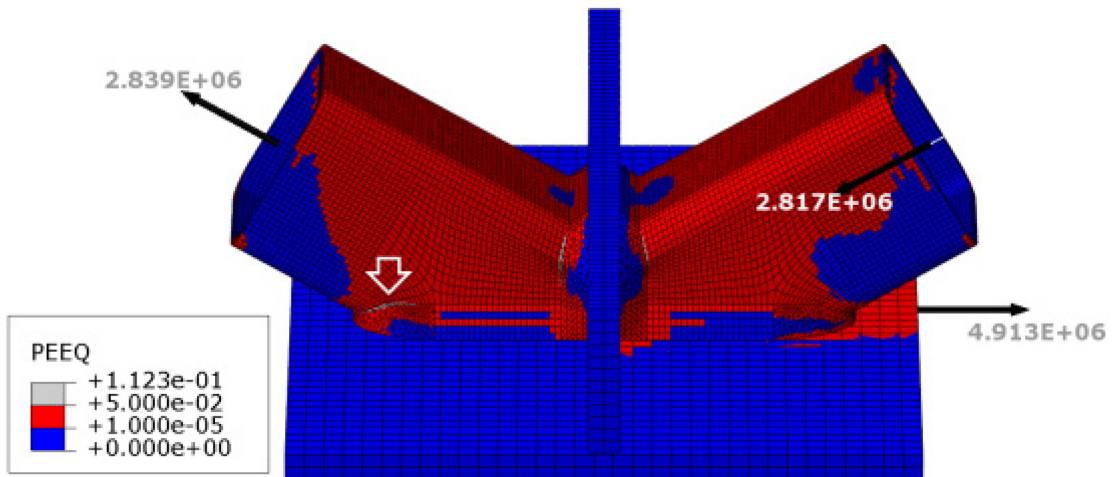


Figure A-2: Equivalent plastic strains of Model 1-2 with steel grade S550.

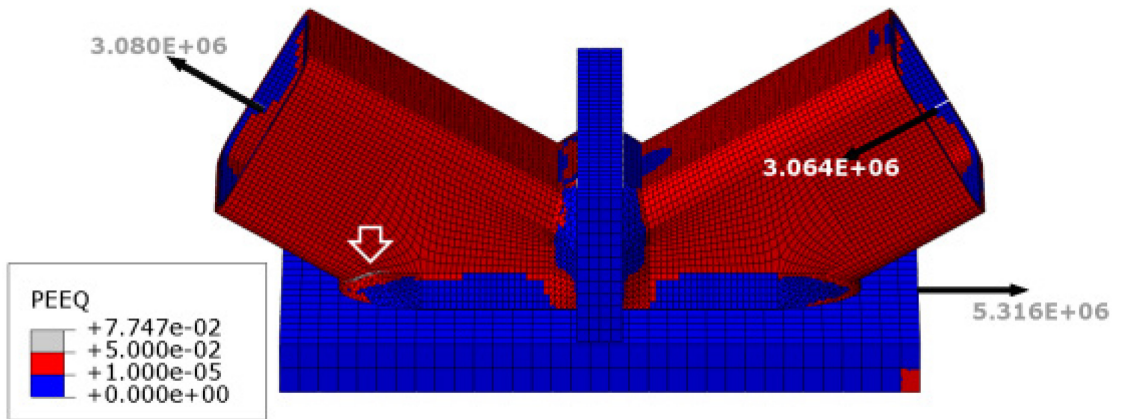


Figure A-3: Equivalent plastic strains of Model 1-3 with steel grade S550.

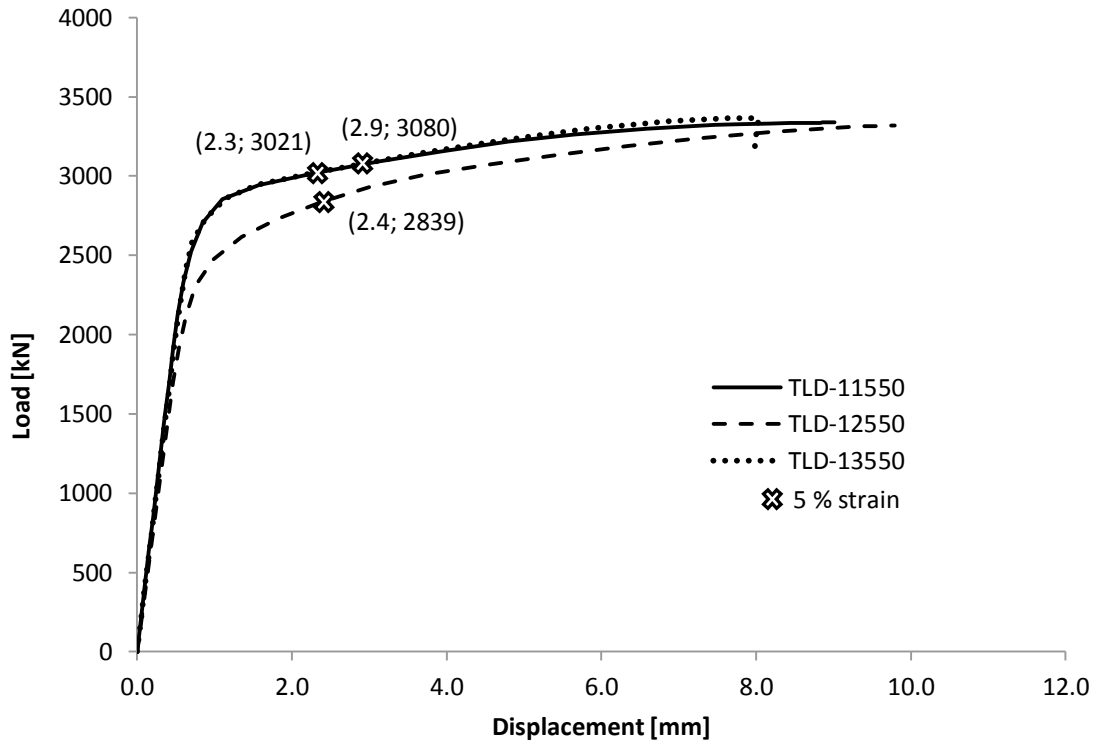


Figure A-4: Load-displacement behaviour of tension bracing member in FE models 1-1, 1-2, and 1-3 with steel grade S550.

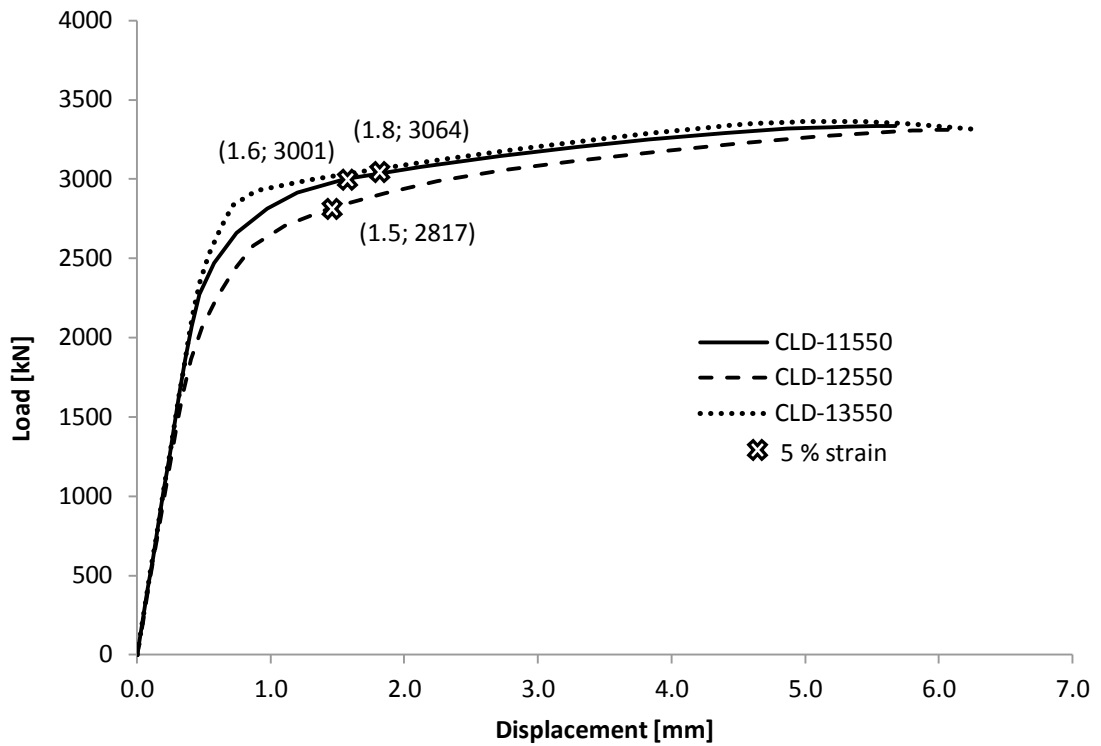


Figure A-5: Load-displacement behaviour of compression bracing member in FE models 1-1, 1-2, and 1-3 with steel grade S550.

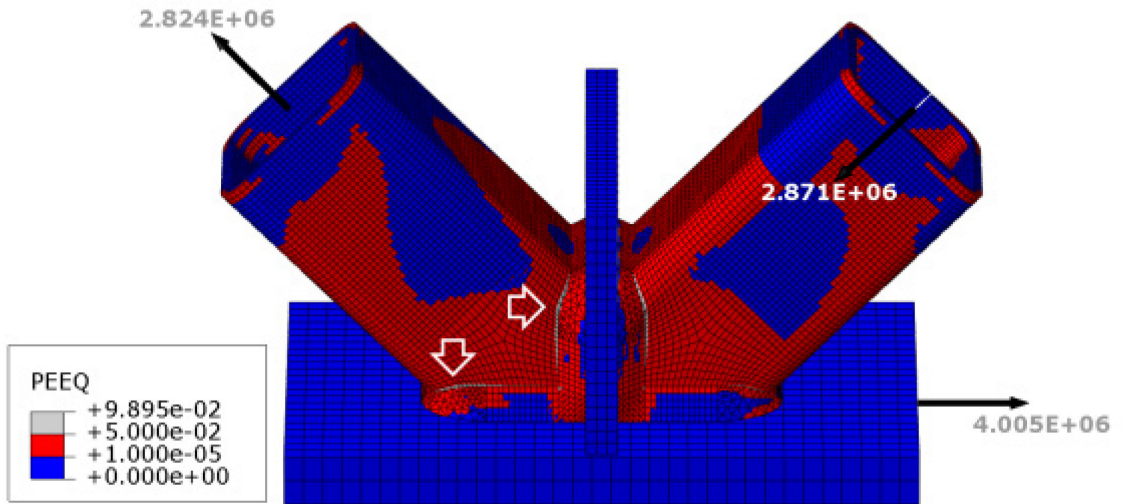


Figure A-6: Equivalent plastic strains of Model 2-1 with steel grade S550.

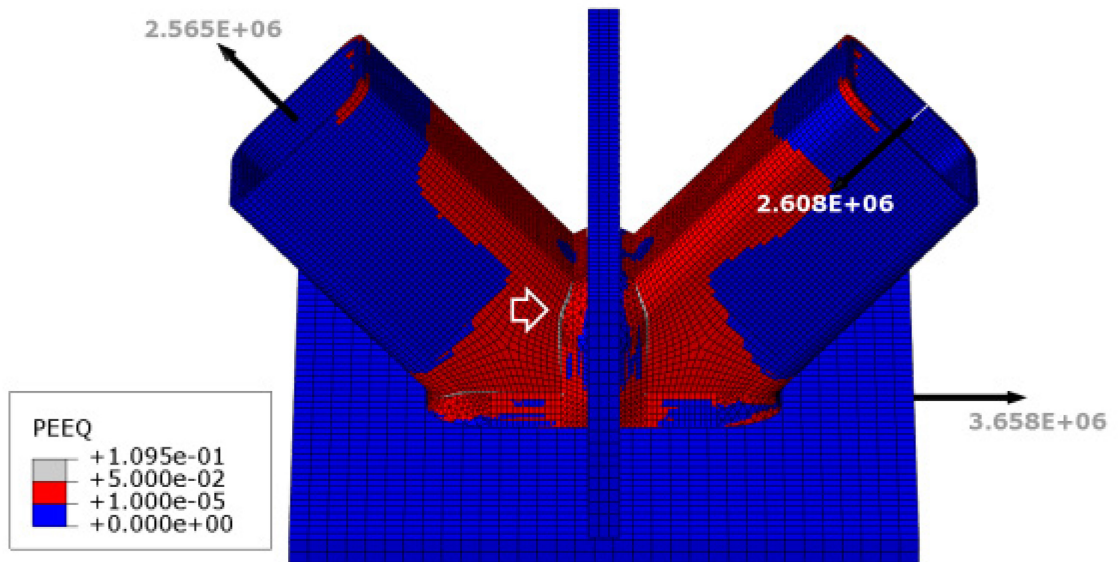


Figure A-7: Equivalent plastic strains of Model 2-2 with steel grade S550.

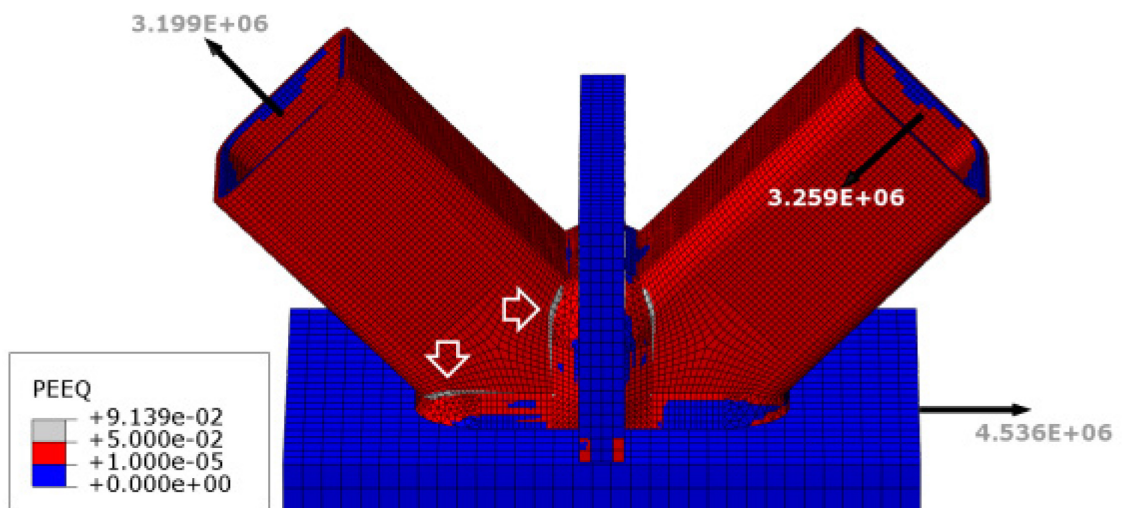


Figure A-8: Equivalent plastic strains of Model 2-3 with steel grade S550.

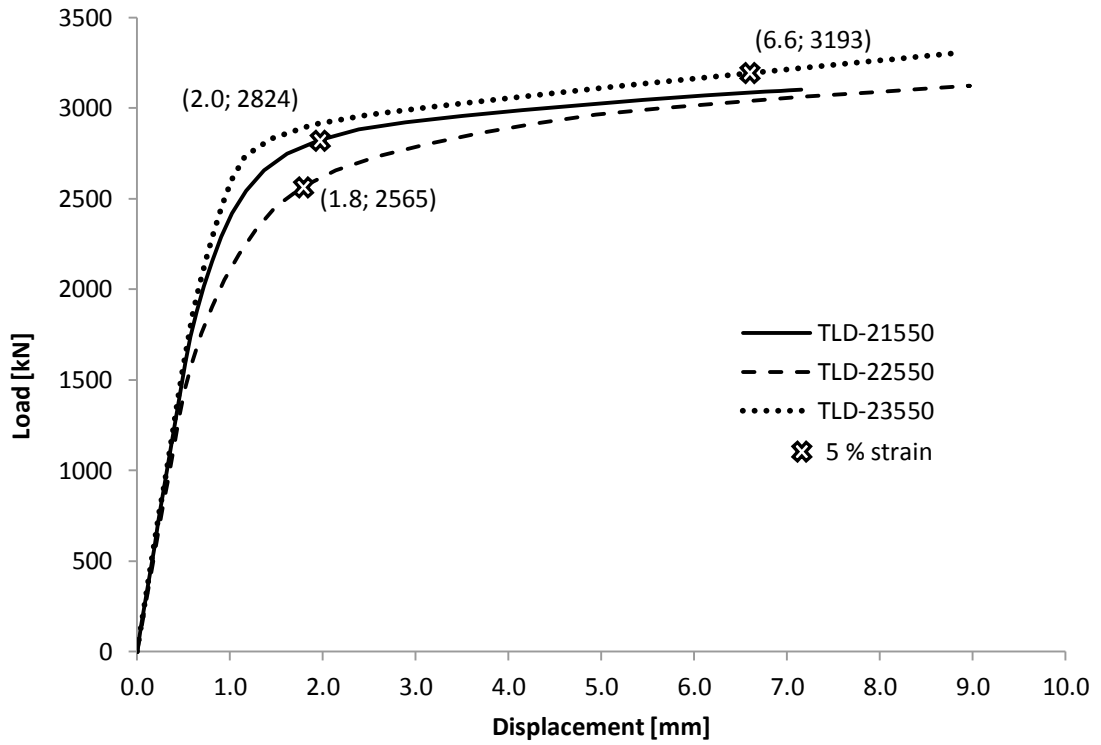


Figure A-9: Load-displacement behaviour of tension bracing member in FE models 2-1, 2-2, and 2-3 with steel grade S550.

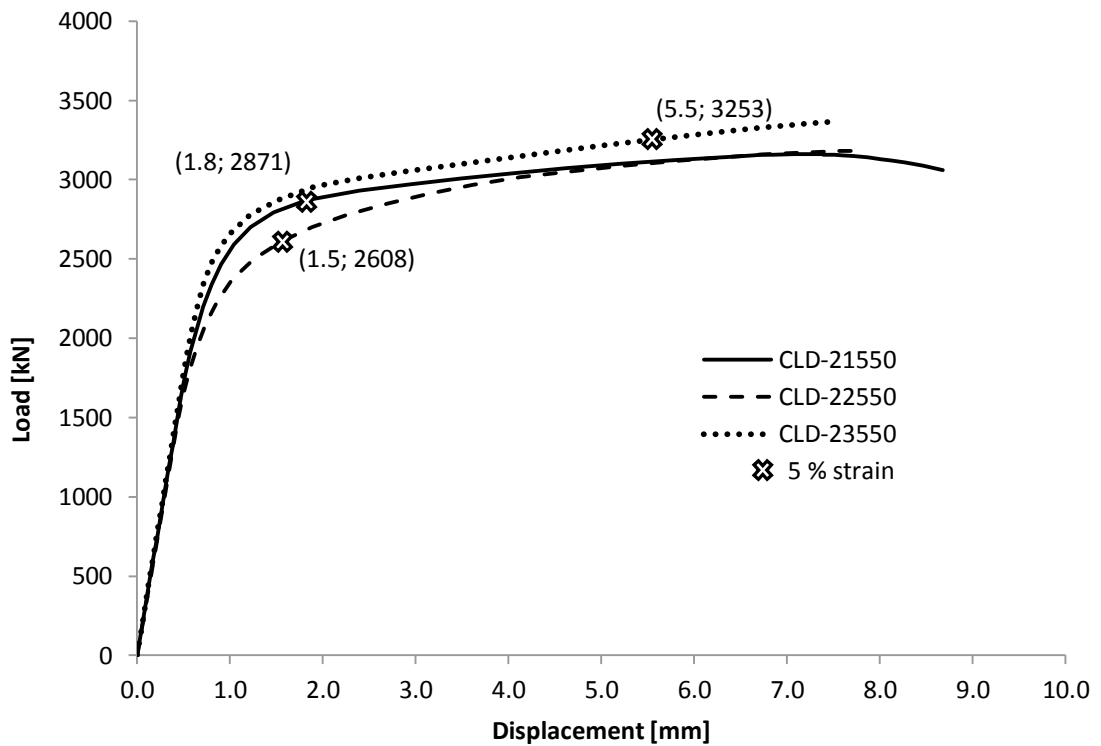


Figure A-10: Load-displacement behaviour of compression bracing member in FE models 2-1, 2-2, and 2-3 with steel grade S550.

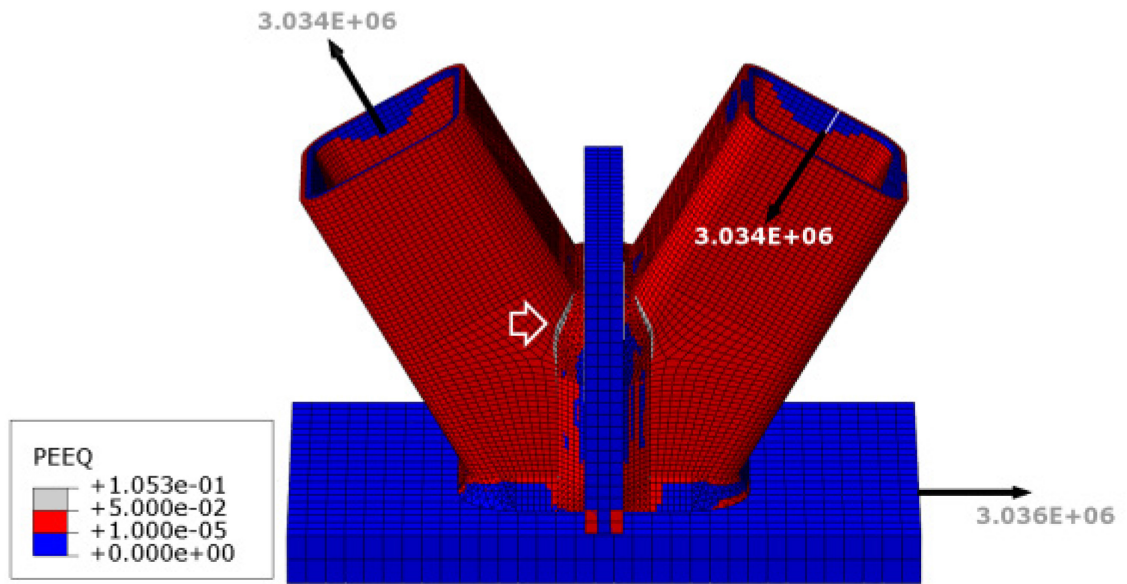


Figure A-11: Equivalent plastic strains of Model 3-1 with steel grade S550.

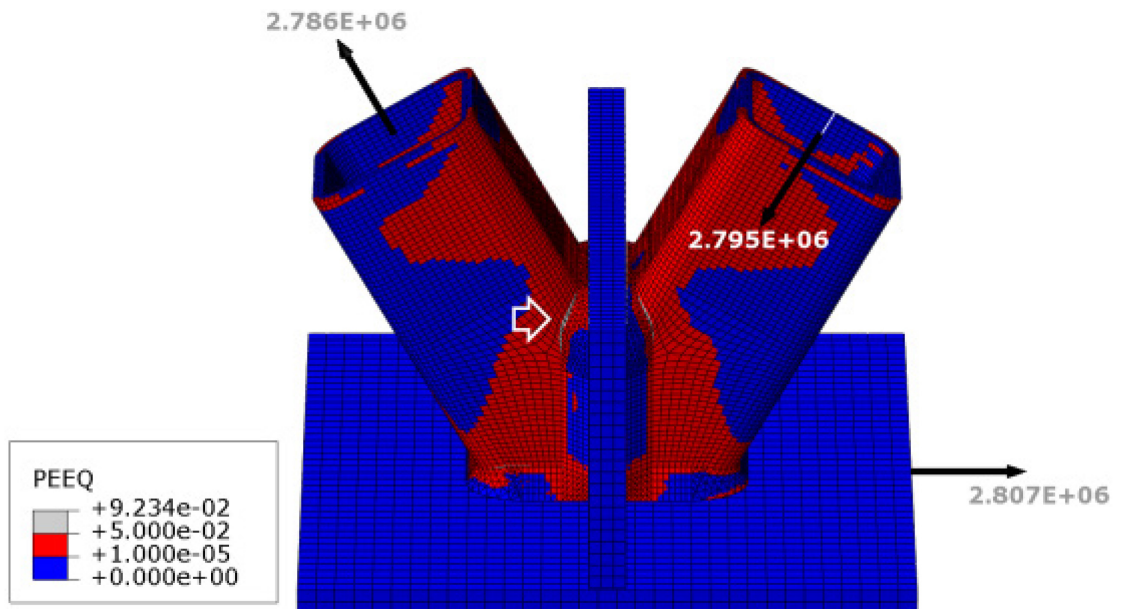


Figure A-12: Equivalent plastic strains of Model 3-2 with steel grade S550.

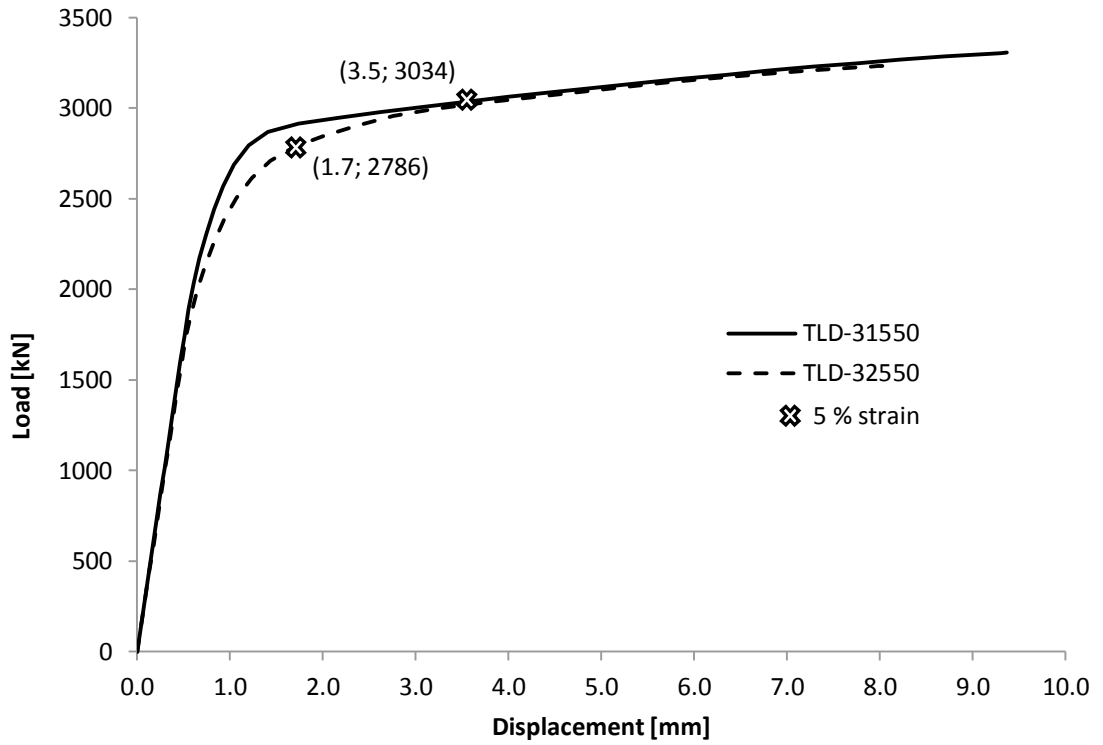


Figure A-13: Load-displacement behaviour of tension bracing member in FE models 3-1 and 3-2 with steel grade S550.

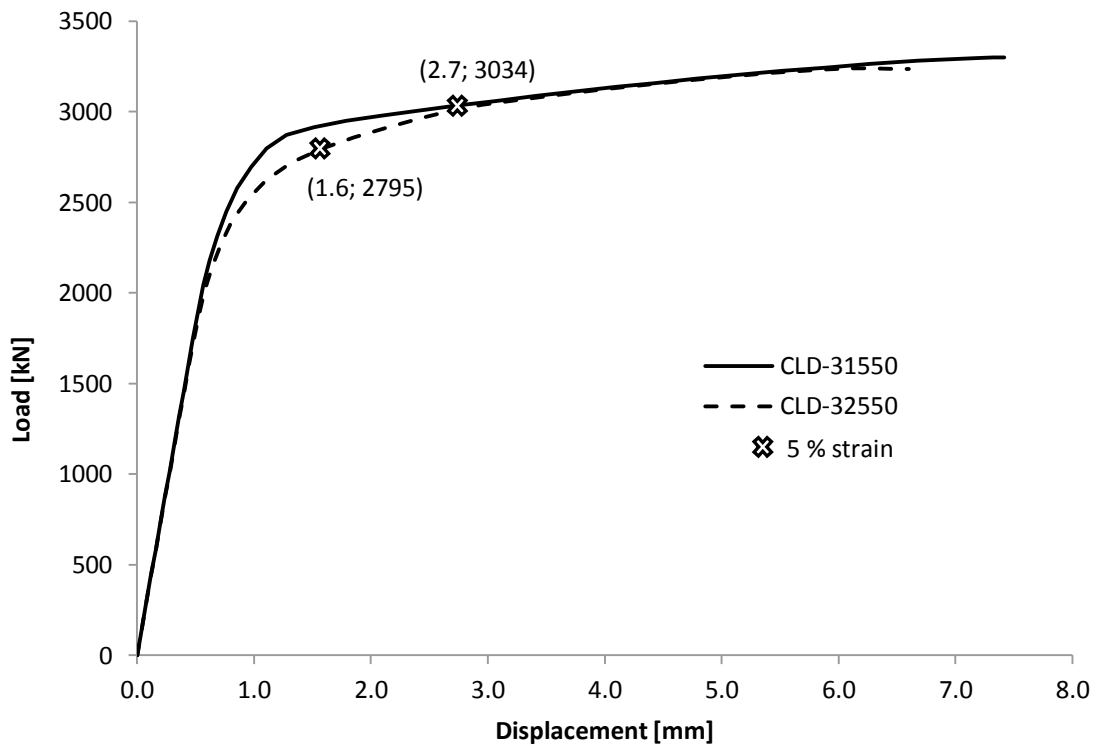


Figure A-14: Load-displacement behaviour of compression bracing member in FE models 3-1 and 3-2 with steel grade S550.

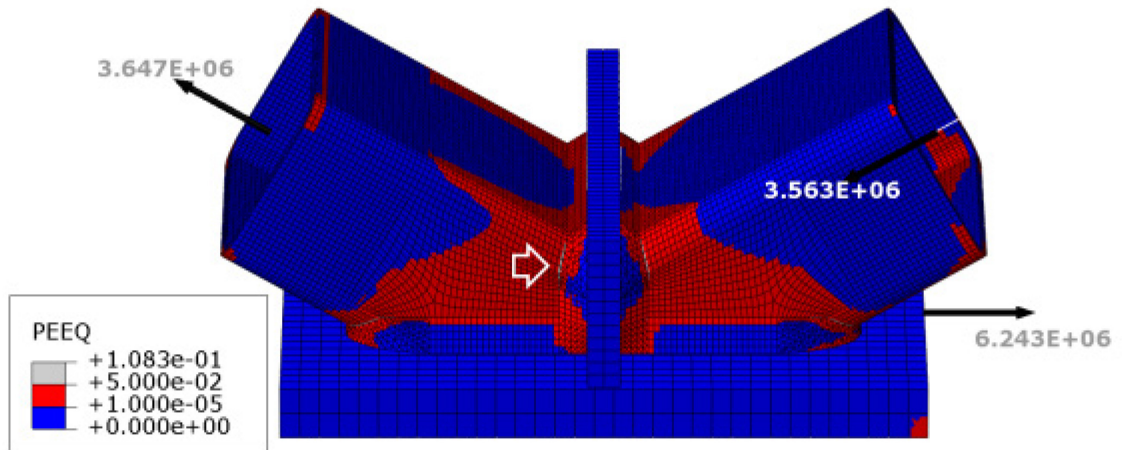


Figure A-15: Equivalent plastic strains of Model 4-1 with steel grade S550.

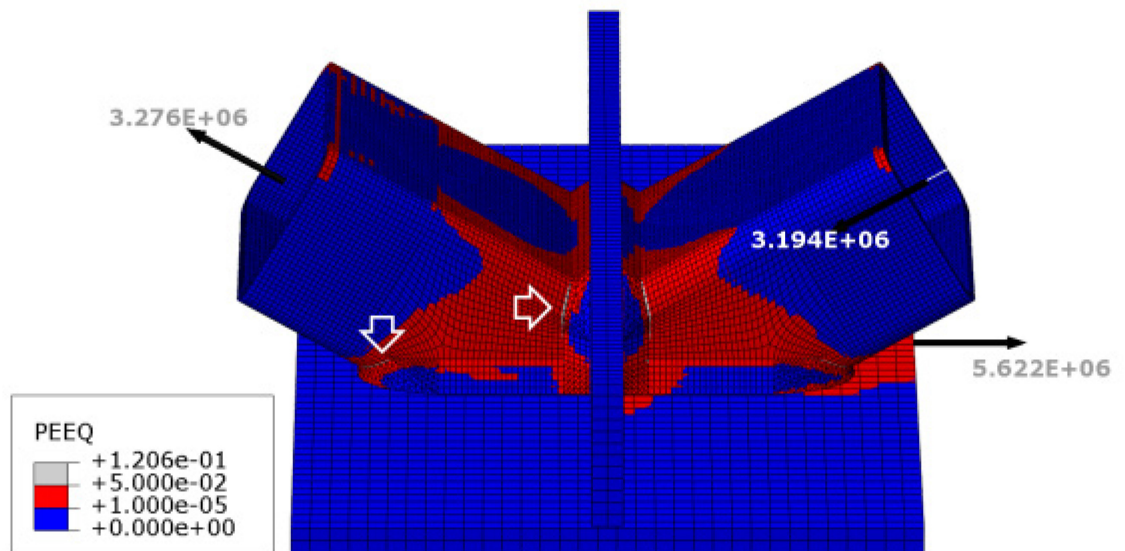


Figure A-16: Equivalent plastic strains of Model 4-2 with steel grade S550.

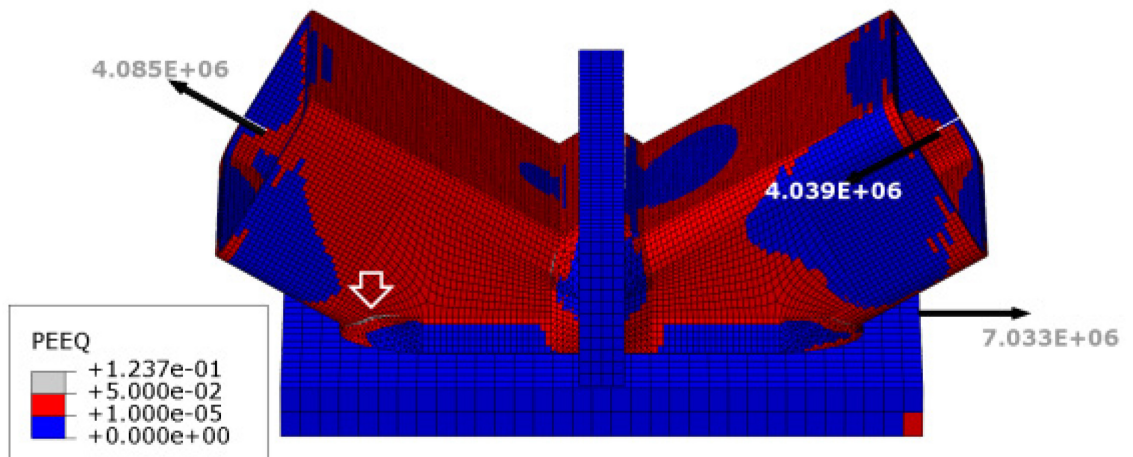


Figure A-17: Equivalent plastic strains of Model 4-3 with steel grade S550.

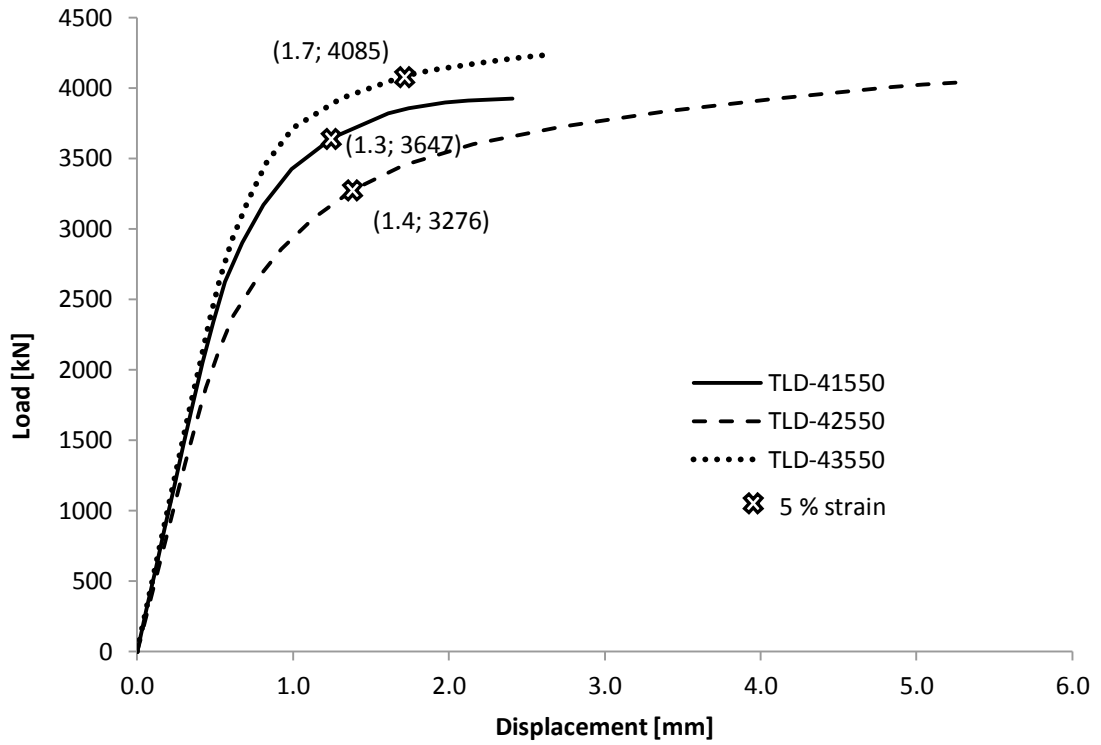


Figure A-18: Load-displacement behaviour of tension bracing member in FE models 4-1, 4-2, and 4-3 with steel grade S550.

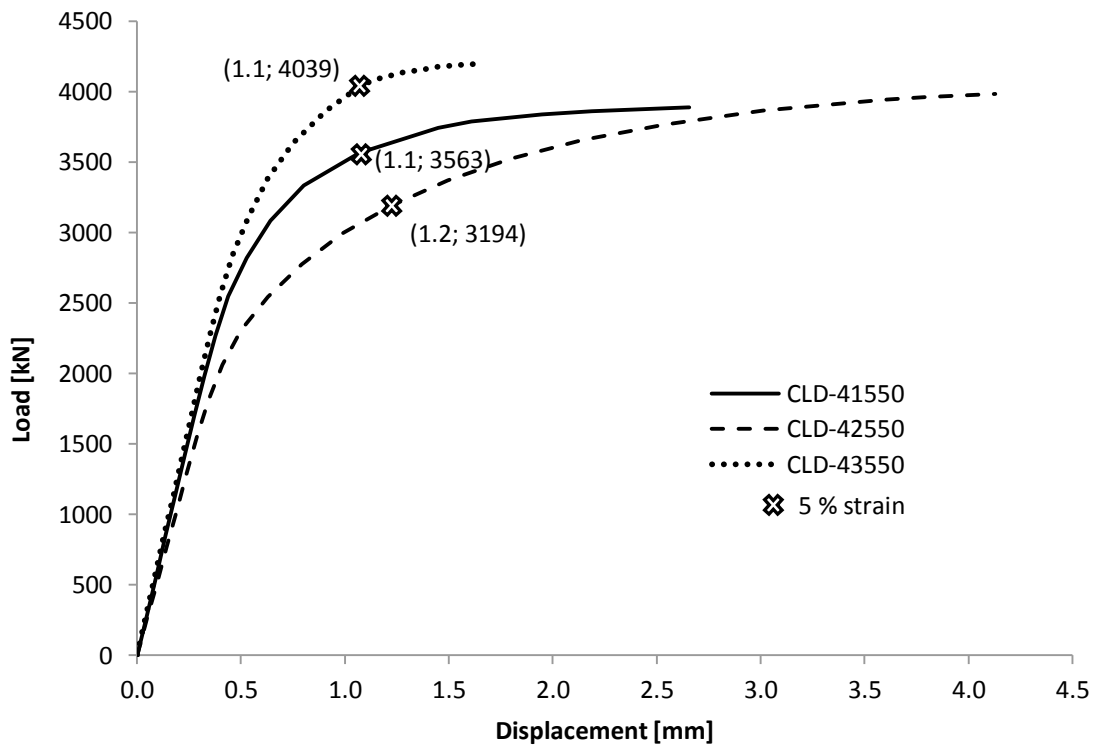


Figure A-19: Load-displacement behaviour of compression bracing member in FE models 4-1, 4-2, and 4-3 with steel grade S550.

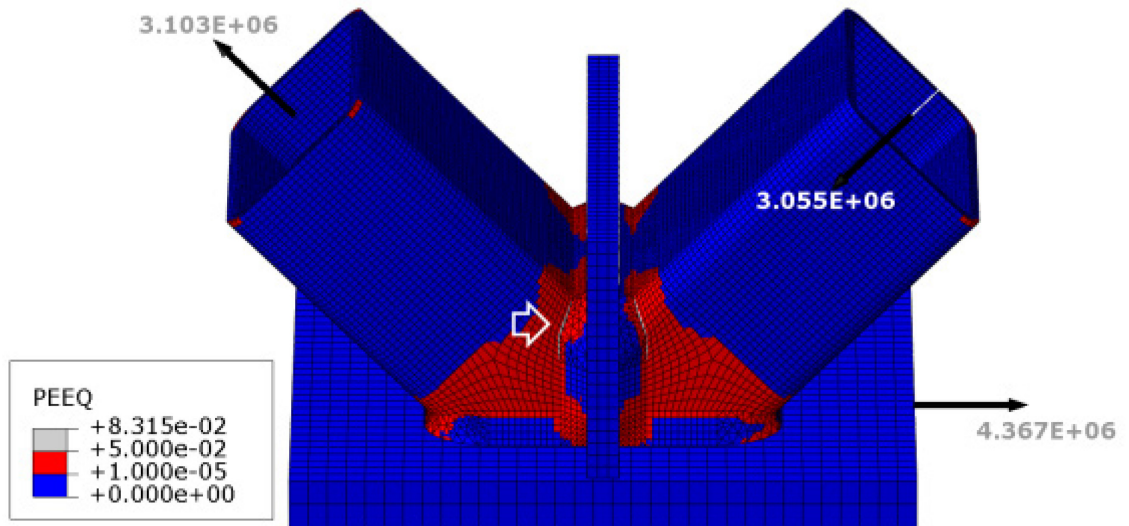


Figure A-20: Equivalent plastic strains of Model 5-1 with steel grade S550.

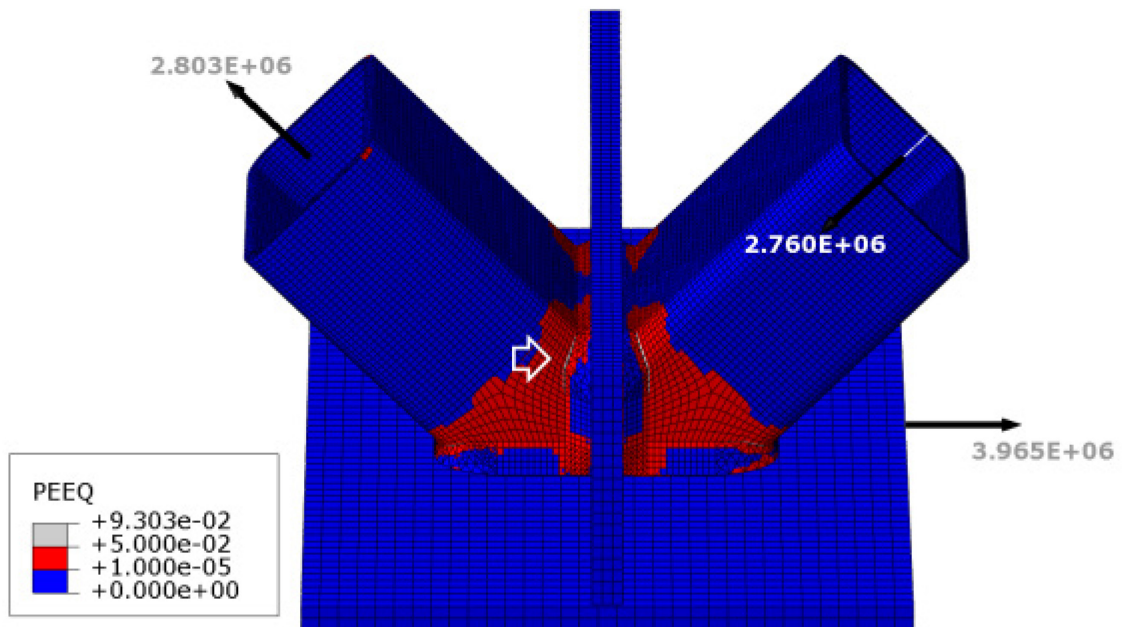


Figure A-21: Equivalent plastic strains of Model 5-2 with steel grade S550.

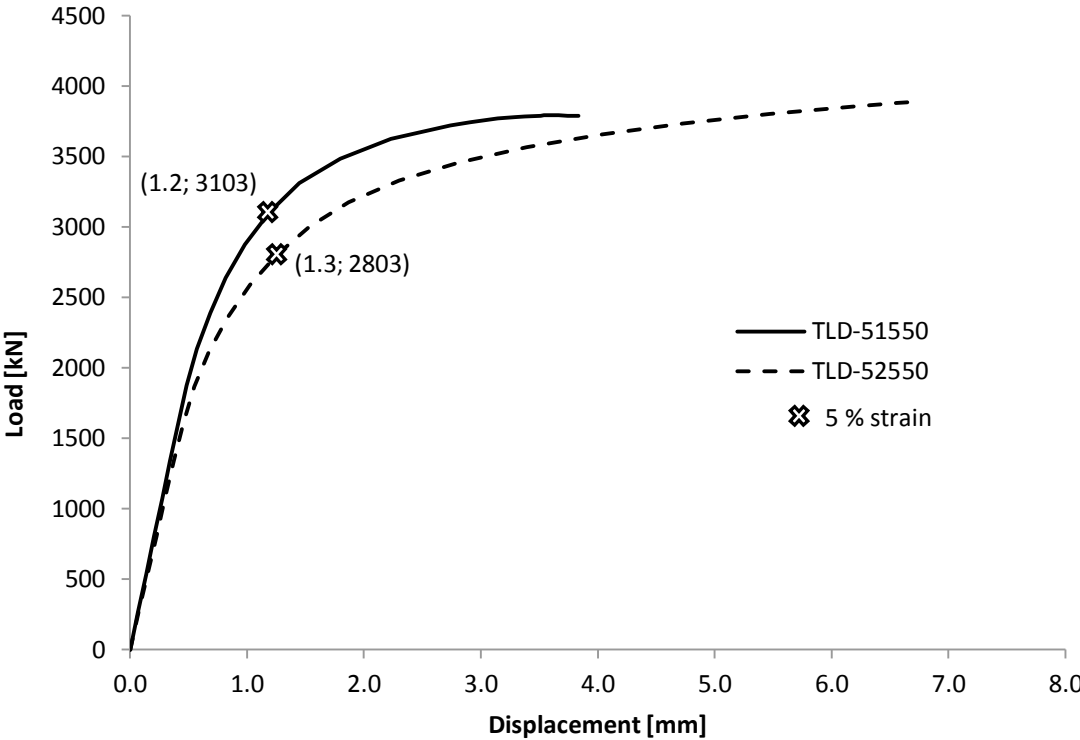


Figure A-22: Load-displacement behaviour of tension bracing member in FE models 5-1 and 5-2 with steel grade S550.

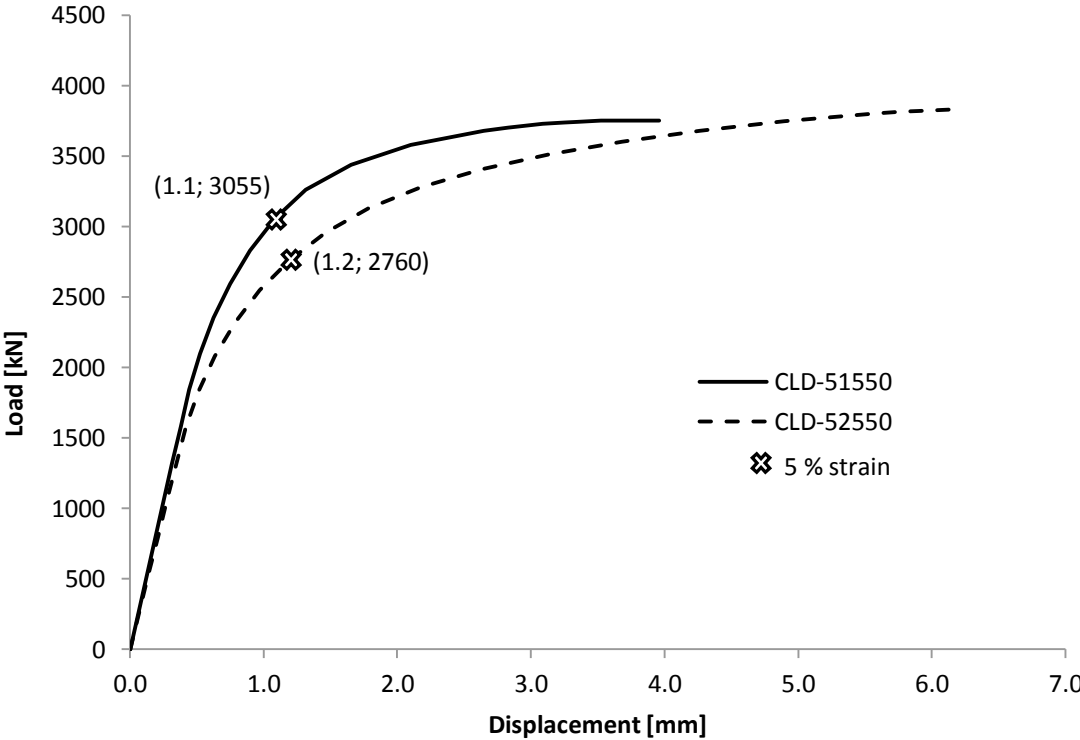


Figure A-23: Load-displacement behaviour of compression bracing member in FE models 5-1 and 5-2 with steel grade S550.

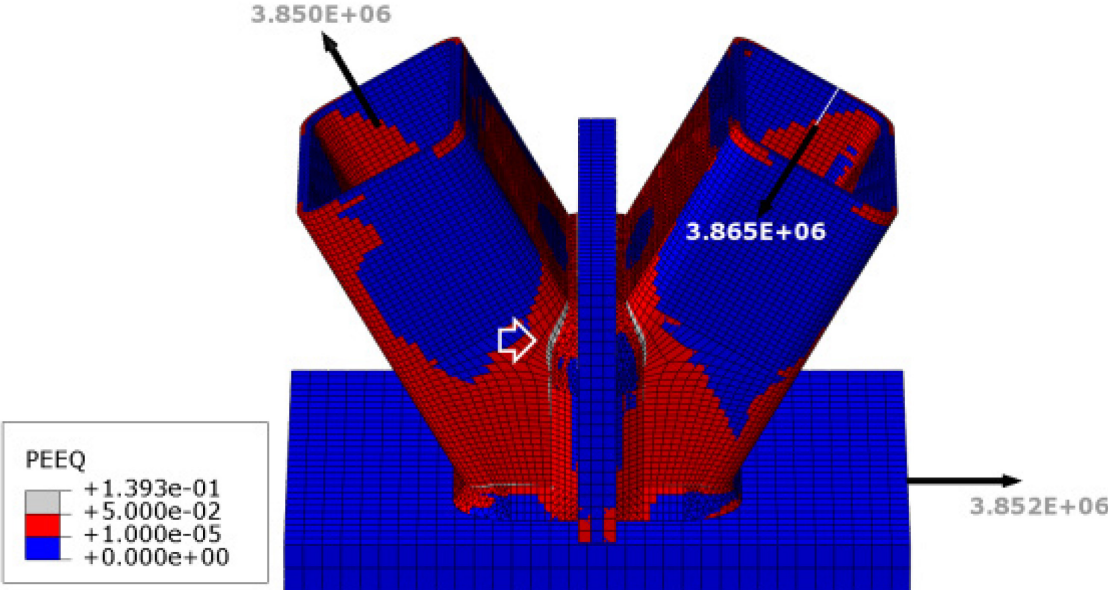


Figure A-24: Equivalent plastic strains of Model 6-1 with steel grade S550.

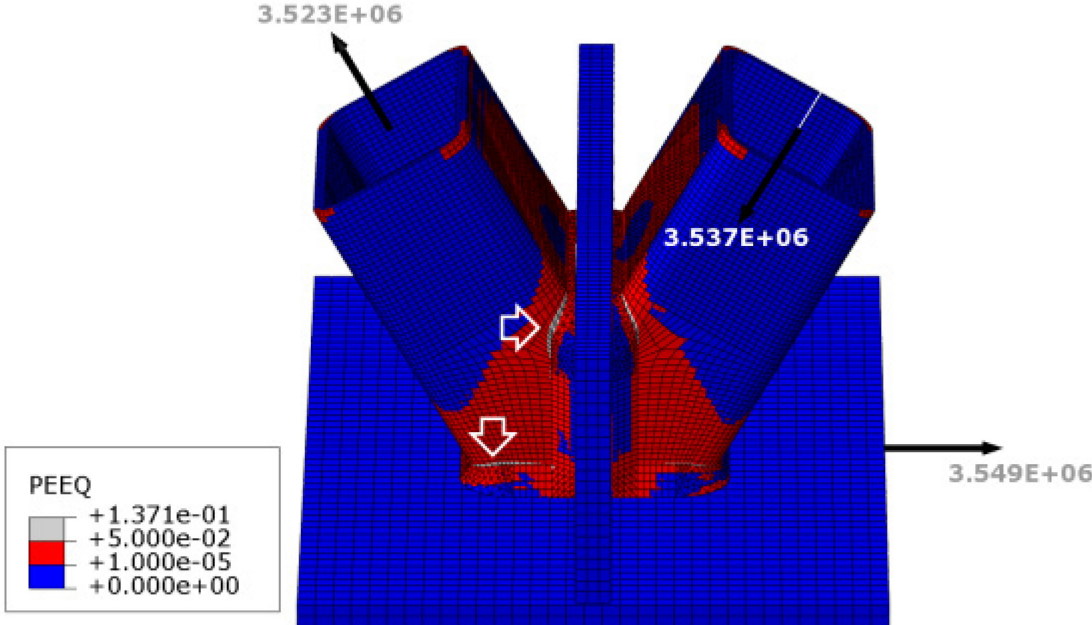


Figure A-25: Equivalent plastic strains of Model 6-2 with steel grade S550.

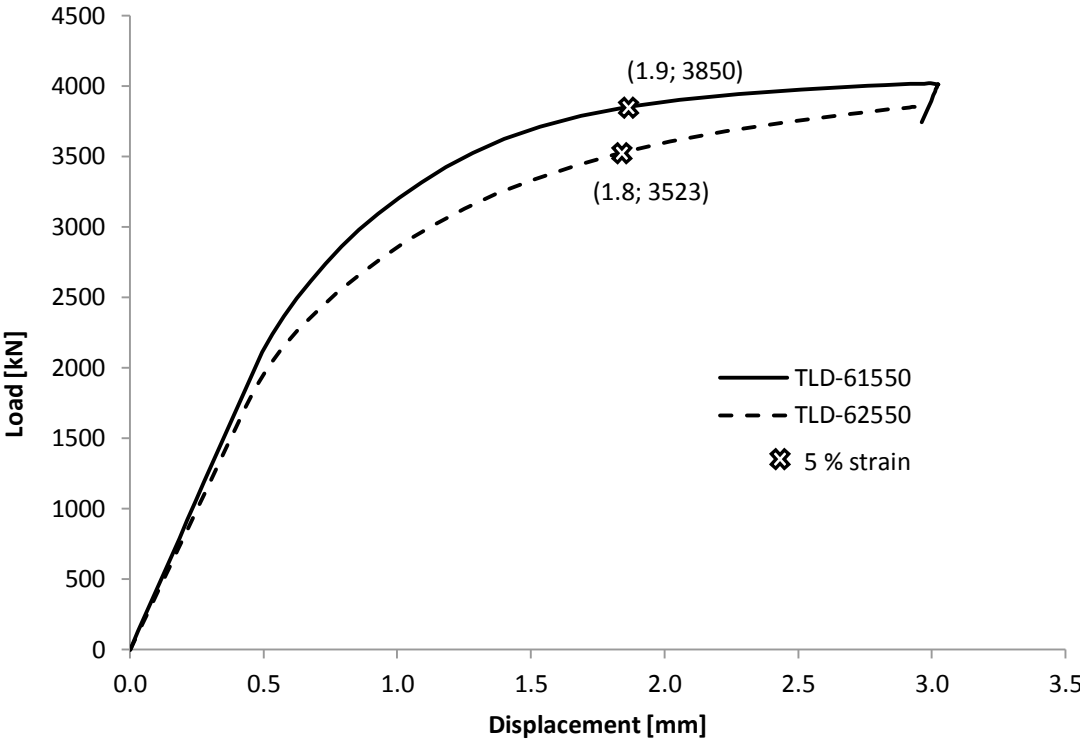


Figure A-26: Load-displacement behaviour of tension bracing member in FE models 6-1 and 6-2 with steel grade S550.

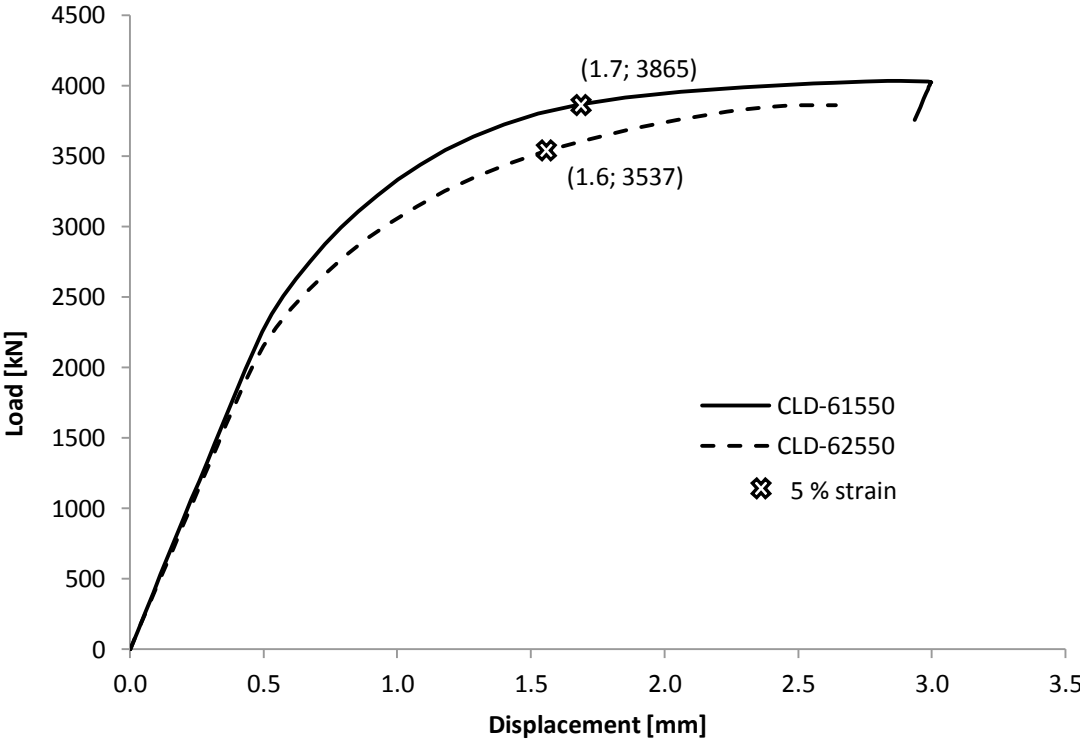


Figure A-27: Load-displacement behaviour of compression bracing member in FE models 6-1 and 6-2 with steel grade S550.